



CMS-HIG-22-007

CERN-EP-2023-284  
2024/02/20

# Search for exotic decays of the Higgs boson to a pair of pseudoscalars in the $\mu\mu bb$ and $\tau\tau bb$ final states

The CMS Collaboration<sup>\*</sup>

## Abstract

A search for exotic decays of the Higgs boson ( $H$ ) with a mass of 125 GeV to a pair of light pseudoscalars  $a_1$  is performed in final states where one pseudoscalar decays to two  $b$  quarks and the other to a pair of muons or  $\tau$  leptons. A data sample of proton-proton collisions at  $\sqrt{s} = 13$  TeV corresponding to an integrated luminosity of  $138 \text{ fb}^{-1}$  recorded with the CMS detector is analyzed. No statistically significant excess is observed over the standard model backgrounds. Upper limits are set at 95% confidence level (CL) on the Higgs boson branching fraction to  $\mu\mu bb$  and to  $\tau\tau bb$ , via a pair of  $a_1$ s. The limits depend on the pseudoscalar mass  $m_{a_1}$  and are observed to be in the range  $(0.17\text{--}3.3)\times 10^{-4}$  and  $(1.7\text{--}7.7)\times 10^{-2}$  in the  $\mu\mu bb$  and  $\tau\tau bb$  final states, respectively. In the framework of models with two Higgs doublets and a complex scalar singlet (2HDM+S), the results of the two final states are combined to determine model-independent upper limits on the branching fraction  $\mathcal{B}(H \rightarrow a_1 a_1 \rightarrow \ell\ell bb)$  at 95% CL, with  $\ell$  being a muon or a  $\tau$  lepton. For different types of 2HDM+S, upper bounds on the branching fraction  $\mathcal{B}(H \rightarrow a_1 a_1)$  are extracted from the combination of the two channels. In most of the Type II 2HDM+S parameter space,  $\mathcal{B}(H \rightarrow a_1 a_1)$  values above 0.23 are excluded at 95% CL for  $m_{a_1}$  values between 15 and 60 GeV.

*Submitted to the European Physical Journal C*



## 1 Introduction

The discovery of the Higgs boson ( $H$ ) by the ATLAS and CMS experiments at the CERN LHC [1–3] strengthened the case for the standard model (SM), which states that the electroweak (EW) symmetry is broken by a complex scalar field [4–9]. However, the SM is not a complete theory as it cannot account for a number of experimental observations. For example, the origin of neutrino mass and dark matter remains unexplained in the SM. Several beyond the SM (BSM) theories address these observations while identifying the 125 GeV resonance as part of an extended group of scalar particles. The Two-Higgs-Doublet Models (2HDMs) [10, 11] predict five physical scalar and pseudoscalar particles and allow different couplings of each scalar to SM fermions. The two real scalar singlet extension [12, 13] of the SM results in three neutral scalar bosons. A broad class of 2HDMs extended with an additional complex scalar singlet (2HDM+S) contains seven physical scalar and pseudoscalar particles [10]. In all these models, one of the scalars is identified as the discovered Higgs boson with a mass of 125 GeV.

Recent measurements of the Higgs boson’s couplings at the LHC do not rule out exotic decays of the Higgs boson to BSM particles. The ATLAS and CMS experiments put, respectively, 12 and 16% upper bounds on the branching fraction of the Higgs boson to undetected particles at 95% confidence level (CL) using data collected in 2016–2018 (Run 2) [14, 15]. Given these bounds, it is crucial to examine the data for direct evidence of new particles coupling to the Higgs boson, in particular, to test possible extensions of the SM.

The exotic decay channels may include the Higgs boson decaying to a pair of light pseudoscalar particles that subsequently decay to pairs of SM particles. This signal can be experimentally discriminated from SM Higgs boson decays. These decays arise naturally in the phenomenology of 2HDM+S, which is described here in more detail. The 2HDM+S couplings are such that a fermion can couple to only one of the scalar doublets to avoid flavor changing neutral currents at tree level. Under this condition, four types of 2HDM+S models are possible [10, 16]. While the SM-like couplings of the Higgs boson to fermions and gauge bosons can be preserved, the singlet state of the 2HDM+S can also serve as a dark matter candidate that couples to the Higgs boson [17, 18]. In 2HDM+S scenarios of Type I, the first doublet,  $\phi_1$ , can couple to any fermion whereas the second doublet,  $\phi_2$ , cannot couple to fermions. In Type II models,  $\phi_2$  couples to down-type quarks and charged leptons while  $\phi_1$  couples to up-type quarks. This model is close to the next-to-minimal supersymmetric SM (NMSSM), which is a special case of 2HDM+S and provides a solution to the so-called  $\mu$ -problem [19]. The NMSSM particle spectrum contains two pseudoscalars,  $a_1$  and  $a_2$ , the lighter  $a_1$  can have a mass smaller than the Higgs boson to allow  $H \rightarrow a_1 a_1$  decays. Another valid extension has quarks coupling to  $\phi_1$  and charged leptons coupling to  $\phi_2$ , referred to as the Type III or “lepton-specific” model. Finally, in the Type IV or “flipped” model,  $\phi_1$  couples to up-type quarks and charged leptons while  $\phi_2$  couples to down-type quarks [10, 16].

The branching fraction,  $\mathcal{B}$ , of  $a_1 a_1 \rightarrow \text{SM}$  particles depends on the type of 2HDM+S model, the mass of the pseudoscalar,  $m_{a_1}$ , and the ratio of the vacuum expectation values of the two doublets,  $\tan \beta$ . The decay width of  $a_1$  to fermion pairs depends, in addition, on the mass of the decay products. In Type II 2HDM+S models,  $\mathcal{B}(a_1 a_1 \rightarrow \tau \tau b b)$  is slightly above 10%, while it can reach up to  $\sim 50\%$  in Type III models. The large predicted branching fraction makes this channel particularly attractive. The decay of  $a_1$  pairs to  $\mu \mu b b$  has a much smaller branching fraction. In Type III models, for  $\tan \beta = 2$ ,  $\mathcal{B}(a_1 a_1 \rightarrow \mu \mu b b)$  is predicted to be about 0.2%. Despite the small branching fraction, this channel can provide competitive results given the high performance of the muon reconstruction and the excellent dimuon mass resolution in CMS. The possibility of the Higgs boson decaying into a pair of  $a_1$ s is studied in this paper for both  $\tau \tau b b$

and  $\mu\mu bb$  decay modes. The gluon-gluon fusion production mechanism ( $ggF$ ) constitutes the dominant Higgs bosons production process, with a cross section of  $\sigma_{ggF} = 48.58 \pm 1.56 \text{ pb}$  [20] at next-to-next-to-next-to-leading order ( $N^3\text{LO}$ ) accuracy in perturbative quantum chromodynamics (QCD) and next-to-leading order (NLO) in EW corrections. The contribution of the Higgs boson production through vector boson fusion (VBF) is also taken into account with a cross section of  $\sigma_{qqH} = 3.72 \pm 0.08 \text{ pb}$  [20], which includes NLO QCD and EW corrections.

Similar searches have been performed at the LHC. The latest analysis by the ATLAS Collaboration [21] has placed a strong bound of  $\mathcal{B}(H \rightarrow a_1 a_1 \rightarrow \mu\mu bb) < (0.2\text{--}4) \times 10^{-4}$  using the LHC Run 2 data at  $\sqrt{s} = 13 \text{ TeV}$ , extending its prior analysis with a partial data sample [22]. The existing CMS search at this center-of-mass energy [23] is based on a data sample corresponding to an integrated luminosity of  $36 \text{ fb}^{-1}$  and results in an upper limit on  $\mathcal{B}(H \rightarrow a_1 a_1 \rightarrow \mu\mu bb)$  of  $(1\text{--}7) \times 10^{-4}$ , considering  $m_{a_1}$  between 20 and  $62.5 \text{ GeV}$ . At  $8 \text{ TeV}$ , the CMS experiment has provided an upper bound of  $\mathcal{B}(H \rightarrow a_1 a_1 \rightarrow \mu\mu bb) < (2\text{--}8) \times 10^{-4}$  [24]. In the  $\tau\tau bb$  final state, an upper limit of  $\mathcal{B}(H \rightarrow a_1 a_1 \rightarrow \tau\tau bb) < (3\text{--}12) \times 10^{-2}$  was reported by CMS using a  $36 \text{ fb}^{-1}$  dataset at  $\sqrt{s} = 13 \text{ TeV}$ , where  $m_{a_1}$  ranged between 15 and  $60 \text{ GeV}$  [25]. The analysis examined both leptonically and hadronically decaying  $\tau$  leptons, the latter denoted by  $\tau_h$ .

This paper reports an extension of CMS searches [23, 25] with the proton-proton (pp) collision data collected in Run 2, corresponding to an integrated luminosity of  $138 \text{ fb}^{-1}$ . Improved techniques in these analyses bring higher sensitivity to the allowed branching fractions. In the  $\mu\mu bb$  final state, in particular, a more in-depth study of the signal achieves a greater gain in sensitivity than that offered by the additional LHC data alone. This channel looks for a bump over the dimuon mass spectrum after a cut-based event selection. A neural network approach to optimize the signal region (SR) selection provides better sensitivity to the signal processes in the  $\tau\tau bb$  channel. The results in the two final states are combined, and interpretations are provided in different types of 2HDM+S models.

The paper is organized as follows: Sections 2 and 3 discuss the CMS detector and the simulated data samples used in these analyses. The event reconstruction and event selection procedures are presented in Sections 4 and 5, respectively. The background prediction methods are described in Section 6. Section 7 presents the signal extraction methods, and the discussion of the systematic uncertainties can be found in Section 8. Results and interpretations are detailed in Section 9 and a summary is presented in Section 10. Tabulated results of this analysis are provided in the HEPData record [26].

## 2 The CMS experiment

The central feature of the CMS apparatus is a superconducting solenoid of 6 m internal diameter, providing a magnetic field of 3.8 T. Within the solenoid volume are a silicon pixel and strip tracker, a lead tungstate crystal electromagnetic calorimeter (ECAL), and a brass and scintillator hadron calorimeter (HCAL), each composed of a barrel and two endcap sections. Forward calorimeters extend the pseudorapidity ( $\eta$ ) coverage provided by the barrel and endcap detectors. Muons are detected in gas-ionization chambers embedded in the steel flux-return yoke outside the solenoid. The collision data are recorded with the help of Level-1 (L1) trigger, high-level trigger (HLT), and data acquisition systems ensuring high efficiency in selecting interesting physics events [27]. A more detailed description of the CMS detector, along with a definition of the coordinate system used and the relevant kinematic variables, can be found in Ref. [28].

### 3 Simulated event samples

Simulated samples are used to design and optimize the analysis strategy and, where needed, to estimate background contributions. A number of Monte Carlo (MC) event generators are used to produce events using either leading order (LO) or NLO matrix element calculations. In all cases, parton showering and fragmentation are implemented using PYTHIA (version 8.212) [29]. The description of parton distribution functions (PDFs) relies on the NNPDF3.1 set [30]. Jets produced at the matrix element level are matched with those generated by PYTHIA using the MLM [31, 32] method for LO samples. The FxFx matching [33] is implemented in the case of NLO samples generated with MADGRAPH5\_aMC@NLO (version 2.2.2 for the simulation of the 2016 data and 2.4.2 for 2017–2018) [34]. For the underlying event description, the CUETP8M1 [35] tune was used for MC samples simulating the 2016 data, while for those simulating the 2017–2018 data, the CP5 [36] tune was employed. The GEANT4 [37, 38] package has been used for the detector simulation. To model the effect of additional collisions within the same or adjacent bunch crossings (pileup), minimum bias interactions are simulated and superimposed on the hard-scattering events. Simulated events are then reweighted to reproduce the pileup distribution in data.

The  $H \rightarrow a_1 a_1 \rightarrow \mu\mu bb$  signal events are generated with the NMSSMHET model [16] using MADGRAPH5\_aMC@NLO (version 2.6.5) at LO [32]. Both ggF and VBF Higgs boson production mechanisms are considered, within the  $a_1$  mass range of 15–60 GeV. While the ggF samples are generated with 5 GeV steps in  $m_{a_1}$ , the VBF samples are generated only for  $m_{a_1}$  of 20, 40, and 60 GeV. Interpolation methods are used to estimate the signal yield and the shape of the dimuon resonance for all mass hypotheses. Similar settings are used to produce  $H \rightarrow a_1 a_1 \rightarrow \tau\tau bb$  signal events at 11  $a_1$  masses between 12 and 60 GeV, for both ggF and VBF Higgs boson production modes.

The major backgrounds for the analyses are the Drell–Yan (DY) process ( $Z/\gamma^* + \text{jets}$ ), the production of a top quark-antiquark pair with additional jets (denoted  $t\bar{t} + \text{jets}$ ), single top quark production, and massive vector boson pair production (Diboson). In the  $\mu\mu bb$  channel, the background estimation is performed using methods fully based on control samples in data with no reference to simulation. Simulated background samples are, however, used to optimize the signal selection criteria. In the  $\tau\tau bb$  channel, only the backgrounds from DY production with  $Z \rightarrow \tau\tau$ , QCD multijet events in the  $e\mu$  final state, and events with jets misidentified as  $\tau_h$  candidates are estimated using control samples in data.

The DY process in the dilepton final state is modeled using MADGRAPH5\_aMC@NLO. Based on the dilepton invariant mass ( $m_{\ell\ell}$ ) threshold at the generator level, two DY samples are considered, one with  $m_{\ell\ell} > 50$  GeV and the other with  $10 < m_{\ell\ell} < 50$  GeV. The high-mass DY samples are produced at (N)LO, with up to four (two) additional partons at the matrix element level. For the low mass, samples are primarily produced at LO with additional partons, similar to those of high mass, while NLO and LO samples inclusive in number of jets are also utilized. In the  $\mu\mu bb$  analysis, the NLO samples at high mass are employed, and at low mass, NLO QCD K-factors are applied to the LO cross section. An uncertainty of 30% is considered on these K-factor corrections, as they are extracted from NLO low-mass samples with limited number of events. The accuracy of the DY sample is found to be sufficient for optimization purposes, which is the only use of the simulated backgrounds in the  $\mu\mu bb$  channel. The  $\tau\tau bb$  analysis makes use of LO DY samples in the entire mass range. The cross sections are normalized to next-to-NLO (NNLO) in QCD using K-factors [39]. In addition, the  $Z$  boson  $p_T$  distribution is corrected by reweighting simulated events to data in bins of  $p_T^{\ell\ell}$  and  $m_{\ell\ell}$ .

The POWHEG BOX v2.0 framework [40–43] event generator is used to produce  $t\bar{t} + \text{jets}$  and sin-

gle top events at NLO. The simulated  $t\bar{t}$ +jets events are reweighted to match the top quark  $p_T$  distribution at NNLO QCD and NLO EW [44] precision. Diboson and  $W$ +jets events are generated by MADGRAPH5\_aMC@NLO. Similar to the high-mass DY sample,  $W$ +jets events are simulated with up to four additional partons at the matrix element level for all years. The  $t\bar{t}$ +jets, DY, and  $W$ +jets samples are normalized to cross section values accurate to NNLO in QCD [45–53]. All SM backgrounds containing the Higgs boson are generated using POWHEG v2.0 at NLO [54–58].

## 4 Object reconstruction

The  $\mu\mu bb$  and  $\tau\tau bb$  analyses together reconstruct a diverse set of final-state particles for a  $H \rightarrow a_1 a_1$  signal. The  $\mu\mu bb$  analysis relies on the presence of two prompt muons. In the  $\tau\tau bb$  channel, on the other hand, final states with at least one  $\tau$  lepton decaying to an electron or muon, i.e.,  $e\mu$ ,  $e\tau_h$ , and  $\mu\tau_h$ , are considered. The  $\tau$  lepton decays resulting in same-flavor leptons, or in two  $\tau_h$  candidates, are not included as they bring negligible sensitivity to the analysis. The signal acceptance of  $\tau_h\tau_h$  is very low due to high trigger thresholds, whereas ee and  $\mu\mu$  final states suffer from low branching fractions.

The particle-flow (PF) algorithm [59] is used to reconstruct and identify each individual particle (PF candidate) in the event, with an optimized combination of information from the various elements of the CMS detector. The energy of photons is measured in ECAL. The energy of electrons is determined from a combination of the electron momentum at the primary interaction vertex as measured by the tracker, the energy of the corresponding ECAL cluster, and the energy sum of all bremsstrahlung photons spatially compatible with originating from the electron track. The energy of muons is obtained from the curvature of the corresponding track. The energy of charged hadrons is evaluated via a combination of their momentum measured in the tracker and the matching of the ECAL and HCAL energy deposits, corrected for the response function of the calorimeters to hadronic showers. Finally, the energy of neutral hadrons is obtained from the corresponding corrected ECAL and HCAL energies.

The primary vertex (PV) is taken to be the vertex corresponding to the hardest scattering in the event, identified using the tracking information alone, as described in Section 9.4.1 of Ref. [60].

Muons can be produced directly in  $a_1$  decays in the  $\mu\mu bb$  final state, or from decays of the  $\tau$  leptons in the  $\tau\tau bb$  channel. In both analyses, muons must lie within  $|\eta| < 2.4$ . The  $p_T$  threshold for muons in the  $\tau\tau bb$  analysis depends on the trigger selection, see Section 5 and Table 1. In the  $\mu\tau_h$  final state, it is required to be 1 GeV greater than the HLT muon  $p_T$  threshold in order to be in a region where the efficiency of the respective trigger is independent of  $p_T$ . The muon  $p_T$  requirement in the  $e\mu$  final state, selected with an  $e\mu$  trigger, is 24 (13) GeV when the muon is the leading (subleading) lepton in the pair. In the  $\mu\mu bb$  analysis, the leading (subleading) muon  $p_T$  must exceed 17 (15) GeV. The two muons are required to have an opposite electric charge and to be separated by a minimum  $\Delta R \equiv \sqrt{(\Delta\eta)^2 + (\Delta\phi)^2} = 0.4$ , where  $\phi$  is the azimuthal angle of the particle’s momentum in the plane perpendicular to the beam line. In cases where more than two muons satisfy these criteria, the pair with the highest  $p_T$  are considered.

In order to suppress contributions from nonprompt decays of hadrons and from their shower penetration in the muon detectors, selected muons must pass dedicated identification requirements. The so-called tight identification [61] is used in the  $\mu\mu bb$  analysis with an efficiency varying between 95 and 99%, depending on  $\eta$ , where the data and simulation agree within 1–3%. Looser requirements for muons, known as medium identification criteria [61], are employed in the  $\tau\tau bb$  analysis, with an overall efficiency of 99.5% for simulated  $W$  and  $Z$  events.

The lepton isolation variable  $I_{\text{rel}}$  is calculated by summing the transverse energy deposited by other particles in a cone of size  $\Delta R = 0.4$  ( $0.3$ ) around the muon (electron) and dividing by the lepton  $p_T$ . The contribution of charged particles from pileup is suppressed by requiring the charged particles to be associated with the PV. An average pileup energy is subtracted from the total energy of neutral particles and photons within the isolation cone, since vertex association is not known in this case. Muons are required to pass  $I_{\text{rel}} < 0.15$  in the  $\tau\tau\text{bb}$  analysis.

In the  $\mu\mu\text{bb}$  analysis, a looser requirement of  $I_{\text{rel}} < 0.25$  is imposed, which results in about 99% efficiency for muons with  $p_T > 20$  GeV, independent of  $\eta$  [61]. Electrons from  $\tau$  lepton decays are selected within  $|\eta| < 2.4$  with different  $p_T$  thresholds, according to the  $\tau\tau\text{bb}$  final state. In the  $e\mu$  channel, the threshold is 24 GeV if the electron is the leading lepton. Otherwise, it is reduced to 13 GeV. In the  $e\tau_h$  channel, the electron  $p_T$  must be more than 1 GeV beyond the HLT threshold. A multivariate analysis (MVA) discriminant is used to identify electrons. The MVA exploits several properties of the electron candidate, including energy deposits in the ECAL, the quality of the associated track, and the shower shape in the calorimeters [62]. The chosen MVA working point has a 90% efficiency to correctly identify an electron. Identified electrons are further required to be isolated, fulfilling  $I_{\text{rel}} < 0.10$ . In the  $e\mu$  channel of the  $\tau\tau\text{bb}$  analysis, the electron must be separated from the muon by  $\Delta R \geq 0.3$  and have an opposite electric charge. For both electrons and muons, correction factors for the reconstruction and identification efficiencies are obtained from data and applied to simulation.

Jets are reconstructed by clustering the charged and neutral PF candidates using the anti- $k_T$  algorithm [63, 64] with a distance parameter of 0.4, up to  $|\eta| < 4.7$  for tagging VBF events. The reconstructed jet energy is corrected for effects from the detector response as a function of the jet  $p_T$  and  $\eta$ . Furthermore, contamination from pileup and electronic noise is subtracted using the charged-hadron subtraction method [59]. To achieve a better agreement between data and simulation, an extra  $\eta$ -dependent smearing is performed on the jet energy in simulated events [65, 66]. Events are required to have at least two jets with  $|\eta| < 2.4$  and  $p_T > 15$  (20) GeV in the  $\mu\mu\text{bb}$  ( $\tau\tau\text{bb}$ ) analysis. Both jets are required to be separated from any selected electron, muon, or  $\tau_h$  by  $\Delta R > 0.4$  (0.5) in the  $\mu\mu\text{bb}$  ( $\tau\tau\text{bb}$ ) analysis.

Both channels rely on identifying jets that likely originate from b quarks. The DEEPJET flavor classification algorithm [67, 68] is used to tag b jets. Three different working points on the b tagging discriminator values correspond to 0.1, 1, and 10% misidentification probabilities, known respectively as tight (T), medium (M), and loose (L) working points. The corresponding b tagging efficiencies are about 65, 80, and 95%, respectively [69]. In the  $\mu\mu\text{bb}$  analysis, the selected jet with the higher b tagging score is required to pass the tight working point whereas the second one fulfills the loose b tagging requirements. In this paper the latter is referred to as the ‘looser’ b jet. In the  $\tau\tau\text{bb}$  analysis, the medium working point is used to identify b jets. The shape of the distribution of the b tagging discriminator, and thus the b tagging efficiencies, can be different between data and simulation. Since the  $\mu\mu\text{bb}$  analysis relies on the b tagging discriminator distribution, shape-based corrections are applied on simulation to match the data. A similar method is used in the  $\tau\tau\text{bb}$  final state, which, by construction corrects the b tagging efficiency for all b tagging discriminator scores.

The hadron-plus-strips algorithm [70] with anti- $k_T$  jets as seeds is used to reconstruct the hadronically decaying  $\tau$  leptons. The algorithm combines one or three tracks with energy deposits in the calorimeters to identify the  $\tau$  lepton decay modes. Neutral pions are reconstructed as strips with a dynamic size in  $\eta$ - $\phi$  from reconstructed electrons and photons, where the strip size varies as a function of the  $p_{\text{TS}}$  of the electron or photon candidate. The  $p_T$  of the  $\tau_h$  candidates are required to be 5 GeV greater than the threshold at the trigger level. In events triggered

by single leptons, the  $\tau_h$   $p_T$  must exceed 20 GeV. The pseudorapidity of the  $\tau_h$  candidate also depends on the trigger. It is restricted to  $|\eta| < 2.1$  if a  $\tau_h$  identification is performed at the HLT, and to  $|\eta| < 2.3$  otherwise. To distinguish genuine  $\tau_h$  decays from electrons, muons, or jets originating from the hadronization of quarks or gluons, the DEEPTAU algorithm [71] is used. Information from all individual reconstructed particles near the  $\tau_h$  candidate axis is combined with properties of the  $\tau_h$  candidate. The probability for a jet to be misidentified as a  $\tau_h$  candidate by the DEEPTAU algorithm depends on the  $p_T$  and the jet flavor. In simulated  $W+jets$  events, the misidentification rate for jets is estimated to be 0.4% for a genuine  $\tau_h$  identification efficiency of 70%. The misidentification rate for electrons (muons) is 2.6% (0.03%) for a genuine  $\tau_h$  identification efficiency of 80% ( $> 99\%$ ). In the  $e\tau_h$  and  $\mu\tau_h$  final states of the  $\tau\tau bb$  channel, the  $\tau_h$  candidate must be separated from the electron or muon by  $\Delta R \geq 0.4$  and they must be oppositely charged.

The missing transverse momentum vector  $\vec{p}_T^{\text{miss}}$  is computed as the negative vector sum of the transverse momenta of all the PF candidates in an event, and its magnitude is denoted as  $p_T^{\text{miss}}$  [72]. The  $\vec{p}_T^{\text{miss}}$  is modified to account for corrections to the energy scale of the reconstructed jets in the event. Anomalous high- $p_T^{\text{miss}}$  events can be due to a variety of reconstruction failures, detector malfunctions or noncollision backgrounds. Such events are rejected by event filters that are designed to identify more than 85–90% of the spurious high- $p_T^{\text{miss}}$  events with a mistagging rate less than 0.1% [72].

## 5 Event selection

Table 1 summarizes the different  $p_T$  criteria for online reconstructed electrons, muons and  $\tau_h$ s in the  $\mu\mu bb$  and  $\tau\tau bb$  channels.

Table 1: The electron, muon, and  $\tau_h$   $p_T$  thresholds in GeV at trigger level for the  $\mu\mu bb$  and  $\tau\tau bb$  channels.

Year	Single/dilepton trigger $p_T$	$\mu\mu bb$			$\tau\tau bb$		
		$\mu$	$e$	$\mu$	$e$	$\tau_h$	$\mu$
2016	Single lepton	24	—	—	25	—	22
	$p_T$ -leading lepton	17	23	23	—	—	—
	$p_T$ -subleading lepton	8	12	8	—	—	19
2017	Single lepton	24	—	—	27, 32	—	24, 27
	$p_T$ -leading lepton	17	23	23	—	30	—
	$p_T$ -subleading lepton	8	12	8	24	—	20
2018	Single lepton	24	—	—	32, 35	—	24, 27
	$p_T$ -leading lepton	17	23	23	—	30	—
	$p_T$ subleading lepton	8	12	8	24	—	20

The  $\mu\mu bb$  event candidates are selected based on the requirement that either one or both muons are reconstructed at the HLT. Passing the double-muon trigger necessitates two isolated muons with  $p_T$  exceeding thresholds of 17 and 8 GeV, which increases to 24 GeV for an isolated muon in the single-muon trigger path. Accepting events from both single- and double-muon triggers improves the trigger efficiency by including events in which the second muon is not reconstructed at the trigger level.

Depending on the decay of the  $\tau$  lepton and the data-taking period, the  $\tau\tau bb$  candidates must pass either a single-electron, single-muon,  $e\mu$ ,  $e\tau_h$ , or  $\mu\tau_h$  trigger selection. The single-muon,

$e\mu$  and  $\mu\tau_h$  triggers require the reconstructed muon to be isolated, while electron isolation is required for the single-electron,  $e\mu$  and  $e\tau_h$  triggers. Two  $e\mu$  dilepton triggers have been used for all data-taking years, having  $p_T$  thresholds of 23 (23) and 12 (8) GeV for the  $p_T$ -leading and -subleading lepton of the trigger in the case of electrons (muons). The single-muon and single-electron triggers with  $p_T$  thresholds of 22 and 25 GeV, respectively, are used for analyzing the 2016 data. The  $p_T$  thresholds of electron and  $\tau_h$  candidates are, respectively, 24 and 30 GeV for the  $e\tau_h$  dilepton trigger in the 2017–2018 data. For the  $\mu\tau_h$  dilepton trigger, the  $p_T$  thresholds of muon and  $\tau_h$  are, respectively, 19 (20) and 20 (27) GeV for the data taken during 2016 (2017–2018). The increase in the  $p_T$  threshold is necessary to control the trigger rate at a larger instantaneous luminosity. Similarly, the  $p_T$  requirements are tightened for single-lepton triggers across the years. This results in two different thresholds for single-electron and muon triggers for 2017–2018.

Offline, in the  $\mu\mu bb$  channel events are required to have two muons and at least two b jets passing the kinematic, identification, and isolation criteria detailed in Section 4. While the final search in this channel is performed for  $m_{a_1}$  between 15 and 62.5 GeV, events are selected with a dimuon invariant mass,  $m_{\mu\mu}$ , between 14 and 70 GeV. The additional sidebands in  $m_{\mu\mu}$  help model the backgrounds at the boundaries. To reduce the background contribution from  $t\bar{t}+jets$ , events with  $p_T^{\text{miss}} > 60 GeV are rejected. The selection yields a total of 109 821 data events while the corresponding expected yield from simulated backgrounds is  $103\,900 \pm 7300$ . The background contribution should be compared with about 80–100 expected signal events, depending on  $m_{a_1}$ , from both ggF and VBF Higgs boson production. The branching fraction  $\mathcal{B}(a_1 a_1 \rightarrow \mu\mu bb)$  is evaluated in the Type III model with  $\tan\beta = 2$ . Figure 1 shows, in data and simulation, the  $p_T$  distributions of the  $p_T$ -leading and -subleading muons and b jets. Although the estimation of backgrounds in this analysis does not rely on simulation, the observed level of agreement between data and simulation justifies the use of simulated events to optimize the sensitivity. Figure 2 shows distributions for the  $p_T$  of the dimuon ( $p_T^{\mu\mu}$ ) and the di-b-jet systems ( $p_T^{bb}$ ).$

To further suppress backgrounds, a  $\chi^2_{\text{tot}}$  variable is defined as  $\chi^2_{\text{tot}} = \chi^2_{bb} + \chi^2_H$ . It examines the compatibility of  $m_{\mu\mu}$  and  $m_{bb}$  with  $m_{a_1}$ , and of  $m_{\mu\mu bb}$  with the Higgs boson mass in signal events. The components of  $\chi^2_{\text{tot}}$  are defined as

$$\chi_{bb} = \frac{(m_{bb} - m_{\mu\mu})}{\sigma_{bb}} \quad \text{and} \quad \chi_H = \frac{(m_{\mu\mu bb} - 125 \text{ GeV})}{\sigma_H}. \quad (1)$$

The variables  $\sigma_{bb}$  and  $\sigma_H$  are the mass resolutions of the di-b-jet system and the Higgs boson candidate, respectively, which are derived from Gaussian fits to simulated distributions of  $m_{bb}$  and the mass of the Higgs boson candidate. While  $\sigma_H$  is found to be constant,  $\sigma_{bb}$  increases linearly with  $m_{a_1}$  and is modeled as a function of  $m_{\mu\mu}$  ( $\sigma_{bb} = am_{\mu\mu} + b$ ), assuming  $m_{\mu\mu} = m_{a_1}$ . The  $\chi^2_{\text{tot}}$  variable is evaluated on an event-by-event basis. It was shown in Ref. [23] that applying a threshold on  $\chi^2_{\text{tot}}$  leads to a large suppression of backgrounds while keeping the majority of signal events. Such a requirement translates to a circle centered at zero in the 2D-plane of  $\chi_{bb}$  and  $\chi_H$ , as shown in Fig. 3. However, the  $\chi_{bb}$  and  $\chi_H$  components are clearly correlated as can be seen in Fig. 3 (right). This leads to a loss of signal efficiency when imposing the circular requirement. In addition, both  $\chi_{bb}$  and  $\chi_H$  distributions are slightly biased away from zero, adding more inefficiencies. Therefore, in the current analysis the definitions of the variables were adjusted to be unbiased and uncorrelated.

The correlation between the  $\chi_{\text{tot}}$  components, as well as their bias, depends on  $m_{a_1}$ . The bias

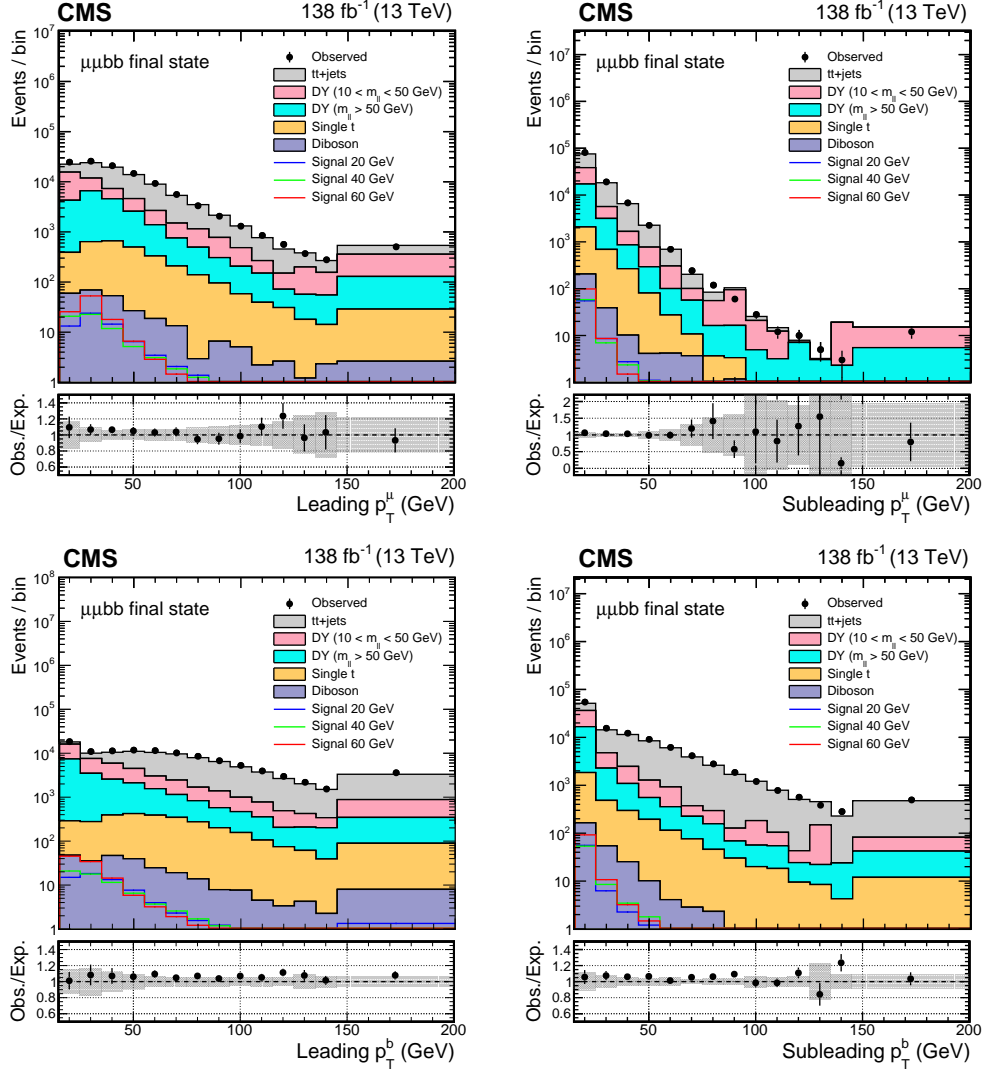


Figure 1: The distributions of leading and subleading (upper) muon  $p_T$  and (lower) b jet  $p_T$  in the selected events. The uncertainty band in the lower panel represents the limited size of the simulated samples together with a 30% uncertainty in the low-mass DY cross section. Simulated samples are normalized using the corresponding theoretical cross sections. To evaluate the normalization of the signal, SM Higgs boson cross sections are multiplied by the  $\mathcal{B}(a_1 a_1 \rightarrow \mu\mu bb)$  value that is calculated in the Type III model with  $\tan \beta = 2$ .

is modeled as a function of  $m_{\mu\mu}$  and is corrected event by event. After applying this correction, a principal component analysis [73] is performed on the bias-corrected variables. The bias-corrected variables are therefore transformed using the eigenvalues,  $\lambda_1$  and  $\lambda_2$ , and eigenvectors  $\begin{pmatrix} a \\ b \end{pmatrix}$ , of the correlation matrix:

$$\begin{pmatrix} \chi_H \\ \chi_{bb} \end{pmatrix}_d = \begin{pmatrix} \frac{a}{\sqrt{\lambda_1}} & \frac{b}{\sqrt{\lambda_1}} \\ \frac{-b}{\sqrt{\lambda_2}} & \frac{a}{\sqrt{\lambda_2}} \end{pmatrix} \begin{pmatrix} \chi_H \\ \chi_{bb} \end{pmatrix}_c, \quad (2)$$

$$\chi_d^2 \equiv \chi_{H,d}^2 + \chi_{bb,d}^2$$

with subscripts  $d$  and  $c$ , respectively, standing for decorrelated and bias-corrected components of  $\chi_{\text{tot}}$ . The transformation matrix in Eq. (2) has three independent parameters,  $a/\sqrt{\lambda_1}$ ,  $a/\sqrt{\lambda_2}$ ,

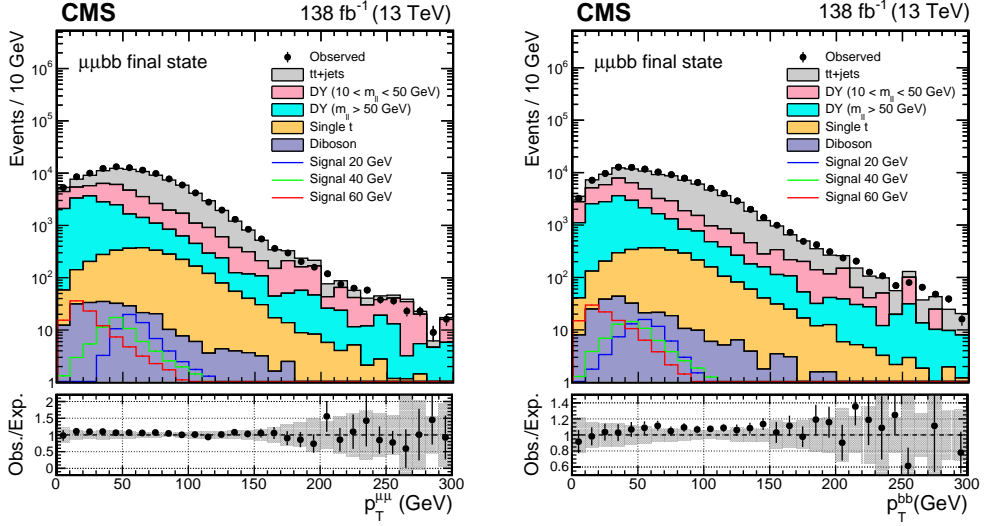


Figure 2: The  $p_T$  distributions of the (left) dimuon systems and (right) di-b-jet system. The uncertainty band in the lower panel represents the limited size of the simulated samples together with a 30% uncertainty in the low-mass DY cross section. Simulated samples are normalized to using the corresponding theoretical cross sections. To evaluate the normalization of the signal, SM Higgs boson cross sections are multiplied by the  $\mathcal{B}(a_1 a_1 \rightarrow \mu\mu bb)$  value that is calculated in the Type III model with  $\tan \beta = 2$ .

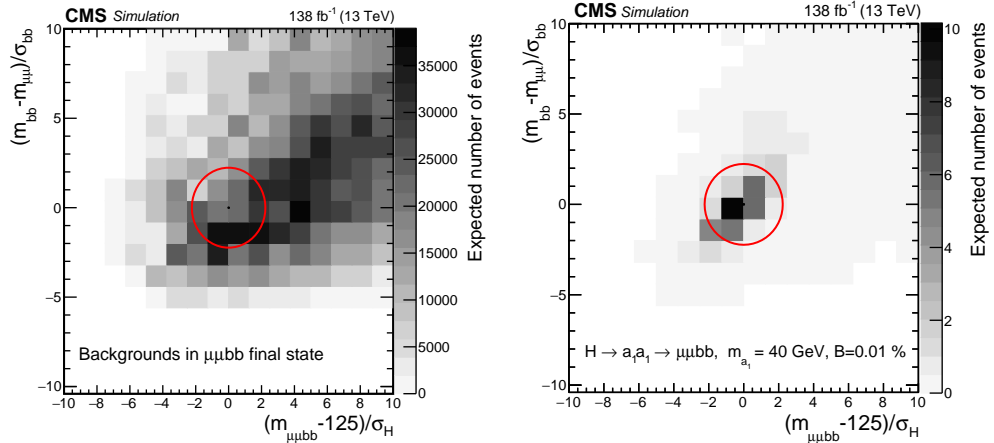


Figure 3: The distribution of  $\chi_{bb}$  versus  $\chi_H$  as defined in Eq. (1) for (left) simulated background processes and (right) the signal process with  $m_{a_1} = 40$  GeV. The contours indicate lines of constant  $\chi^2_{\text{tot}}$ . The gray scale represents the expected yields in data. To evaluate the yield of the signal, SM Higgs boson cross sections are multiplied by the  $\mathcal{B}(a_1 a_1 \rightarrow \mu\mu bb)$  value that is calculated in the Type III model with  $\tan \beta = 2$ .

and  $b/a$ , that are modeled as functions of  $m_{a_1}$ . Figure 4 compares the performance of the selection based on  $\chi_d^2$  and  $\chi_{\text{tot}}^2$  variables in terms of the signal ( $m_{a_1} = 40$  GeV) efficiency and background rejection probability. Based on the optimization studies, events with  $\chi_d^2 < 1.5$  are selected.

Table 2 summarizes the number of observed events in data together with the expected yields for the main backgrounds and the signal for different  $m_{a_1}$  hypotheses.

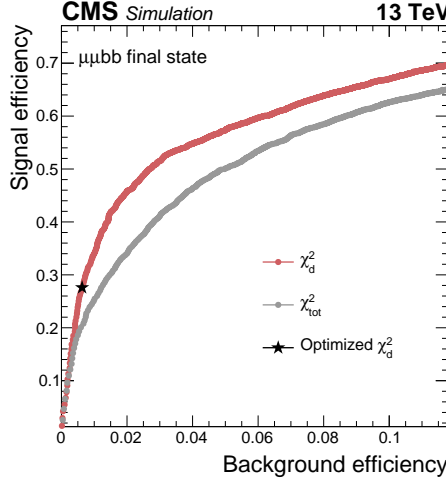


Figure 4: Signal ( $m_{a_1} = 40 \text{ GeV}$ ) versus background efficiency for different thresholds on  $\chi^2_{\text{tot}}$  (gray) and  $\chi^2_d$  (red) variables. The black star indicates signal efficiency versus that of background for the optimized  $\chi^2_d$  requirement.

Table 2: Event yields in the  $\mu\mu\text{bb}$  channel for simulated processes and the number of observed events in data after applying  $\chi^2_d < 1.5$ . The expected number of simulated events is normalized to the integrated luminosity of  $138 \text{ fb}^{-1}$ . The Type III parametrization of 2HDM+S with  $\tan \beta = 2$  is used to evaluate  $\mathcal{B}(a_1 a_1 \rightarrow \mu\mu\text{bb})$ .

Process	Yield
tt+jets	$86.3 \pm 2.2$
DY ( $10 < m_{\ell\ell} < 50 \text{ GeV}$ )	$289.6 \pm 89.5$
DY ( $m_{\ell\ell} > 50 \text{ GeV}$ )	$200.2 \pm 31.9$
Diboson	$1.5 \pm 0.9$
Single top	$11.4 \pm 1.6$
Total expected background	$589.1 \pm 95.1$
Data	641
<hr/>	
Signal for ggH ( $\mu\mu\text{bb}$ )	
$m_{a_1} = 20 \text{ GeV}$	$m_{a_1} = 40 \text{ GeV}$
$15.4 \pm 0.2$	$18.7 \pm 0.2$
	$m_{a_1} = 60 \text{ GeV}$
	$40.5 \pm 0.3$

Events are further categorized according to the jet  $p_T$ , the b tagging score of the jets, and additional jet activity in the event compatible with the VBF signature. Events containing at least one of the two selected b jets with  $p_T < 20 \text{ GeV}$  are put in a separate category (Low  $p_T$ ). This category brings extra sensitivity to the signals with lower  $m_{a_1}$  values and contains about 70% (40%) background (ggF signal) events. For the VBF category, events must have at least two jets, in addition to b jets, with  $p_T > 30 \text{ GeV}$ ,  $|\eta| < 4.7$ , and an invariant mass  $m_{jj} > 250 \text{ GeV}$ . About 50% of VBF signal events fall in this category. The remaining events are categorized based on the b tagging score of the looser b jet. Three exclusive categories are defined where the second jet passes the loose but fails the medium (TL), passes the medium but fails the tight (TM), and passes the tight (TT) b tagging working point. This categorization relies on the fact that events with genuine and misidentified b quark jets are distributed differently among those categories. About 20% of backgrounds as well as the ggF signal events fall into the TL category. The TM and TT categories almost equally receive 20% of the ggF signal and 5% of the background

events. Table 3 summarizes the categories of the current analysis, whereas the expected yields in different categories are presented in Table 4.

Table 3: Summary of the categorization requirements in the  $\mu\mu bb$  channel. Events in these categories contain two muons and two b jets. As stated in the text, L, M, and T stand for the loose, medium, and tight b tagging criteria, respectively.

Categories for selected events		
Low $p_T$	At least one b jet with $p_T < 20 \text{ GeV}$	
VBF	Two additional jets with $p_T > 30 \text{ GeV}$ , $ \eta  < 4.7$ , and $m_{jj} > 250 \text{ GeV}$	
TL	Looser b jet passes L but fails M	
TM	Looser b jet passes M but fails T	
TT	Looser b jet passes T	

Table 4: The expected yields for backgrounds and different signal hypotheses in each category of the  $\mu\mu bb$  channel.

Category	Signal for ggH ( $\mu\mu bb$ )			Expected background
	$m_{a_1} = 20 \text{ GeV}$	$m_{a_1} = 40 \text{ GeV}$	$m_{a_1} = 60 \text{ GeV}$	
Low $p_T$	$7.4 \pm 0.1$	$7.3 \pm 0.1$	$17 \pm 0.2$	$421 \pm 88$
VBF	$0.2 \pm (<0.1)$	$1.0 \pm (<0.1)$	$1.1 \pm 0.4$	$5 \pm 2$
TL	$2.1 \pm 0.1$	$2.8 \pm 0.1$	$6.7 \pm 0.1$	$109 \pm 30$
TM	$2.7 \pm 0.1$	$3.3 \pm 0.1$	$7.7 \pm 0.1$	$27 \pm 15$
TT	$2.8 \pm 0.1$	$4.2 \pm 0.1$	$8.1 \pm 0.1$	$28 \pm 11$
Total	$15.4 \pm 0.2$	$18.7 \pm 0.2$	$40.5 \pm 0.3$	$589 \pm 95$

In the  $\tau\tau bb$  channel, the offline signal event signature constitutes at least one b jet, and depending on the  $\tau$  lepton decay mode, an  $e\mu$ , an  $e\tau_h$ , or a  $\mu\tau_h$  pair. Any event with an additional electron or muon is rejected to reduce the contribution from DY and multilepton processes. The selection and identification requirements for all objects are discussed in Section 4.

Each final state is subdivided into two categories based on the presence of exactly one b jet or at least two b jets in the event. Requiring at least two b jets in the event introduces an additional category compared to Ref. [25], capable of reconstructing the full signal hypothesis and bringing further signal-to-background discrimination power. In total there are six event categories, considering the number of b jets and the decay modes of the  $\tau$  leptons. A deep neural network (DNN) with two hidden layers and 40 nodes is used to discriminate signal from background events in each category. The DNNs are trained using simulated events.

Kinematic properties of the decay products are utilized to construct variables that are inputs to the DNN training, such as the  $p_T$  and transverse mass ( $m_T$ ) of the leptons and b jets,  $p_T$  and  $\eta$  of the di- $\tau$  system, the invariant mass of each system made of a lepton and a b jet, and  $\Delta R$  between various combinations of the identified particles. One of the most important discriminating observables used in the training is the invariant mass of the decay products of the  $\tau$  leptons and the  $p_T$ -leading b jet, denoted by  $m_{b\tau\tau}$ . The  $m_{b\tau\tau}$  value is typically smaller for signal than for background events. Similarly, angular separation and other invariant mass variables can be reconstructed with different combinations of the four final-state particles, employing the

correlation between the resonance decay products. The  $m_T$  between an e or  $\mu$  and  $p_T^{\text{miss}}$  is one of the discriminating variables and is defined as

$$m_T(e/\mu, p_T^{\text{miss}}) \equiv \sqrt{2p_T^{e/\mu} p_T^{\text{miss}} [1 - \cos(\Delta\phi)]}, \quad (3)$$

where  $p_T^{e/\mu}$  is the transverse momentum of the lepton and  $\Delta\phi$  is the azimuthal angle between the lepton direction and  $\vec{p}_T^{\text{miss}}$ . Events from tt+jets and misidentified  $\tau_h$  backgrounds, such as W+jets, have larger  $p_T^{\text{miss}}$ , thus result in higher  $m_T$  values.

Another variable useful in the training is  $D_\zeta$ , defined as

$$D_\zeta \equiv p_\zeta - 0.85p_\zeta^{\text{vis}}, \quad (4)$$

where the bisector of the directions of the visible  $\tau$  decay products transverse to the beam direction is denoted as the  $\zeta$  axis. The quantity  $p_\zeta$  is defined as the component of the  $\vec{p}_T^{\text{miss}}$  along the  $\zeta$  axis, and  $p_\zeta^{\text{vis}}$  to be the sum of the components of the lepton transverse momentum along the same direction [74]. The  $Z \rightarrow \tau\tau$  background corresponds to large  $D_\zeta$  values because the  $p_T^{\text{miss}}$  is approximately collinear to the  $\tau\tau$  system. The tt+jets events tend to have small  $D_\zeta$  values due to a large  $p_T^{\text{miss}}$  that is not aligned with the  $\tau\tau$  system. The signal has intermediate  $D_\zeta$  values because the  $p_T^{\text{miss}}$  is approximately aligned with the  $\tau\tau$  system, but its magnitude is small.

For events in the category with two or more b jets, a variable can be constructed to measure the difference between the invariant mass of the two b jets and the invariant mass of the  $\tau\tau$  system ( $m_{\tau\tau}$ ):

$$\Delta m_{a_1} \equiv (m_{bb} - m_{\tau\tau})/m_{\tau\tau}. \quad (5)$$

This variable is of particular interest since it peaks at zero for signal events. The  $m_{\tau\tau}$  distribution reconstructed with the SVfit algorithm [75] is used to test the presence of signal, and thus is not directly included as an input to the DNN.

Figure 5 shows, as an example, the DNN score distributions in the  $\mu\tau_h$  channel separated for events with one or at least two b jets. The distributions are obtained by comparing the estimated signal and background distributions of the DNN score to that of the data before the fit described in Section 7 (pre-fit).

In each category, subregions are defined using a threshold on the DNN score. The expected limits are scanned by varying the DNN thresholds to obtain the highest sensitivity to the simulated signal. This optimization method also ensures that the expected number of background events in each subregion is large enough to perform the final likelihood fit of the  $m_{\tau\tau}$  distribution. There are three SRs for events containing one b jet: SR1, SR2, and SR3, whereas events with two b jets are divided into two categories: SR1 and SR2. The only exception is the  $e\tau_h$  final state in the two-b-jet category where no significant gain was observed when adding a second signal region. The remaining subregion containing events with the lowest DNN scores is used as a control region (CR) to constrain various background normalizations in the final likelihood fit.

## 6 Background estimation

The presence of a  $\mu\mu bb$  signal is expected to appear as a peak over the  $m_{\mu\mu}$  distribution centered at  $m_{a_1}$ . The background shape and its normalization in this channel are collectively determined from data with no reference to simulation. Different parameterizations of polynomials

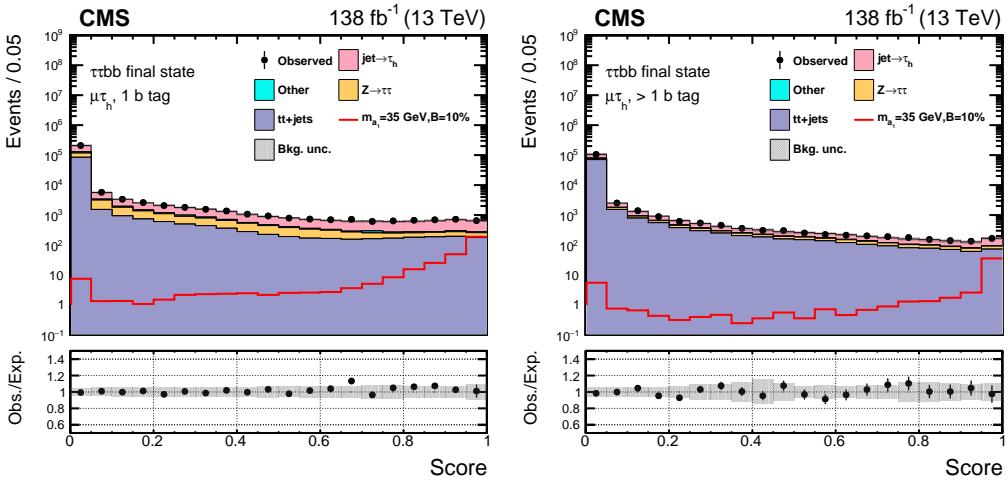


Figure 5: Pre-fit distributions of the DNN score for the  $\mu\tau_h$  channel divided into events with one (left) or at least two (right) b jets. The shape of the  $H \rightarrow a_1 a_1$  signal, where  $m_{a_1} = 35$  GeV, is indicated assuming  $\mathcal{B}(H \rightarrow a_1 a_1 \rightarrow \tau\tau bb)$  to be 10%. The lower panel shows the ratio of the observed data to the expected yields. The gray band represents the unconstrained statistical and systematic uncertainties.

are used to model the  $m_{\mu\mu}$  distribution in data of every category, separately. For each group of models, a maximum degree of the polynomial, determined through statistical tests, is imposed. This is to ensure that the data are not overfit. Parameters of every selected model vary within their uncertainties in the final fit to extract the signal strength, defined as the ratio of the observed signal rate to that predicted by the SM. The latter uses the discrete profiling method [76–78] where every functional form of the selected background models is treated as a discrete nuisance parameter. Along with the determination of the signal strength, one of the background models, its parameters, and the corresponding normalization are determined by the fit, as described in Section 7.

A major background contribution to the  $\tau\tau bb$  channel is  $Z \rightarrow \tau\tau$ , which is estimated from data using an embedding technique [79]. The method is based on the reconstruction of  $Z \rightarrow \mu\mu$  events in data where the muons are replaced with simulated  $\tau$  leptons with the same kinematic properties. In comparison with the simulation of the  $Z \rightarrow \tau\tau$  process, this technique allows a more accurate description of variables related to  $p_T^{\text{miss}}$  and jet activity. The embedded sample also estimates other SM processes with two genuine  $\tau$  leptons, such as  $tt+jets$  and Diboson.

The QCD multijet contribution to the  $e\mu$  final state of the  $\tau\tau bb$  channel is estimated using the data in a sideband (SB) region with same-sign  $e\mu$  pairs. The event selection in the SB region is otherwise identical to that in the  $e\mu$  SRs. The contributions of other processes in the SB are taken from simulation and subtracted from the data. The resulting number of data events in the SB is scaled by the ratio of the expected multijet contribution in the SR to the expected multijet contribution in the SB. Scale factors are calculated in data orthogonal to the SR, as functions of the jet multiplicity and the  $\Delta R$  separation between the electron and the muon, in order to account for possible kinematic differences between the two regions.

Backgrounds with hadronic jets that are misidentified as  $\tau_h$  candidates contribute significantly to  $e\tau_h$  and  $\mu\tau_h$  final states and are estimated from data. This background includes the  $W+jets$ , QCD multijets, and  $tt+jets$  processes with at least one top quark decaying to hadrons. In a data sideband region, events are required to pass all the baseline  $e\tau_h/\mu\tau_h$  selection criteria, but fail the  $\tau_h$  isolation. The data in this SB are reweighted with a factor  $f/(1-f)$ , where  $f$  is the

probability for a jet to be misidentified as a  $\tau_h$  candidate and is evaluated as a function of the  $p_T(\tau_h)$ . The  $Z \rightarrow \mu\mu + \text{jets}$  events in data are used to measure the misidentification probability. The final state must contain a dimuon pair compatible with the decay of the  $Z$  boson, as well as a  $\tau_h$  candidate. Simulation is used to subtract from data the contribution from events with a genuine  $\tau_h$  lepton. The measurement is done separately for the  $e\tau_h$  and  $\mu\tau_h$  final states. This is because the antilepton discrimination working points in the  $\tau_h$  identification change depending on the lepton selected is an electron or a muon [71]. The difference between the two fake rate measurements is observed to be around 10%. The misidentification probability also depends on the jet multiplicity, which characterizes the hadronic activity in the event.

Another dominant background is  $t\bar{t} + \text{jets}$ , which has to be carefully estimated from simulation. Because  $t\bar{t} + \text{jets}$  events with two genuine  $\tau$  leptons in the final state are an irreducible contribution to the embedded sample described above, the  $t\bar{t} + \text{jets}$  background estimate from simulation described here does not include these events. It also does not include  $t\bar{t} + \text{jets}$  events in which a reconstructed  $\tau_h$  candidate arises from a simulated jet, as the estimation of the misidentified  $\tau_h$  background is derived from data SBs, as described above. The normalization of backgrounds is free to vary within a range limited by the a priori uncertainty estimates in the final fit for the signal extraction.

The presence of a  $\tau\tau bb$  signal is expected to appear as a peak over the  $m_{\tau\tau}$  distribution centered at  $m_{a_1}$ . A fit to the  $m_{\tau\tau}$  distribution is performed simultaneously in the SRs and CRs described in Section 5.

## 7 Signal extraction

In the  $\mu\mu bb$  final state, an unbinned maximum likelihood fit to the data  $m_{\mu\mu}$  distributions is carried out simultaneously in all event categories. The fit is performed in the range  $15 < m_{\mu\mu} < 62.5 \text{ GeV}$ , using parametric models for signal and background. The parametric model of the signal is a weighted sum of a Voigt profile and a Crystal Ball (CB) function [80], where the mean values of the two are constrained to be identical [23].

Simulated samples are used to determine the parameters of the signal model that may depend on  $m_{a_1}$ . The studies are performed separately on signal samples simulated for different years. This is to account for the effect of muon reconstruction details on the signal model in different data-taking periods. Most of the parameters are found to be independent of  $m_{a_1}$  and fixed in the final fit. Only the resolutions of the Voigt profile and CB function demonstrate linear variation with the pseudoscalar mass. The slope of the linear models are floating parameters in the signal extraction fit. In each category, contributions from different years are normalized considering the signal selection efficiency and acceptance, and are used to construct the expected signal distribution in data. The expected signal efficiency and acceptance are interpolated for  $m_{a_1}$  values not covered by simulation.

To evaluate the background contribution, every selected functional form is treated as a discrete nuisance parameter as discussed earlier. In addition, the parameters of every model, as well as the normalization, are part of the background parameter space. A likelihood  $\mathcal{L}$  is constructed using the signal and the background models in all categories, including systematic uncertainties associated with the signal, as nuisance parameters. In the minimization process of the negative logarithm of the likelihood, the discrete profiling method chooses a best fit background model as the physics parameter of interest, the signal strength, varies. The method incorporates the systematic uncertainty in the background model by taking the envelope of the models

provided to the fit.

In practice, a penalty term is added to the likelihood to account for the number of free parameters in the final background model. The penalized likelihood,  $\tilde{\mathcal{L}}$ , is a function of the measured signal strength,  $\mu$ , the continuous nuisance parameters,  $\vec{\theta}$ , and the background models,  $\vec{b}$ . The penalized likelihood ratio is defined as

$$-2 \ln \frac{\tilde{\mathcal{L}}(\text{data}|\mu, \hat{\theta}_\mu, \hat{b}_\mu)}{\tilde{\mathcal{L}}(\text{data}|\hat{\mu}, \hat{\theta}, \hat{b})}, \quad (6)$$

with the numerator being the maximum  $\tilde{\mathcal{L}}$  for a given  $\mu$  at the best fit values of nuisance parameters and background functions. The denominator is the global maximum of  $\tilde{\mathcal{L}}$ , obtained at  $\mu = \hat{\mu}$ ,  $\theta = \hat{\theta}$ , and  $b = \hat{b}$ . The background function maximizing  $\tilde{\mathcal{L}}$  at any  $\mu$  is used to derive the confidence interval on  $\mu$  at any  $m_{a_1}$  [76]. It is verified that the fit is unbiased using studies where signals at several  $m_{a_1}$  values are injected with different strengths. The relative change in signal strength is found to be less than  $10^{-4}$ . The best fit background models together with their uncertainties are shown in Fig. 6 for all event categories in the  $\mu\mu\text{bb}$  analysis.

In the  $\tau\tau\text{bb}$  channel, a binned maximum likelihood fit is performed on the  $m_{\tau\tau}$  distribution with systematic uncertainties included as nuisance parameters. The subregions of event categories from all final states are included in a simultaneous fit. Figures 7–9 show the post-fit  $m_{\tau\tau}$  distributions in different subregions and categories for the  $\mu\tau_h$  final state.

The limits and confidence intervals are obtained using the modified frequentist  $\text{CL}_s$  approach [81, 82] with an asymptotic approximation to the distribution of the profile likelihood ratio test statistic [83]. Pseudoscalar masses between 12 and 60 GeV are considered using simulated samples described in Section 3.

The  $m_{\mu\mu}$  and  $m_{\tau\tau}$  expected distributions are compared to data in a combined fit, integrating over the  $a_1$  decay modes. Integrating over  $a_1$  decays makes the combination model dependent since the branching fraction of  $a_1$  to fermion pairs depends on the model. The 2HDM+S and the theoretical predictions of Ref. [84] are used for the branching fractions of  $a_1$  to muons,  $\tau$  leptons, and  $b$  quarks which are fixed in the fit. The selected events are mutually exclusive in the two analyses as events with an extra muon and/or electron are vetoed in the  $\tau\tau\text{bb}$  selection. A correlation model is employed between the two analyses for the systematic uncertainties that are in common.

## 8 Systematic uncertainties

The sensitivity of the two analyses,  $\mu\mu\text{bb}$  and  $\tau\tau\text{bb}$ , is mainly affected by the uncertainties arising from the finite size of the data sample. Nevertheless, several sources of systematic uncertainties are included in the determination of the results. Most of the systematic uncertainties are common between the two analyses, although their impact on the result may differ. In this class of uncertainties fall those associated with the modeling and acceptance of the signal, including the PDFs, the strong coupling constant, and the renormalization and factorization scales. In addition, experimental uncertainties associated with, e.g., the jet energy calibrations,  $b$  tagging, and muon reconstruction and identification are in common between the two analyses, although the uncertainties related to the background estimations are not. In the  $\mu\mu\text{bb}$  analysis, uncertainties associated with the parameters of the dimuon resonance model in the signal are taken into account.

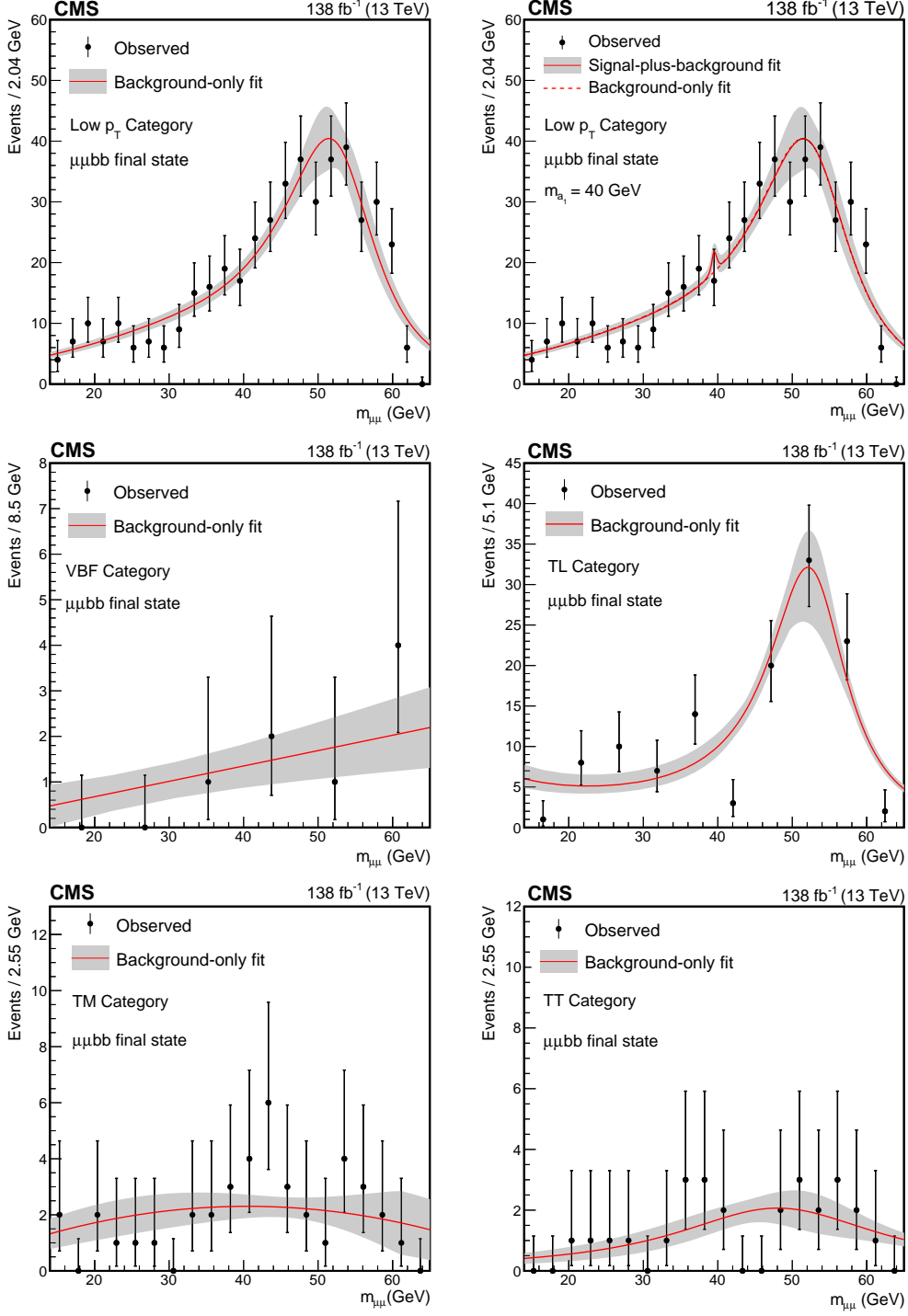


Figure 6: The best fit background models for the  $\mu\mu bb$  channel together with a 68% CL uncertainty band from the fit to the data under the background-only hypothesis for the (upper left) Low  $p_T$  category, (middle left) VBF category, (middle right) TL category, (lower left) TM category, and (lower right) TT category. For comparison, the signal-plus-background is shown for the (upper right) Low  $p_T$  category for a signal with  $m_{a_1} = 40$  GeV. The expected signal yield is evaluated assuming the SM production of the Higgs boson and a  $\mathcal{B}(a_1 a_1 \rightarrow \mu\mu bb)$  as predicted in the Type III 2HDM+S with  $\tan \beta = 2$ . The bin widths depend on statistics, irrelevant for the final fit.

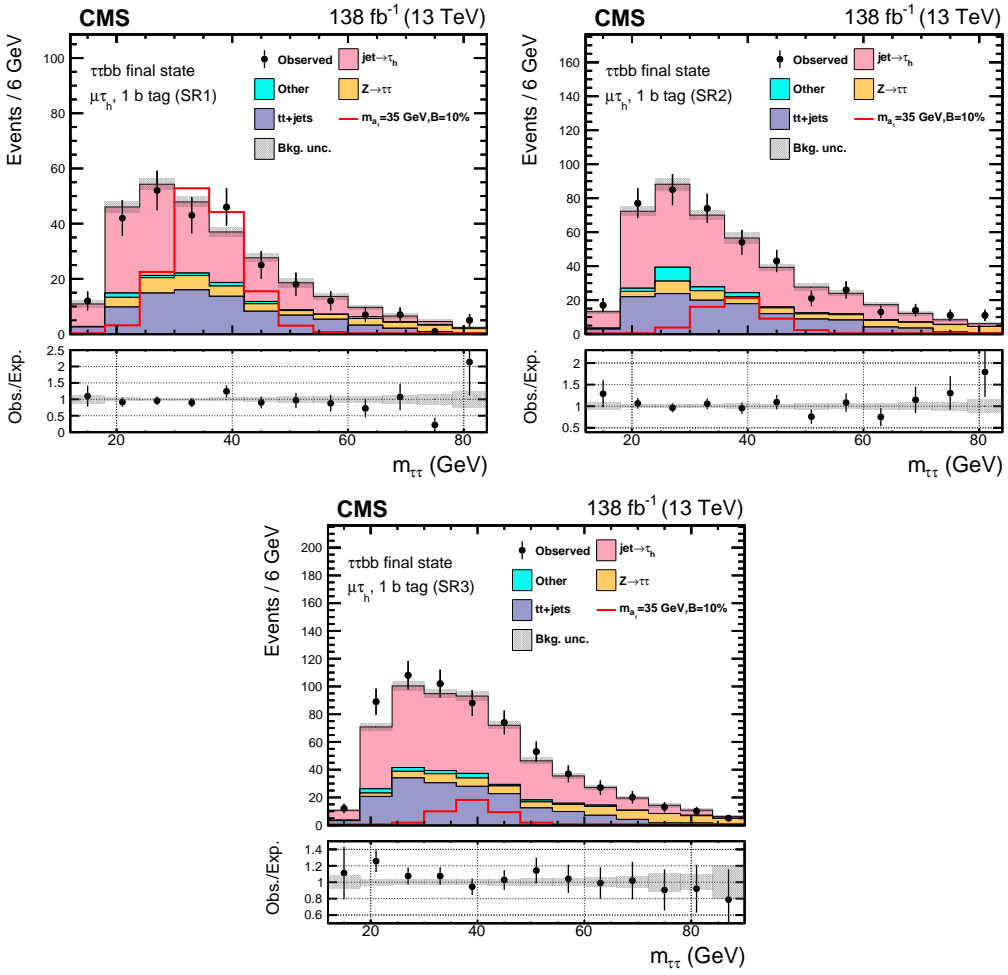


Figure 7: Post-fit distributions of  $m_{\tau\tau}$  for the  $\mu\tau_h$  channel signal regions in events with exactly one b tagged jet: SR1 (upper left), SR2 (upper right), and SR3 (lower). The shape of the  $H \rightarrow a_1 a_1$  signal, where  $m_{a_1} = 35$  GeV, is indicated assuming  $\mathcal{B}(H \rightarrow a_1 a_1 \rightarrow \tau\tau bb) = 10\%$ .

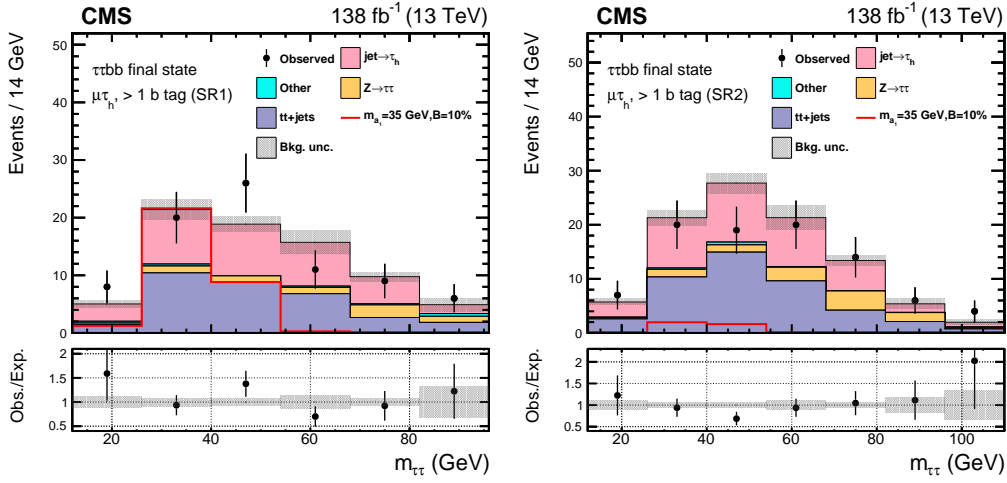


Figure 8: Post-fit distributions of the  $m_{\tau\tau}$  for the  $\mu\tau_h$  channel signal regions in events with at least two b tagged jets: SR1 (left) and SR2 (right). The shape of the  $H \rightarrow a_1 a_1$  signal, where  $m_{a_1} = 35$  GeV, is indicated assuming  $\mathcal{B}(H \rightarrow a_1 a_1 \rightarrow \tau\tau bb)$  to be 10%.

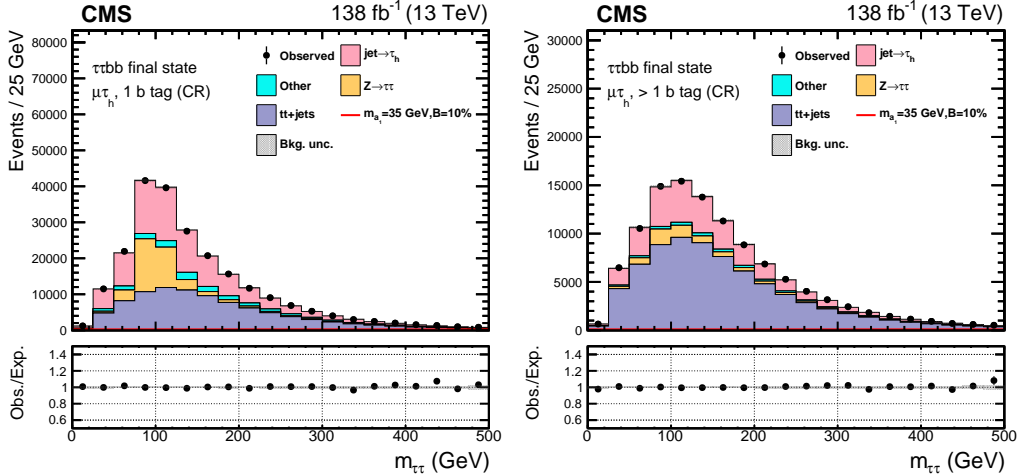


Figure 9: Post-fit distributions of the  $m_{\tau\tau}$  for the  $\mu\tau_h$  channel control regions in events with exactly one b tagged jet (left) and at least two b tagged jets (right). The contamination from the  $H \rightarrow a_1 a_1$  signal, where  $m_{a_1} = 35$  GeV, is barely visible assuming  $\mathcal{B}(H \rightarrow a_1 a_1 \rightarrow \tau\tau bb)$  to be 10%.

The unbinned maximum likelihood fit of the  $\mu\mu bb$  analysis accounts for the shape uncertainties in a different way. The impact of systematic variations is found to be negligible on the parametric model of the signal for all  $m_{a_1}$  hypotheses. On the other hand, the modeling of the  $m_{\mu\mu}$  resolution with  $m_{a_1}$  (discussed in Section 7) has an uncertainty that is included in the fit with a Gaussian profile. Uncertainties associated with the background model are evaluated by means of the discrete profiling method as described earlier and contribute to the statistical uncertainty of the result. Depending on the signal mass hypothesis, they constitute about 10–25% of the total uncertainty in the  $\mu\mu bb$  results. Contributions from uncertainties in the signal efficiency and acceptance are significantly smaller. In the following, details are provided for several sources of uncertainties.

All uncertainties are included as nuisance parameters in the final fit for the signal extraction. Uncertainties affecting the event yields in categories, i.e., normalization uncertainties, are as-

signed via multiplicative corrections, with a log-normal probability density function. In the binned maximum likelihood fit of the  $\tau\tau bb$  analysis, nuisance parameters that modify the shapes of the  $m_{\tau\tau}$  distributions are assumed to have a Gaussian profile. This means that for every nuisance parameter of this type, two alternate distributions are provided to the fit: one with the distribution resulting from an increase of the nuisance parameter by one standard deviation and the other with the distribution resulting from a decrease by one standard deviation. The dominant systematic uncertainty is found to be associated with the signal model, followed by the normalization of the QCD multijet background in the  $e\mu$  final state and the uncertainties in the  $t\bar{t}+jets$  cross section.

**Integrated luminosity:** the integrated luminosity of the data recorded by CMS for physics analyses is evaluated separately for different years of the Run 2 data taking [85–87]. The uncertainty in the measured integrated luminosity of a given year has a component that is uncorrelated across the years. It amounts to 1.0, 2.0, and 1.5%, for the 2016, 2017, and 2018 periods, respectively. Another component is correlated across all three years and is 0.6% in 2016, 0.9% in 2017, and 2.0% in 2018. Furthermore, the luminosity measurements in 2017–2018 have additional uncertainties, of 0.6 and 0.2%, respectively, that are considered correlated between the two years. The overall uncertainty in integrated luminosity for the 2016–2018 period is 1.6%.

**Pileup:** the uncertainty associated with the number of pileup interactions per bunch crossing is estimated by varying the total inelastic pp cross section by 4.6% [88], fully correlated across the years.

**ECAL timing shift:** during the 2016–2017 data-taking periods, a gradual shift in the timing of the ECAL L1 trigger inputs occurred in the forward endcap region,  $|\eta| > 2.4$  [89]. This led to a specific inefficiency due to erroneous association of detector readout to the previous bunch crossing in a small fraction of the collision events. A correction to this effect was determined using an unbiased data sample and found to be relevant in events containing high- $p_T$  jets with  $2.4 < |\eta| < 3.0$ . This correction is applied to simulation and is accompanied by a 20% uncertainty. The uncertainty predominantly affects the VBF category in the  $\mu\mu bb$  analysis, with a negligible effect on the results in this channel.

**Jet energy corrections:** the jet energy scale (JES) uncertainties include several sources parameterized as a function of the jet  $p_T$  and  $\eta$  [90]. Those variations can modify the content of the selected event sample. They also introduce event migration between categories. In the  $\mu\mu bb$  analysis, the event  $p_T^{\text{miss}}$  changes as a result of variations in the jet kinematics whereas in the  $\tau\tau bb$  analysis, JES uncertainties affect the  $m_{\tau\tau}$  distribution. Variations in the expected signal yield are between 15–50% in the  $\mu\mu bb$  analysis. In the  $\tau\tau bb$  channel, distributions vary between 10–15% of the nominal. Depending on the source, JES uncertainties are considered as uncorrelated, fully correlated, or partially correlated (50%) across the years. The jet energy resolution is also considered, where the smearing corrections are varied within their uncertainties, uncorrelated across the years.

**b tagging:** sources of systematic uncertainty that affect the data-to-simulation corrections of the b tagging discriminant distribution are JES, the light flavor or gluon (LF) jet contamination in the b jet sample, the heavy flavor (HF) jet contamination in the LF jet sample, and the statistical fluctuations in data and MC [68]. The JES variations in b tagging are obtained together with the JES uncertainties on jet kinematics and follow the same correlation pattern across the years. The statistical components of the b tagging uncertainties are uncorrelated while the rest are assumed correlated between different periods.

**Muon reconstruction:** the data-to-simulation correction factors for the muon tracking, recon-

struction and selection efficiencies are estimated using a “tag-and-probe” method [91] in DY data and simulated samples. These uncertainties include the pileup dependence of the correction factors and are correlated across the years since common procedural uncertainties are the dominant source. The requirements between the two analyses are slightly different, mainly because of a different impact parameter in  $\tau \rightarrow \mu$  decays. The corrections, and therefore associated systematic uncertainties, are applied in bins of muon  $p_T$  and  $|\eta|$  in the  $\mu\mu bb$  analysis [61]. In the  $\tau\tau bb$  analysis, a 2% uncertainty, independent of  $p_T$  and  $\eta$ , per muon is used [92] and treated as uncorrelated between simulated and  $\tau$ -embedded events. The muon momentum scale varies within 0.4–2.7% [61] and is accounted for in systematic uncertainties on the signal and background  $m_{\tau\tau}$  distribution. Its impact is found to be negligible in the  $\mu\mu bb$  analysis.

**Electron reconstruction:** the electron energy scale uncertainties in  $e\mu$  and  $e\tau_h$  final states are accounted for using methods outlined in Ref. [93]. The reconstruction and selection efficiencies are accompanied by a 2% uncertainty per electron, independent of  $p_T$  and  $\eta$  [62]. Similar to muons, these uncertainties are uncorrelated between simulated and  $\tau$ -embedded events. Uncertainties in the electron energy scale also affect the shapes of the  $m_{\tau\tau}$  distributions and are accounted for.

**Hadronically decaying  $\tau$  lepton reconstruction:** in  $\mu\tau_h$  and  $e\tau_h$  final states, there are uncertainties associated with  $\tau_h$  identification efficiencies and energy scale corrections where the variations depend on  $p_T(\tau_h)$  and decay mode, ranging from 3–5% and 0.2–1.1%, respectively. Systematic variations in the selected event yields as well as in the shapes of the distributions are taken into account. Uncertainties are considered uncorrelated across the bins of  $p_T(\tau_h)$  and different years for the MC [70]. Uncertainties of the same source are treated as 50% correlated between the embedded DY background and simulated samples. For events with a genuine  $\tau_h$  lepton matched at the generator level, energy scale uncertainties are considered using shape variations. In the case of muons and electrons misidentified as  $\tau_h$  candidates, energy scale corrections are applied in bins of  $p_T$ ,  $\eta$ , and decay mode of the misidentified  $\tau_h$ . These corrections are associated with uncertainties. A 50% correlation is considered between the embedded and MC samples for these lepton energy scale uncertainties.

**Trigger efficiencies:** an uncertainty of 1% is assigned to the HLT efficiency in the  $\mu\mu bb$  analysis. In the  $\tau\tau bb$  channel, an uncertainty of 2% is applied per single-lepton trigger and 5–10% on the dilepton triggers with a  $\tau_h$  requirement. Uncertainties associated with trigger efficiencies affect the shape of the distributions in this channel. The shape effects are taken into account in both simulated and embedded backgrounds, where a 50% correlation is considered between the two.

**Background estimations in  $\tau\tau bb$  final state:** the Z boson  $p_T$  reweighting uncertainty in DY samples, which amounts to 10% of the nominal value, is taken as a  $m_{\tau\tau}$  shape uncertainty. The embedded samples include a 4% normalization uncertainty [79]. Moreover, shape uncertainties related to tracking efficiencies and contamination from non-DY events in the embedded sample are considered. Since the contribution of the QCD multijet background in the  $e\mu$  channel is obtained from a same-sign sideband region with a limited number of events, the validity of the method is tested in independent same-sign SBs. This test results in a 20% normalization uncertainty. The uncertainty in the scale factor between the same-sign SBs and opposite-sign SRs is modeled using shape variations in the fit used to obtain the nominal values. The misidentification probability,  $f$ , of a jet as a  $\tau_h$  candidate depends on the jet multiplicity. A 20% normalization uncertainty is applied to the estimate of the W+jets and QCD multijet backgrounds due to  $f$  being measured in  $Z \rightarrow \mu\mu$  events with different jet multiplicities. In addition, shape variations due to different measurements of  $f$  are considered.

**Limited size of the samples:** to account for the limited size of the simulated samples, as well as the data in SBs used to estimate backgrounds, a bin-by-bin statistical uncertainty is considered where a Poisson nuisance parameter per bin is assigned to distributions in those samples [94]. This uncertainty is specific to the  $\tau\tau bb$  analysis.

**Modeling uncertainties:** a total uncertainty of 3.6% is assigned to the sum of the ggF and VBF Higgs boson production cross sections [20] predicted by the SM and used to describe the upper limits on  $\mathcal{B}(H \rightarrow a_1 a_1 \rightarrow \mu\mu bb/\tau\tau bb)$ . It includes uncertainties from the perturbative QCD calculations, PDFs, and  $\alpha_S$ . In the  $\tau\tau bb$  analysis, PDF and  $\alpha_S$  uncertainties are considered for simulated backgrounds, namely: 4.2% for  $t\bar{t}$ +jets, 5% for Diboson, and 5% for single top quark processes. These uncertainties are obtained following the PDF4LHC prescription [95]. To account for variations in the signal acceptance in both channels, the renormalization and factorization scales are doubled and halved simultaneously in simulation. In addition, the eigenvectors of the NNPDF3.1 PDF set are varied within their uncertainties in the final fit. The value of  $\alpha_S$ , computed at the energy scale of the Z boson mass, is also varied within its uncertainty in the PDF set. For the parton shower simulation, uncertainties are separately assessed for initial- and final-state radiation, by varying the respective scales up and down by factors of two. Using the same model assumptions and procedures, the aforementioned uncertainties are considered fully correlated across the data-taking years.

## 9 Results

No excess of events over the expected SM backgrounds is observed in either of the  $\mu\mu bb$  and  $\tau\tau bb$  channels. Upper limits are placed, at 95% CL, on  $\mathcal{B}(H \rightarrow a_1 a_1 \rightarrow \ell\ell bb)$  as a function of  $m_{a_1}$ , with  $\ell$  being either a  $\tau$  lepton or muon. The two final states are combined to set upper limits on  $\mathcal{B}(H \rightarrow a_1 a_1)$ , assuming fixed decay fractions of  $a_1$ . The branching fraction  $\mathcal{B}(a_1 \rightarrow ff)$  depends on the 2HDM+S parameters, where  $f$  indicates either muon, b quark, or  $\tau$  lepton. Since the results in both channels are statistically limited, the combination mostly benefits from the additional data. The combined results are still dominated by the statistical uncertainties. At  $m_{a_1} = 35$  GeV, all systematic uncertainties amount to about 6% of the total uncertainty, with the dominant contributions corresponding to JES in the  $\mu\mu bb$  channel, followed by the theoretical uncertainties in the signal, and finally the uncertainties in the QCD multijet backgrounds in the  $e\mu$  final state of the  $\tau\tau bb$  analysis.

Figure 10 shows the upper limits on  $\mathcal{B}(H \rightarrow a_1 a_1 \rightarrow \mu\mu bb)$  at 95% CL, assuming SM predictions for the Higgs boson production cross section. The  $\mu\mu bb$  search is optimized for  $m_{a_1}$  values between 15 and 60 GeV, with signal sensitivity falling rapidly below  $m_{a_1} = 20$  GeV. This is mainly because the two b jets start to merge as a result of a higher momentum for  $a_1$ . At 95% CL, the observed upper limits are  $(0.17\text{--}3.3) \times 10^{-4}$  for the mass range 15 to 62.5 GeV, while the expected limits are  $(0.35\text{--}2.6) \times 10^{-4}$ .

Figure 11 shows the observed and expected 95% CL upper limits on  $\mathcal{B}(H \rightarrow a_1 a_1 \rightarrow \tau\tau bb)$  as functions of  $m_{a_1}$ . Only the  $e\mu$  channel provides sensitivity to the 12 GeV mass point, as in this channel the baseline selection on the  $\Delta R$  between the two  $\tau$  candidates is the lowest. For small  $m_{a_1}$  values, the decay products appear as boosted and may not be reconstructed as two separate objects. The low  $\Delta R$  requirement allows a selection of more signal events where the two  $\tau$  candidates are close to each other. The  $\mu\tau_h$  final state is the most sensitive, where limits as low as around 1.8% (1.7%) are observed (expected) in the intermediate mass range at  $m_{a_1} = 35$  GeV. Combining all final states in the  $\tau\tau bb$  channel, observed limits on the branching

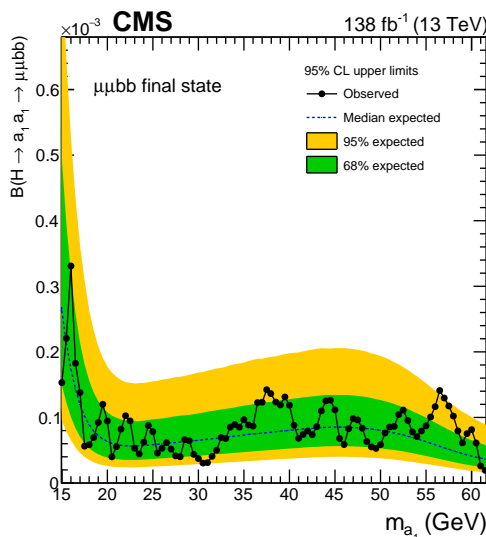


Figure 10: Observed and expected upper limits at 95% CL on  $\mathcal{B}(H \rightarrow a_1 a_1 \rightarrow \mu\mu bb)$  as functions of  $m_{a_1}$ . The inner and outer bands indicate the regions containing the distribution of limits located within 68 and 95% confidence intervals, respectively, of the expectation under the background-only hypothesis.

fraction are found to be in the range 1.7–7.7%, for a pseudoscalar mass between 12 and 60 GeV, with corresponding expected limits in the range 1.5–5.7% at 95% CL.

Figure 12 shows the observed and expected limits at 95% CL on  $\mathcal{B}(H \rightarrow a_1 a_1 \rightarrow \ell\ell bb)$ , where  $\ell$  stands for muons or  $\tau$  leptons. Using decay width expression from Ref. [84], the signal strength of each channel is scaled with a type and  $\tan\beta$  independent factor to obtain this limit in the context of 2HDM+S models. The observed and expected ranges are 0.6–7.7% and 0.8–5.7% respectively, depending on  $m_{a_1}$ .

The combined branching fraction  $\mathcal{B}(H \rightarrow a_1 a_1)$  is obtained upon reinterpretation of the  $\mu\mu bb$  and  $\tau\tau bb$  results in different types of 2HDM+S and  $\tan\beta$  values for  $15 < m_{a_1} < 60, illustrated in Fig. 13. Upper limits in the range 5–23% are observed at 95% CL for all Type II scenarios with  $\tan\beta > 1.0$ . The tightest constraint is obtained for the Type III scenario with  $\tan\beta = 2.0$ . At 95% CL, the observed upper limits on the combined branching fraction are in the range 1–7%, with a similar range for the expected upper limits. For the Type IV scenario, the observed upper limits on  $\mathcal{B}(H \rightarrow a_1 a_1)$  at 95% CL are between about 3 and 15% for  $\tan\beta = 0.5$ , with corresponding expected limits between about 3 and 11%.$

The allowed values of  $\tan\beta$  and  $m_{a_1}$  are shown in Fig. 14 in the context of Type III and Type IV 2HDM+S. The dashed contours represent the upper limits at 95% CL on Higgs boson to pseudoscalar decays, assuming the branching fraction to be either 100 or 16%. Here 16% corresponds to the combined upper limit on Higgs boson to BSM particle decays obtained from previous Run 2 results [15].

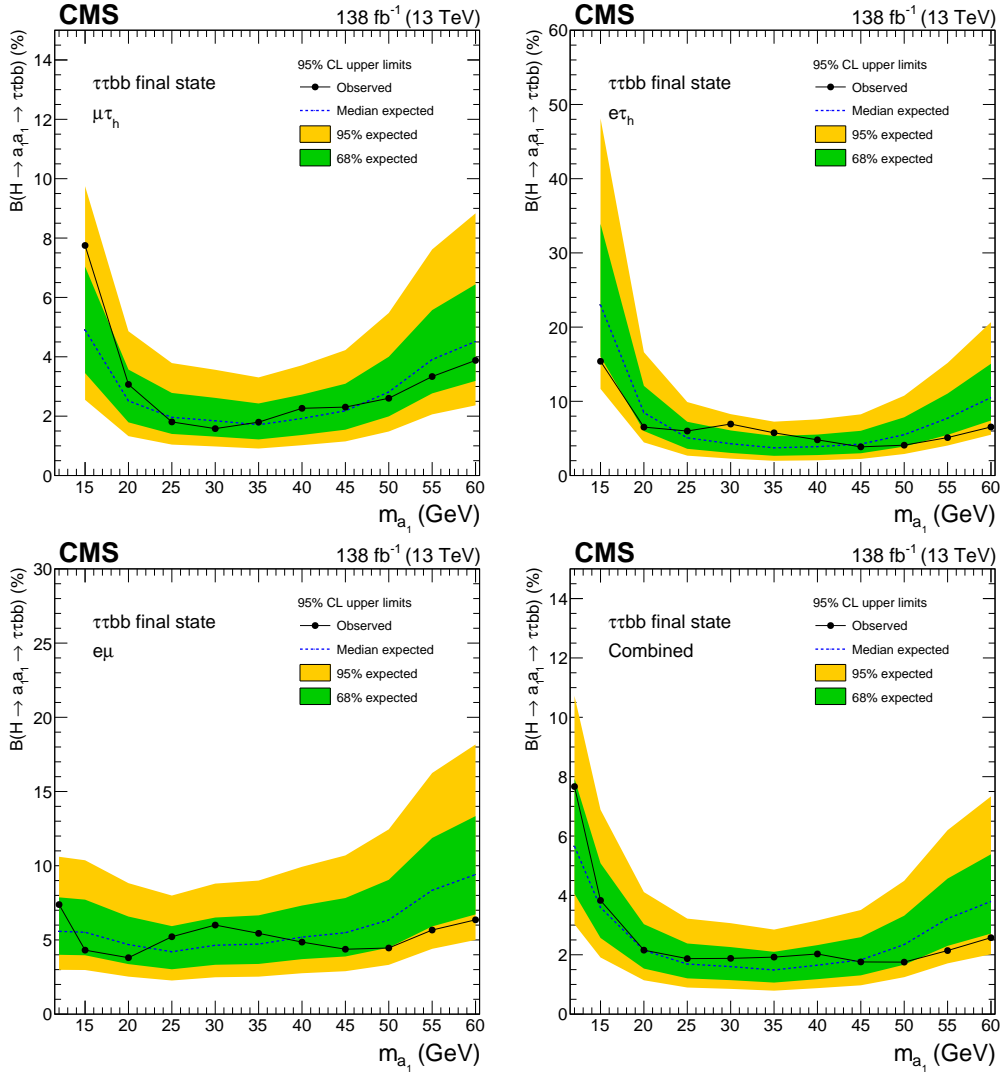


Figure 11: Observed and expected 95% CL exclusion limits on  $\mathcal{B}(H \rightarrow a_1 a_1 \rightarrow \tau\tau bb)$  in percent, for the (upper left)  $\mu\tau_h$ , (upper right)  $e\tau_h$ , (lower left)  $e\mu$  channels, and (lower right) for the combination of all the channels.

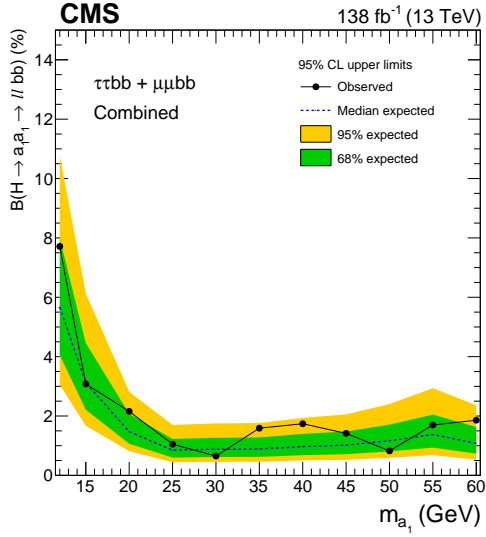


Figure 12: Observed and expected 95% CL upper limits on  $\mathcal{B}(H \rightarrow a_1 a_1 \rightarrow \ell\ell bb)$  in %, where  $\ell$  stands for muons or  $\tau$  leptons, obtained from the combination of the  $\mu\mu bb$  and  $\tau\tau bb$  channels. The results are obtained as functions of  $m_{a_1}$  for 2HDM+S models, independent of the type and  $\tan\beta$  parameter.

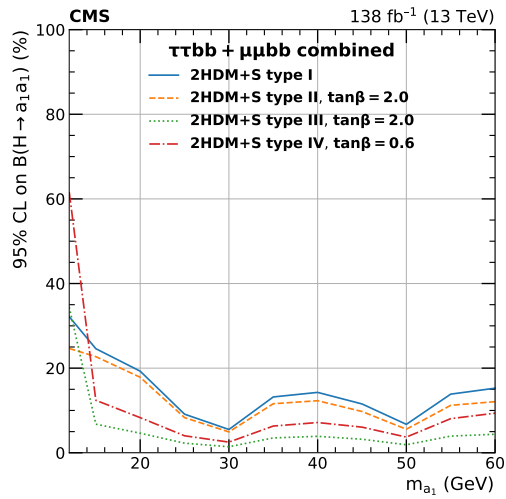


Figure 13: Observed and expected 95% CL upper limits on  $\mathcal{B}(H \rightarrow a_1 a_1)$  in %, obtained from the combination of the  $\mu\mu bb$  and  $\tau\tau bb$  channels. The results are obtained as functions of  $m_{a_1}$  for 2HDM+S Type I (independent of  $\tan\beta$ ), Type II ( $\tan\beta = 2.0$ ), Type III ( $\tan\beta = 2.0$ ), and Type IV ( $\tan\beta = 0.6$ ), respectively.

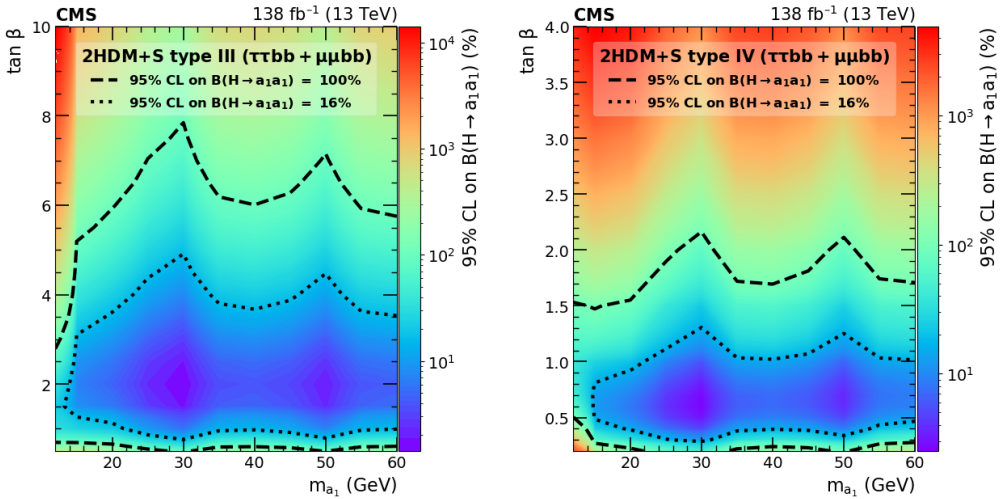


Figure 14: Observed 95% CL upper limits on  $\mathcal{B}(H \rightarrow a_1 a_1)$  in %, for the combination of the  $\mu\mu bb$  and  $\tau\tau bb$  channels for Type III (left) and Type IV (right) 2HDM+S in the  $\tan \beta$  vs.  $m_{a_1}$  parameter space. The limits are calculated in a grid of 5 GeV in  $m_{a_1}$  and 0.1–0.5 in  $\tan \beta$ , interpolating the points in between. The contours corresponding to branching fractions of 100 and 16% are drawn using dashed lines, where 16% refers to the combined upper limit on Higgs boson to undetected particle decays from previous Run 2 results [15]. All points inside the contour are allowed within that upper limit.

## 10 Summary

A search for an exotic decay of the 125 GeV Higgs boson ( $H$ ) to a pair of light pseudoscalar bosons ( $a_1$ ) in the final state with two  $b$  quarks and two muons or two  $\tau$  leptons has been presented. The results are based on a data sample of proton-proton collisions corresponding to an integrated luminosity of  $138 \text{ fb}^{-1}$ , accumulated by the CMS experiment at the LHC during Run 2 at a center-of-mass energy of 13 TeV. Final states with at least one leptonic  $\tau$  decay are studied in the  $\tau\tau bb$  channel, excluding those with two muons or two electrons. The results show significant improvement, with respect to the earlier CMS analyses at 13 TeV, beyond what is merely expected from the increase in the size of the data sample. A more thorough analysis of the signal properties using a single discriminating variable improves the  $\mu\mu bb$  analysis, while the  $\tau\tau bb$  analysis gains from a deep neural network based signal categorization. No significant excess in the data over the standard model backgrounds is observed. Upper limits are set, at 95% confidence level, on branching fractions  $\mathcal{B}(H \rightarrow a_1 a_1 \rightarrow \mu\mu bb)$  and  $\mathcal{B}(H \rightarrow a_1 a_1 \rightarrow \tau\tau bb)$ , in the  $\mu\mu bb$  and  $\tau\tau bb$  analyses, respectively. Both analyses provide the most stringent expected limits to date. In the  $\mu\mu bb$  channel, the observed limits are in the range  $(0.17\text{--}3.3) \times 10^{-4}$  for a pseudoscalar mass,  $m_{a_1}$ , between 15 and 62.5 GeV. Combining all final states in the  $\tau\tau bb$  channel, limits are observed to be in the range 1.7–7.7% for  $m_{a_1}$  between 12 and 60 GeV. By combining the  $\mu\mu bb$  and  $\tau\tau bb$  channels, model-independent limits are set on the branching fraction  $\mathcal{B}(H \rightarrow a_1 a_1 \rightarrow \ell\ell bb)$ , where  $\ell$  stands for muons or  $\tau$  leptons. The observed upper limits range between 0.6 and 7.7% depending on the  $m_{a_1}$ . The results can also be interpreted in different types of 2HDM+S models. For  $m_{a_1}$  values between 15 and 60 GeV,  $\mathcal{B}(H \rightarrow a_1 a_1)$  values above 23% are excluded, at 95% confidence level, in most of the Type II scenarios. In Types III and IV, observed upper limits as low as 1 and 3% are obtained, respectively, for  $\tan\beta = 2.0$  and 0.5.

## Acknowledgments

We congratulate our colleagues in the CERN accelerator departments for the excellent performance of the LHC and thank the technical and administrative staffs at CERN and at other CMS institutes for their contributions to the success of the CMS effort. In addition, we gratefully acknowledge the computing centers and personnel of the Worldwide LHC Computing Grid and other centers for delivering so effectively the computing infrastructure essential to our analyses. Finally, we acknowledge the enduring support for the construction and operation of the LHC, the CMS detector, and the supporting computing infrastructure provided by the following funding agencies: SC (Armenia), BMBWF and FWF (Austria); FNRS and FWO (Belgium); CNPq, CAPES, FAPERJ, FAPERGS, and FAPESP (Brazil); MES and BNSF (Bulgaria); CERN; CAS, MoST, and NSFC (China); MINCIENCIAS (Colombia); MSES and CSF (Croatia); RIF (Cyprus); SENESCYT (Ecuador); ERC PRG, RVTT3 and MoER TK202 (Estonia); Academy of Finland, MEC, and HIP (Finland); CEA and CNRS/IN2P3 (France); SRNSF (Georgia); BMBF, DFG, and HGF (Germany); GSRI (Greece); NKFIH (Hungary); DAE and DST (India); IPM (Iran); SFI (Ireland); INFN (Italy); MSIP and NRF (Republic of Korea); MES (Latvia); LMTLT (Lithuania); MOE and UM (Malaysia); BUAP, CINVESTAV, CONACYT, LNS, SEP, and UASLP-FAI (Mexico); MOS (Montenegro); MBIE (New Zealand); PAEC (Pakistan); MES and NSC (Poland); FCT (Portugal); MESTD (Serbia); MCIN/AEI and PCTI (Spain); MOSTR (Sri Lanka); Swiss Funding Agencies (Switzerland); MST (Taipei); MHESI and NSTDA (Thailand); TUBITAK and TENMAK (Turkey); NASU (Ukraine); STFC (United Kingdom); DOE and NSF (USA).

Individuals have received support from the Marie-Curie program and the European Research Council and Horizon 2020 Grant, contract Nos. 675440, 724704, 752730, 758316, 765710, 824093, 101115353, and COST Action CA16108 (European Union); the Leventis Foundation; the Alfred P. Sloan Foundation; the Alexander von Humboldt Foundation; the Science Committee, project no. 22rl-037 (Armenia); the Belgian Federal Science Policy Office; the Fonds pour la Formation à la Recherche dans l'Industrie et dans l'Agriculture (FRIA-Belgium); the Agentschap voor Innovatie door Wetenschap en Technologie (IWT-Belgium); the F.R.S.-FNRS and FWO (Belgium) under the "Excellence of Science – EOS" – be.h project n. 30820817; the Beijing Municipal Science & Technology Commission, No. Z191100007219010 and Fundamental Research Funds for the Central Universities (China); the Ministry of Education, Youth and Sports (MEYS) of the Czech Republic; the Shota Rustaveli National Science Foundation, grant FR-22-985 (Georgia); the Deutsche Forschungsgemeinschaft (DFG), under Germany's Excellence Strategy – EXC 2121 "Quantum Universe" – 390833306, and under project number 400140256 - GRK2497; the Hellenic Foundation for Research and Innovation (HFRI), Project Number 2288 (Greece); the Hungarian Academy of Sciences, the New National Excellence Program - ÚNKP, the NKFIH research grants K 124845, K 124850, K 128713, K 128786, K 129058, K 131991, K 133046, K 138136, K 143460, K 143477, 2020-2.2.1-ED-2021-00181, and TKP2021-NKTA-64 (Hungary); the Council of Science and Industrial Research, India; ICSC – National Research Center for High Performance Computing, Big Data and Quantum Computing, funded by the EU NexGeneration program (Italy); the Latvian Council of Science; the Ministry of Education and Science, project no. 2022/WK/14, and the National Science Center, contracts Opus 2021/41/B/ST2/01369 and 2021/43/B/ST2/01552 (Poland); the Fundação para a Ciência e a Tecnologia, grant CEECIND/01334/2018 (Portugal); the National Priorities Research Program by Qatar National Research Fund; MCIN/AEI/10.13039/501100011033, ERDF "a way of making Europe", and the Programa Estatal de Fomento de la Investigación Científica y Técnica de Excelencia María de Maeztu, grant MDM-2017-0765 and Programa Severo Ochoa del Principado de Asturias (Spain); the Chulalongkorn Academic into Its 2nd Century Project Advancement Project, and the National Science, Research and Innovation Fund via the Program Management Unit for Human Resources & Institutional Development, Research and Innovation, grant B37G660013 (Thailand); the Kavli Foundation; the Nvidia Corporation; the SuperMicro Corporation; the Welch Foundation, contract C-1845; and the Weston Havens Foundation (USA).

## References

- [1] ATLAS Collaboration, "Observation of a new particle in the search for the Standard Model Higgs boson with the ATLAS detector at the LHC", *Phys. Lett. B* **716** (2012) 1, doi:10.1016/j.physletb.2012.08.020, arXiv:1207.7214.
- [2] CMS Collaboration, "Observation of a new boson at a mass of 125 GeV with the CMS experiment at the LHC", *Phys. Lett. B* **716** (2012) 30, doi:10.1016/j.physletb.2012.08.021, arXiv:1207.7235.
- [3] CMS Collaboration, "Observation of a new boson with mass near 125 GeV in  $pp$  collisions at  $\sqrt{s} = 7$  and 8 TeV", *JHEP* **06** (2013) 081, doi:10.1007/JHEP06(2013)081, arXiv:1303.4571.
- [4] F. Englert and R. Brout, "Broken Symmetry and the Mass of Gauge Vector Mesons", *Phys. Rev. Lett.* **13** (1964) 321, doi:10.1103/PhysRevLett.13.321.

- [5] P. W. Higgs, "Broken symmetries, massless particles and gauge fields", *Phys. Lett.* **12** (1964) 132, doi:10.1016/0031-9163(64)91136-9.
- [6] P. W. Higgs, "Broken symmetries and the masses of gauge bosons", *Phys. Rev. Lett.* **13** (1964) 508, doi:10.1103/PhysRevLett.13.508.
- [7] G. S. Guralnik, C. R. Hagen, and T. W. B. Kibble, "Global conservation laws and massless particles", *Phys. Rev. Lett.* **13** (1964) 585, doi:10.1103/PhysRevLett.13.585.
- [8] P. W. Higgs, "Spontaneous symmetry breakdown without massless bosons", *Phys. Rev.* **145** (1966) 1156, doi:10.1103/PhysRev.145.1156.
- [9] T. W. B. Kibble, "Symmetry breaking in non-abelian gauge theories", *Phys. Rev.* **155** (1967) 1554, doi:10.1103/PhysRev.155.1554.
- [10] G. C. Branco et al., "Theory and phenomenology of two-Higgs-doublet models", *Phys. Rept.* **516** (2012) 1, doi:10.1016/j.physrep.2012.02.002, arXiv:1106.0034.
- [11] A. Djouadi, "The Anatomy of electro-weak symmetry breaking. II. The Higgs bosons in the minimal supersymmetric model", *Phys. Rept.* **459** (2008) 1, doi:10.1016/j.physrep.2007.10.005, arXiv:hep-ph/0503173.
- [12] T. Robens and T. Stefaniak, "Status of the Higgs Singlet Extension of the Standard Model after LHC Run 1", *Eur. Phys. J. C* **75** (2015) 104, doi:10.1140/epjc/s10052-015-3323-y, arXiv:1501.02234.
- [13] T. Robens, T. Stefaniak, and J. Wittbrodt, "Two-real-scalar-singlet extension of the SM: LHC phenomenology and benchmark scenarios", *Eur. Phys. J. C* **80** (2020) 151, doi:10.1140/epjc/s10052-020-7655-x, arXiv:1908.08554.
- [14] ATLAS Collaboration, "A detailed map of Higgs boson interactions by the ATLAS experiment ten years after the discovery", *Nature* **607** (2022) 52, doi:10.1038/s41586-022-04893-w, arXiv:2207.00092. [Erratum: doi:10.1038/s41586-022-05581-5].
- [15] CMS Collaboration, "A portrait of the Higgs boson by the CMS experiment ten years after the discovery", *Nature* **607** (2022) 60, doi:10.1038/s41586-022-04892-x, arXiv:2207.00043.
- [16] D. Curtin et al., "Exotic decays of the 125 GeV Higgs boson", *Phys. Rev. D* **90** (2014) 075004, doi:10.1103/PhysRevD.90.075004, arXiv:1312.4992.
- [17] B. Grzadkowski and P. Osland, "Tempered Two-Higgs-Doublet Model", *Phys. Rev. D* **82** (2010) 125026, doi:10.1103/PhysRevD.82.125026, arXiv:0910.4068.
- [18] A. Drozd, B. Grzadkowski, J. F. Gunion, and Y. Jiang, "Extending two-Higgs-doublet models by a singlet scalar field - the Case for Dark Matter", *JHEP* **11** (2014) 105, doi:10.1007/JHEP11(2014)105, arXiv:1408.2106.
- [19] S. Ramos-Sanchez, "The  $\mu$ -problem, the NMSSM and string theory", *Fortschritte der Phys.* **58** (2010) 748, doi:10.1002/prop.201000058, arXiv:1003.1307.
- [20] D. de Florian et al., "Handbook of LHC Higgs cross sections: 4. Deciphering the nature of the Higgs sector", CERN Report CERN-2017-002-M, 2016. doi:10.23731/CYRM-2017-002, arXiv:1610.07922.

- [21] ATLAS Collaboration, “Search for Higgs boson decays into a pair of pseudoscalar particles in the  $bb\mu\mu$  final state with the ATLAS detector in  $pp$  collisions at  $\sqrt{s} = 13$  TeV”, *Phys. Rev. D* **105** (2022) 012006, doi:10.1103/physrevd.105.012006, arXiv:2110.00313.
- [22] ATLAS Collaboration, “Search for Higgs boson decays into a pair of light bosons in the  $bb\mu\mu$  final state in  $pp$  collision at  $\sqrt{s} = 13$  TeV with the ATLAS detector”, *Phys. Lett. B* **790** (2019) 1, doi:10.1016/j.physletb.2018.10.073, arXiv:1807.00539.
- [23] CMS Collaboration, “Search for an exotic decay of the Higgs boson to a pair of light pseudoscalars in the final state with two muons and two b quarks in  $pp$  collisions at 13 TeV”, *Phys. Lett. B* **795** (2019) 398, doi:10.1016/j.physletb.2019.06.021, arXiv:1812.06359.
- [24] CMS Collaboration, “Search for light bosons in decays of the 125 GeV Higgs boson in proton-proton collisions at  $\sqrt{s} = 8$  TeV”, *JHEP* **10** (2017) 076, doi:10.1007/JHEP10(2017)076, arXiv:1701.02032.
- [25] CMS Collaboration, “Search for an exotic decay of the Higgs boson to a pair of light pseudoscalars in the final state with two b quarks and two  $\tau$  leptons in proton-proton collisions at  $\sqrt{s} = 13$  TeV”, *Phys. Lett. B* **785** (2018) 462, doi:10.1016/j.physletb.2018.08.057, arXiv:1805.10191.
- [26] HEPData record for this analysis, 2024. doi:10.17182/hepdata.145999.
- [27] CMS Collaboration, “The CMS trigger system”, *JINST* **12** (2017) P01020, doi:10.1088/1748-0221/12/01/P01020, arXiv:1609.02366.
- [28] CMS Collaboration, “The CMS experiment at the CERN LHC”, *JINST* **3** (2008) S08004, doi:10.1088/1748-0221/3/08/S08004.
- [29] T. Sjöstrand et al., “An Introduction to PYTHIA 8.2”, *Comput. Phys. Commun.* **191** (2015) 159, doi:10.1016/j.cpc.2015.01.024, arXiv:1410.3012.
- [30] NNPDF Collaboration, “Parton distributions from high-precision collider data”, *Eur. Phys. J. C* **77** (2017) 663, doi:10.1140/epjc/s10052-017-5199-5, arXiv:1706.00428.
- [31] J. Alwall, S. de Visscher, and F. Maltoni, “QCD radiation in the production of heavy colored particles at the LHC”, *JHEP* **02** (2009) 017, doi:10.1088/1126-6708/2009/02/017, arXiv:0810.5350.
- [32] J. Alwall et al., “Comparative study of various algorithms for the merging of parton showers and matrix elements in hadronic collisions”, *Eur. Phys. J. C* **53** (2008) 473, doi:10.1140/epjc/s10052-007-0490-5, arXiv:0706.2569.
- [33] R. Frederix and S. Frixione, “Merging meets matching in MC@NLO”, *JHEP* **12** (2012) 061, doi:10.1007/JHEP12(2012)061, arXiv:1209.6215.
- [34] J. Alwall et al., “The automated computation of tree-level and next-to-leading order differential cross sections, and their matching to parton shower simulations”, *JHEP* **07** (2014) 079, doi:10.1007/JHEP07(2014)079, arXiv:1405.0301.

- [35] P. Skands, S. Carrazza, and J. Rojo, “Tuning PYTHIA 8.1: the Monash 2013 Tune”, *Eur. Phys. J. C* **74** (2014) 3024, doi:10.1140/epjc/s10052-014-3024-y, arXiv:1404.5630.
- [36] CMS Collaboration, “Extraction and validation of a new set of CMS PYTHIA8 tunes from underlying-event measurements”, *Eur. Phys. J. C* **80** (2020) 4, doi:10.1140/epjc/s10052-019-7499-4, arXiv:1903.12179.
- [37] GEANT4 Collaboration, “GEANT4—a simulation toolkit”, *Nucl. Instrum. Meth. A* **506** (2003) 250, doi:10.1016/S0168-9002(03)01368-8.
- [38] J. Allison et al., “Geant4 developments and applications”, *IEEE Trans. Nucl. Sci.* **53** (2006) 270, doi:10.1109/TNS.2006.869826.
- [39] CMS Collaboration, “Measurements of Higgs boson production in the decay channel with a pair of  $\tau$  leptons in proton–proton collisions at  $\sqrt{s} = 13$  TeV”, *Eur. Phys. J. C* **83** (2023), no. 7, 562, doi:10.1140/epjc/s10052-023-11452-8, arXiv:2204.12957.
- [40] P. Nason, “A New method for combining NLO QCD with shower Monte Carlo algorithms”, *JHEP* **11** (2004) 040, doi:10.1088/1126-6708/2004/11/040, arXiv:hep-ph/0409146.
- [41] S. Frixione, P. Nason, and C. Oleari, “Matching NLO QCD computations with Parton Shower simulations: the POWHEG method”, *JHEP* **11** (2007) 070, doi:10.1088/1126-6708/2007/11/070, arXiv:0709.2092.
- [42] S. Alioli, P. Nason, C. Oleari, and E. Re, “A general framework for implementing NLO calculations in shower Monte Carlo programs: the POWHEG BOX”, *JHEP* **06** (2010) 043, doi:10.1007/JHEP06(2010)043, arXiv:1002.2581.
- [43] S. Alioli et al., “Jet pair production in POWHEG”, *JHEP* **04** (2011) 081, doi:10.1007/JHEP04(2011)081, arXiv:1012.3380.
- [44] M. Czakon et al., “Top-pair production at the LHC through NNLO QCD and NLO EW”, *JHEP* **10** (2017) 186, doi:10.1007/JHEP10(2017)186, arXiv:1705.04105.
- [45] M. Czakon and A. Mitov, “Top++: A Program for the Calculation of the Top-Pair Cross-Section at Hadron Colliders”, *Comput. Phys. Commun.* **185** (2014) 2930, doi:10.1016/j.cpc.2014.06.021, arXiv:1112.5675.
- [46] M. Botje et al., “The PDF4LHC Working Group interim recommendations”, 2011. arXiv:1101.0538.
- [47] A. D. Martin, W. J. Stirling, R. S. Thorne, and G. Watt, “Uncertainties on alpha(S) in global PDF analyses and implications for predicted hadronic cross sections”, *Eur. Phys. J. C* **64** (2009) 653, doi:10.1140/epjc/s10052-009-1164-2, arXiv:0905.3531.
- [48] J. Gao et al., “CT10 next-to-next-to-leading order global analysis of QCD”, *Phys. Rev. D* **89** (2014), no. 3, 033009, doi:10.1103/PhysRevD.89.033009, arXiv:1302.6246.
- [49] R. D. Ball et al., “Parton distributions with LHC data”, *Nucl. Phys. B* **867** (2013) 244, doi:10.1016/j.nuclphysb.2012.10.003, arXiv:1207.1303.
- [50] J. Campbell, T. Neumann, and Z. Sullivan, “Single-top-quark production in the  $t$ -channel at NNLO”, *JHEP* **02** (2021) 040, doi:10.1007/JHEP02(2021)040, arXiv:2012.01574.

- [51] PDF4LHC Working Group Collaboration, “The PDF4LHC21 combination of global PDF fits for the LHC Run III”, *J. Phys. G* **49** (2022), no. 8, 080501, doi:10.1088/1361-6471/ac7216, arXiv:2203.05506.
- [52] K. Melnikov and F. Petriello, “Electroweak gauge boson production at hadron colliders through  $O(\alpha_s^2)$ ”, *Phys. Rev. D* **74** (2006) 114017, doi:10.1103/PhysRevD.74.114017, arXiv:hep-ph/0609070.
- [53] A. D. Martin, W. J. Stirling, R. S. Thorne, and G. Watt, “Parton distributions for the LHC”, *Eur. Phys. J. C* **63** (2009) 189–285, doi:10.1140/epjc/s10052-009-1072-5, arXiv:0901.0002.
- [54] S. Alioli, P. Nason, C. Oleari, and E. Re, “NLO Higgs boson production via gluon fusion matched with shower in POWHEG”, *JHEP* **04** (2009) 002, doi:10.1088/1126-6708/2009/04/002, arXiv:0812.0578.
- [55] E. Bagnaschi, G. Degrassi, P. Slavich, and A. Vicini, “Higgs production via gluon fusion in the POWHEG approach in the SM and in the MSSM”, *JHEP* **02** (2012) 088, doi:10.1007/JHEP02(2012)088, arXiv:1111.2854.
- [56] P. Nason and C. Oleari, “NLO Higgs boson production via vector-boson fusion matched with shower in POWHEG”, *JHEP* **02** (2010) 037, doi:10.1007/JHEP02(2010)037, arXiv:0911.5299.
- [57] G. Luisoni, P. Nason, C. Oleari, and F. Tramontano, “HW $^\pm$ /HZ + 0 and 1 jet at NLO with the POWHEG BOX interfaced to GoSam and their merging within MiNLO”, *JHEP* **10** (2013) 083, doi:10.1007/JHEP10(2013)083, arXiv:1306.2542.
- [58] H. B. Hartanto, B. Jager, L. Reina, and D. Wackerlo, “Higgs boson production in association with top quarks in the POWHEG BOX”, *Phys. Rev. D* **91** (2015) 094003, doi:10.1103/PhysRevD.91.094003, arXiv:1501.04498.
- [59] CMS Collaboration, “Particle-flow reconstruction and global event description with the CMS detector”, *JINST* **12** (2017) P10003, doi:10.1088/1748-0221/12/10/P10003, arXiv:1706.04965.
- [60] CMS Collaboration, “Technical proposal for the Phase-II upgrade of the Compact Muon Solenoid”, CMS Technical Proposal CERN-LHCC-2015-010, CMS-TDR-15-02, 2015.
- [61] CMS Collaboration, “Performance of the CMS muon detector and muon reconstruction with proton-proton collisions at  $\sqrt{s} = 13$  TeV”, *JINST* **13** (2018) P06015, doi:10.1088/1748-0221/13/06/P06015, arXiv:1804.04528.
- [62] CMS Collaboration, “Electron and photon reconstruction and identification with the CMS experiment at the CERN LHC”, *JINST* **16** (2021) P05014, doi:10.1088/1748-0221/16/05/p05014, arXiv:2012.06888.
- [63] M. Cacciari, G. P. Salam, and G. Soyez, “The anti- $k_t$  jet clustering algorithm”, *JHEP* **04** (2008) 063, doi:10.1088/1126-6708/2008/04/063, arXiv:0802.1189.
- [64] M. Cacciari, G. P. Salam, and G. Soyez, “FastJet User Manual”, *Eur. Phys. J. C* **72** (2012) 1896, doi:10.1140/epjc/s10052-012-1896-2, arXiv:1111.6097.
- [65] CMS Collaboration, “Jet algorithms performance in 13 TeV data”, CMS Physics Analysis Summary CMS-PAS-JME-16-003, 2017.

- [66] CMS Collaboration, “Determination of Jet Energy Calibration and Transverse Momentum Resolution in CMS”, *JINST* **6** (2011) P11002, doi:[10.1088/1748-0221/6/11/P11002](https://doi.org/10.1088/1748-0221/6/11/P11002), arXiv:[1107.4277](https://arxiv.org/abs/1107.4277).
- [67] E. Bols et al., “Jet Flavour Classification Using DeepJet”, *JINST* **15** (2020) P12012, doi:[10.1088/1748-0221/15/12/P12012](https://doi.org/10.1088/1748-0221/15/12/P12012), arXiv:[2008.10519](https://arxiv.org/abs/2008.10519).
- [68] CMS Collaboration, “Identification of heavy-flavour jets with the CMS detector in pp collisions at 13 TeV”, *JINST* **13** (2018) P05011, doi:[10.1088/1748-0221/13/05/P05011](https://doi.org/10.1088/1748-0221/13/05/P05011), arXiv:[1712.07158](https://arxiv.org/abs/1712.07158).
- [69] CMS Collaboration, “Performance of the DeepJet b tagging algorithm using 41.9/fb of data from proton-proton collisions at 13 TeV with Phase 1 CMS detector”, CMS Detector Performance Note CMS-DP-2018-058, 2018.
- [70] CMS Collaboration, “Performance of reconstruction and identification of  $\tau$  leptons decaying to hadrons and  $\nu_\tau$  in pp collisions at  $\sqrt{s} = 13$  TeV”, *JINST* **13** (2018) P10005, doi:[10.1088/1748-0221/13/10/P10005](https://doi.org/10.1088/1748-0221/13/10/P10005), arXiv:[1809.02816](https://arxiv.org/abs/1809.02816).
- [71] CMS Collaboration, “Identification of hadronic tau lepton decays using a deep neural network”, *JINST* **17** (2022) P07023, doi:[10.1088/1748-0221/17/07/P07023](https://doi.org/10.1088/1748-0221/17/07/P07023), arXiv:[2201.08458](https://arxiv.org/abs/2201.08458).
- [72] CMS Collaboration, “Performance of missing transverse momentum reconstruction in proton-proton collisions at  $\sqrt{s} = 13$  TeV using the CMS detector”, *JINST* **14** (2019) P07004, doi:[10.1088/1748-0221/14/07/P07004](https://doi.org/10.1088/1748-0221/14/07/P07004), arXiv:[1903.06078](https://arxiv.org/abs/1903.06078).
- [73] J. Lever, M. Krzywinski, and N. Altman, “Principal component analysis”, *Nature Methods* **14** (2017) 641, doi:[10.1038/nmeth.4346](https://doi.org/10.1038/nmeth.4346).
- [74] CDF Collaboration, “Search for neutral Higgs bosons of the minimal supersymmetric standard model decaying to  $\tau$  pairs in  $p\bar{p}$  collisions at  $\sqrt{s} = 1.96$  TeV”, *Phys. Rev. Lett.* **96** (2006) 011802, doi:[10.1103/PhysRevLett.96.011802](https://doi.org/10.1103/PhysRevLett.96.011802), arXiv:[hep-ex/0508051](https://arxiv.org/abs/hep-ex/0508051).
- [75] L. Bianchini et al., “Reconstruction of the Higgs mass in events with Higgs bosons decaying into a pair of tau leptons using matrix element technique”, *Nucl. Instrum. Meth. A* **862** (2017) 54, doi:[10.1016/j.nima.2017.05.001](https://doi.org/10.1016/j.nima.2017.05.001), arXiv:[1603.05910](https://arxiv.org/abs/1603.05910).
- [76] P. D. Dauncey, M. Kenzie, N. Wardle, and G. J. Davies, “Handling uncertainties in background shapes: the discrete profiling method”, *JINST* **10** (2015) P04015, doi:[10.1088/1748-0221/10/04/P04015](https://doi.org/10.1088/1748-0221/10/04/P04015), arXiv:[1408.6865](https://arxiv.org/abs/1408.6865).
- [77] CMS Collaboration, “Observation of the diphoton decay of the Higgs boson and measurement of its properties”, *Eur. Phys. J. C* **74** (2014) 3076, doi:[10.1140/epjc/s10052-014-3076-z](https://doi.org/10.1140/epjc/s10052-014-3076-z), arXiv:[1407.0558](https://arxiv.org/abs/1407.0558).
- [78] ATLAS, CMS Collaboration, “Combined Measurement of the Higgs Boson Mass in  $pp$  Collisions at  $\sqrt{s} = 7$  and 8 TeV with the ATLAS and CMS Experiments”, *Phys. Rev. Lett.* **114** (2015) 191803, doi:[10.1103/PhysRevLett.114.191803](https://doi.org/10.1103/PhysRevLett.114.191803), arXiv:[1503.07589](https://arxiv.org/abs/1503.07589).
- [79] CMS Collaboration, “An embedding technique to determine  $\tau\tau$  backgrounds in proton-proton collision data”, *JINST* **14** (2019) P06032, doi:[10.1088/1748-0221/14/06/P06032](https://doi.org/10.1088/1748-0221/14/06/P06032), arXiv:[1903.01216](https://arxiv.org/abs/1903.01216).

- [80] M. J. Oreglia, “A study of the reactions  $\psi' \rightarrow \gamma\gamma\psi$ ”. PhD thesis, Stanford University, 1980. SLAC Report SLAC-R-236.
- [81] T. Junk, “Confidence level computation for combining searches with small statistics”, *Nucl. Instrum. Meth. A* **434** (1999) 435, doi:10.1016/S0168-9002(99)00498-2, arXiv:hep-ex/9902006.
- [82] A. L. Read, “Presentation of search results: The  $CL_s$  technique”, *J. Phys. G* **28** (2002) 2693, doi:10.1088/0954-3899/28/10/313.
- [83] G. Cowan, K. Cranmer, E. Gross, and O. Vitells, “Asymptotic formulae for likelihood-based tests of new physics”, *Eur. Phys. J. C* **71** (2011) 1554, doi:10.1140/epjc/s10052-011-1554-0, arXiv:1007.1727. [Erratum: doi:10.1140/epjc/s10052-013-2501-z].
- [84] U. Haisch, J. F. Kamenik, A. Malinauskas, and M. Spira, “Collider constraints on light pseudoscalars”, *JHEP* **03** (2018) 178, doi:10.1007/JHEP03(2018)178, arXiv:1802.02156.
- [85] CMS Collaboration, “Precision luminosity measurement in proton-proton collisions at  $\sqrt{s} = 13$  TeV in 2015 and 2016 at CMS”, *Eur. Phys. J. C* **81** (2021) 800, doi:10.1140/epjc/s10052-021-09538-2, arXiv:2104.01927.
- [86] CMS Collaboration, “CMS luminosity measurement for the 2017 data-taking period at  $\sqrt{s} = 13$  TeV”, CMS Physics Analysis Summary CMS-PAS-LUM-17-004, 2018.
- [87] CMS Collaboration, “CMS luminosity measurement for the 2018 data-taking period at  $\sqrt{s} = 13$  TeV”, CMS Physics Analysis Summary CMS-PAS-LUM-18-002, 2019.
- [88] CMS Collaboration, “Measurement of the inelastic proton-proton cross section at  $\sqrt{s} = 13$  TeV”, *JHEP* **07** (2018) 161, doi:10.1007/JHEP07(2018)161, arXiv:1802.02613.
- [89] CMS Collaboration, “Performance of the CMS Level-1 trigger in proton-proton collisions at  $\sqrt{s} = 13$  TeV”, *JINST* **15** (2020) P10017, doi:10.1088/1748-0221/15/10/P10017, arXiv:2006.10165.
- [90] CMS Collaboration, “Jet energy scale and resolution in the CMS experiment in pp collisions at 8 TeV”, *JINST* **12** (2017), no. 02, P02014, doi:10.1088/1748-0221/12/02/P02014, arXiv:1607.03663.
- [91] CMS Collaboration, “Measurement of the Inclusive W and Z Production Cross Sections in  $pp$  Collisions at  $\sqrt{s} = 7$  TeV”, *JHEP* **10** (2011) 132, doi:10.1007/JHEP10(2011)132, arXiv:1107.4789.
- [92] CMS Collaboration, “Measurement of the inclusive and differential Higgs boson production cross sections in the decay mode to a pair of  $\tau$  leptons in pp collisions at  $\sqrt{s} = 13$  TeV”, *Phys. Rev. Lett.* **128** (2022) 081805, doi:10.1103/PhysRevLett.128.081805, arXiv:2107.11486.
- [93] CMS Collaboration, “Performance of electron reconstruction and selection with the CMS detector in proton-proton collisions at  $\sqrt{s} = 8$  TeV”, *JINST* **10** (2015) P06005, doi:10.1088/1748-0221/10/06/P06005, arXiv:1502.02701.
- [94] R. J. Barlow and C. Beeston, “Fitting using finite Monte Carlo samples”, *Comput. Phys. Commun.* **77** (1993) 219, doi:10.1016/0010-4655(93)90005-W.

- [95] J. Butterworth et al., “PDF4LHC recommendations for LHC Run II”, *J. Phys. G* **43** (2016) 023001, doi:10.1088/0954-3899/43/2/023001, arXiv:1510.03865.

## A The CMS Collaboration

### **Yerevan Physics Institute, Yerevan, Armenia**

A. Hayrapetyan, A. Tumasyan<sup>1</sup> 

### **Institut für Hochenergiephysik, Vienna, Austria**

W. Adam , J.W. Andrejkovic, T. Bergauer , S. Chatterjee , K. Damanakis , M. Dragicevic , A. Escalante Del Valle , P.S. Hussain , M. Jeitler<sup>2</sup> , N. Krammer , D. Liko , I. Mikulec , J. Schieck<sup>2</sup> , R. Schöfbeck , D. Schwarz , M. Sonawane , S. Templ , W. Waltenberger , C.-E. Wulz<sup>2</sup> 

### **Universiteit Antwerpen, Antwerpen, Belgium**

M.R. Darwish<sup>3</sup> , T. Janssen , P. Van Mechelen 

### **Vrije Universiteit Brussel, Brussel, Belgium**

E.S. Bols , J. D'Hondt , S. Dansana , A. De Moor , M. Delcourt , H. El Faham , S. Lowette , I. Makarenko , D. Müller , A.R. Sahasransu , S. Tavernier , M. Tytgat<sup>4</sup> , S. Van Putte , D. Vannerom 

### **Université Libre de Bruxelles, Bruxelles, Belgium**

B. Clerbaux , G. De Lentdecker , L. Favart , D. Hohov , J. Jaramillo , A. Khalilzadeh, K. Lee , M. Mahdavikhorrami , A. Malara , S. Paredes , L. Pétré , N. Postiau, L. Thomas , M. Vanden Bemden , C. Vander Velde , P. Vanlaer 

### **Ghent University, Ghent, Belgium**

M. De Coen , D. Dobur , Y. Hong , J. Knolle , L. Lambrecht , G. Mestdach, C. Rendón, A. Samalan, K. Skovpen , N. Van Den Bossche , L. Wezenbeek 

### **Université Catholique de Louvain, Louvain-la-Neuve, Belgium**

A. Benecke , G. Bruno , C. Caputo , C. Delaere , I.S. Donertas , A. Giannanco , K. Jaffel , Sa. Jain , V. Lemaitre, J. Lidrych , P. Mastrapasqua , K. Mondal , T.T. Tran , S. Wertz 

### **Centro Brasileiro de Pesquisas Fisicas, Rio de Janeiro, Brazil**

G.A. Alves , E. Coelho , C. Hensel , T. Menezes De Oliveira , A. Moraes , P. Rebello Teles , M. Soeiro

### **Universidade do Estado do Rio de Janeiro, Rio de Janeiro, Brazil**

W.L. Aldá Júnior , M. Alves Gallo Pereira , M. Barroso Ferreira Filho , H. Brandao Malbouisson , W. Carvalho , J. Chinellato<sup>5</sup>, E.M. Da Costa , G.G. Da Silveira<sup>6</sup> , D. De Jesus Damiao , S. Fonseca De Souza , J. Martins<sup>7</sup> , C. Mora Herrera , K. Mota Amarilo , L. Mundim , H. Nogima , A. Santoro , S.M. Silva Do Amaral , A. Sznajder , M. Thiel , A. Vilela Pereira 

### **Universidade Estadual Paulista, Universidade Federal do ABC, São Paulo, Brazil**

C.A. Bernardes<sup>6</sup> , L. Calligaris , T.R. Fernandez Perez Tomei , E.M. Gregores , P.G. Mercadante , S.F. Novaes , B. Orzari , Sandra S. Padula 

### **Institute for Nuclear Research and Nuclear Energy, Bulgarian Academy of Sciences, Sofia, Bulgaria**

A. Aleksandrov , G. Antchev , R. Hadjiiska , P. Iaydjiev , M. Misheva , M. Shopova , G. Sultanov 

### **University of Sofia, Sofia, Bulgaria**

A. Dimitrov , T. Ivanov , L. Litov , B. Pavlov , P. Petkov , A. Petrov , E. Shumka 

**Instituto De Alta Investigación, Universidad de Tarapacá, Casilla 7 D, Arica, Chile**

S. Keshri , S. Thakur 

**Beihang University, Beijing, China**

T. Cheng , Q. Guo, T. Javaid , M. Mittal , L. Yuan 

**Department of Physics, Tsinghua University, Beijing, China**

G. Bauer<sup>8,9</sup>, Z. Hu , K. Yi<sup>8,10</sup> 

**Institute of High Energy Physics, Beijing, China**

G.M. Chen<sup>11</sup> , H.S. Chen<sup>11</sup> , M. Chen<sup>11</sup> , F. Iemmi , C.H. Jiang, A. Kapoor<sup>12</sup> , H. Liao , Z.-A. Liu<sup>13</sup> , F. Monti , M.A. Shahzad<sup>11</sup>, R. Sharma<sup>14</sup> , J.N. Song<sup>13</sup>, J. Tao , C. Wang<sup>11</sup>, J. Wang , Z. Wang<sup>11</sup>, H. Zhang 

**State Key Laboratory of Nuclear Physics and Technology, Peking University, Beijing, China**

A. Agapitos , Y. Ban , A. Levin , C. Li , Q. Li , X. Lyu, Y. Mao, S.J. Qian , X. Sun , D. Wang , H. Yang, C. Zhou 

**Sun Yat-Sen University, Guangzhou, China**

Z. You 

**University of Science and Technology of China, Hefei, China**

N. Lu 

**Institute of Modern Physics and Key Laboratory of Nuclear Physics and Ion-beam Application (MOE) - Fudan University, Shanghai, China**

X. Gao<sup>15</sup> , D. Leggat, H. Okawa , Y. Zhang 

**Zhejiang University, Hangzhou, Zhejiang, China**

Z. Lin , C. Lu , M. Xiao 

**Universidad de Los Andes, Bogota, Colombia**

C. Avila , D.A. Barbosa Trujillo, A. Cabrera , C. Florez , J. Fraga , J.A. Reyes Vega

**Universidad de Antioquia, Medellin, Colombia**

J. Mejia Guisao , F. Ramirez , M. Rodriguez , J.D. Ruiz Alvarez 

**University of Split, Faculty of Electrical Engineering, Mechanical Engineering and Naval Architecture, Split, Croatia**

D. Giljanovic , N. Godinovic , D. Lelas , A. Sculac 

**University of Split, Faculty of Science, Split, Croatia**

M. Kovac , T. Sculac 

**Institute Rudjer Boskovic, Zagreb, Croatia**

P. Bargassa , V. Brigljevic , B.K. Chitroda , D. Ferencek , S. Mishra , A. Starodumov<sup>16</sup> , T. Susa 

**University of Cyprus, Nicosia, Cyprus**

A. Attikis , K. Christoforou , S. Konstantinou , J. Mousa , C. Nicolaou, F. Ptochos , P.A. Razis , H. Rykaczewski, H. Saka , A. Stepennov 

**Charles University, Prague, Czech Republic**

M. Finger , M. Finger Jr. , A. Kveton 

**Escuela Politecnica Nacional, Quito, Ecuador**

E. Ayala 

**Universidad San Francisco de Quito, Quito, Ecuador**E. Carrera Jarrin **Academy of Scientific Research and Technology of the Arab Republic of Egypt, Egyptian Network of High Energy Physics, Cairo, Egypt**S. Elgammal<sup>17</sup>, A. Ellithi Kamel<sup>18</sup>**Center for High Energy Physics (CHEP-FU), Fayoum University, El-Fayoum, Egypt**A. Lotfy , M.A. Mahmoud **National Institute of Chemical Physics and Biophysics, Tallinn, Estonia**R.K. Dewanjee<sup>19</sup> , K. Ehataht , M. Kadastik, T. Lange , S. Nandan , C. Nielsen , J. Pata , M. Raidal , L. Tani , C. Veelken **Department of Physics, University of Helsinki, Helsinki, Finland**H. Kirschenmann , K. Osterberg , M. Voutilainen **Helsinki Institute of Physics, Helsinki, Finland**S. Bharthuar , E. Brücken , F. Garcia , J. Havukainen , K.T.S. Kallonen , M.S. Kim , R. Kinnunen, T. Lampén , K. Lassila-Perini , S. Lehti , T. Lindén , M. Lotti, L. Martikainen , M. Myllymäki , M.m. Rantanen , H. Siikonen , E. Tuominen , J. Tuominiemi **Lappeenranta-Lahti University of Technology, Lappeenranta, Finland**P. Luukka , H. Petrow , T. Tuuva<sup>†</sup>**IRFU, CEA, Université Paris-Saclay, Gif-sur-Yvette, France**M. Besancon , F. Couderc , M. Dejardin , D. Denegri, J.L. Faure, F. Ferri , S. Ganjour , P. Gras , G. Hamel de Monchenault , V. Lohezic , J. Malcles , J. Rander, A. Rosowsky , M.Ö. Sahin , A. Savoy-Navarro<sup>20</sup> , P. Simkina , M. Titov **Laboratoire Leprince-Ringuet, CNRS/IN2P3, Ecole Polytechnique, Institut Polytechnique de Paris, Palaiseau, France**C. Baldenegro Barrera , F. Beaudette , A. Buchot Perraguin , P. Busson , A. Cappati , C. Charlot , F. Damas , O. Davignon , A. De Wit , G. Falmagne , B.A. Fontana Santos Alves , S. Ghosh , A. Gilbert , R. Granier de Cassagnac , A. Hakimi , B. Harikrishnan , L. Kalipoliti , G. Liu , J. Motta , M. Nguyen , C. Ochando , L. Portales , R. Salerno , U. Sarkar , J.B. Sauvan , Y. Sirois , A. Tarabini , E. Vernazza , A. Zabi , A. Zghiche **Université de Strasbourg, CNRS, IPHC UMR 7178, Strasbourg, France**J.-L. Agram<sup>21</sup> , J. Andrea , D. Apparu , D. Bloch , J.-M. Brom , E.C. Chabert , C. Collard , S. Falke , U. Goerlach , C. Grimault, R. Haeberle , A.-C. Le Bihan , M.A. Sessini , P. Van Hove **Institut de Physique des 2 Infinis de Lyon (IP2I ), Villeurbanne, France**S. Beauceron , B. Blançon , G. Boudoul , N. Chanon , J. Choi , D. Contardo , P. Depasse , C. Dozen<sup>22</sup> , H. El Mamouni, J. Fay , S. Gascon , M. Gouzevitch , C. Greenberg, G. Grenier , B. Ille , I.B. Laktineh, M. Lethuillier , L. Mirabito, S. Perries, M. Vander Donckt , P. Verdier , J. Xiao **Georgian Technical University, Tbilisi, Georgia**A. Khvedelidze<sup>16</sup> , I. Lomidze , Z. Tsamalaidze<sup>16</sup> **RWTH Aachen University, I. Physikalisches Institut, Aachen, Germany**

V. Botta [ID](#), L. Feld [ID](#), K. Klein [ID](#), M. Lipinski [ID](#), D. Meuser [ID](#), A. Pauls [ID](#), N. Röwert [ID](#), M. Teroerde [ID](#)

#### **RWTH Aachen University, III. Physikalisches Institut A, Aachen, Germany**

S. Diekmann [ID](#), A. Dodonova [ID](#), N. Eich [ID](#), D. Eliseev [ID](#), F. Engelke [ID](#), M. Erdmann [ID](#), P. Fackeldey [ID](#), B. Fischer [ID](#), T. Hebbeker [ID](#), K. Hoepfner [ID](#), F. Ivone [ID](#), A. Jung [ID](#), M.y. Lee [ID](#), L. Mastrolorenzo, M. Merschmeyer [ID](#), A. Meyer [ID](#), S. Mukherjee [ID](#), D. Noll [ID](#), A. Novak [ID](#), F. Nowotny, A. Pozdnyakov [ID](#), Y. Rath, W. Redjeb [ID](#), F. Rehm, H. Reithler [ID](#), V. Sarkisovi [ID](#), A. Schmidt [ID](#), S.C. Schuler, A. Sharma [ID](#), A. Stein [ID](#), F. Torres Da Silva De Araujo<sup>23</sup> [ID](#), L. Vigilante, S. Wiedenbeck [ID](#), S. Zaleski

#### **RWTH Aachen University, III. Physikalisches Institut B, Aachen, Germany**

C. Dzwik [ID](#), G. Flügge [ID](#), W. Haj Ahmad<sup>24</sup> [ID](#), T. Kress [ID](#), A. Nowack [ID](#), O. Pooth [ID](#), A. Stahl [ID](#), T. Ziemons [ID](#), A. Zottz [ID](#)

#### **Deutsches Elektronen-Synchrotron, Hamburg, Germany**

H. Aarup Petersen [ID](#), M. Aldaya Martin [ID](#), J. Alimena [ID](#), S. Amoroso, Y. An [ID](#), S. Baxter [ID](#), M. Bayatmakou [ID](#), H. Becerril Gonzalez [ID](#), O. Behnke [ID](#), A. Belvedere [ID](#), S. Bhattacharya [ID](#), F. Blekman<sup>25</sup> [ID](#), K. Borras<sup>26</sup> [ID](#), D. Brunner [ID](#), A. Campbell [ID](#), A. Cardini [ID](#), C. Cheng, F. Colombina [ID](#), S. Consuegra Rodríguez [ID](#), G. Correia Silva [ID](#), M. De Silva [ID](#), G. Eckerlin, D. Eckstein [ID](#), L.I. Estevez Banos [ID](#), O. Filatov [ID](#), E. Gallo<sup>25</sup> [ID](#), A. Geiser [ID](#), A. Giraldi [ID](#), G. Greau, V. Guglielmi [ID](#), M. Guthoff [ID](#), A. Hinzmann [ID](#), A. Jafari<sup>27</sup> [ID](#), L. Jeppe [ID](#), N.Z. Jomhari [ID](#), B. Kaech [ID](#), M. Kasemann [ID](#), H. Kaveh [ID](#), C. Kleinwort [ID](#), R. Kogler [ID](#), M. Komm [ID](#), D. Krücker [ID](#), W. Lange, D. Leyva Pernia [ID](#), K. Lipka<sup>28</sup> [ID](#), W. Lohmann<sup>29</sup> [ID](#), R. Mankel [ID](#), I.-A. Melzer-Pellmann [ID](#), M. Mendizabal Morentin [ID](#), J. Metwally, A.B. Meyer [ID](#), G. Milella [ID](#), A. Mussgiller [ID](#), A. Nürnberg [ID](#), Y. Otarid, D. Pérez Adán [ID](#), E. Ranken [ID](#), A. Raspereza [ID](#), B. Ribeiro Lopes [ID](#), J. Rübenach, A. Saggio [ID](#), M. Scham<sup>30,26</sup> [ID](#), S. Schnake<sup>26</sup> [ID](#), P. Schütze [ID](#), C. Schwanenberger<sup>25</sup> [ID](#), D. Selivanova [ID](#), M. Shchedrolosiev [ID](#), R.E. Sosa Ricardo [ID](#), L.P. Sreelatha Pramod [ID](#), D. Stafford, F. Vazzoler [ID](#), A. Ventura Barroso [ID](#), R. Walsh [ID](#), Q. Wang [ID](#), Y. Wen [ID](#), K. Wichmann, L. Wiens<sup>26</sup> [ID](#), C. Wissing [ID](#), S. Wuchererl [ID](#), Y. Yang [ID](#), A. Zimermann Castro Santos [ID](#)

#### **University of Hamburg, Hamburg, Germany**

A. Albrecht [ID](#), S. Albrecht [ID](#), M. Antonello [ID](#), S. Bein [ID](#), L. Benato [ID](#), M. Bonanomi [ID](#), P. Connor [ID](#), M. Eich, K. El Morabit [ID](#), Y. Fischer [ID](#), A. Fröhlich, C. Garbers [ID](#), E. Garutti [ID](#), A. Grohsjean [ID](#), M. Hajheidari, J. Haller [ID](#), H.R. Jabusch [ID](#), G. Kasieczka [ID](#), P. Keicher, R. Klanner [ID](#), W. Korcari [ID](#), T. Kramer [ID](#), V. Kutzner [ID](#), F. Labe [ID](#), J. Lange [ID](#), A. Lobanov [ID](#), C. Matthies [ID](#), A. Mehta [ID](#), L. Moureaux [ID](#), M. Mrowietz, A. Nigamova [ID](#), Y. Nissan, A. Paasch [ID](#), K.J. Pena Rodriguez [ID](#), T. Quadfasel [ID](#), B. Raciti [ID](#), M. Rieger [ID](#), D. Savoiu [ID](#), J. Schindler [ID](#), P. Schleper [ID](#), M. Schröder [ID](#), J. Schwandt [ID](#), M. Sommerhalder [ID](#), H. Stadie [ID](#), G. Steinbrück [ID](#), A. Tews, M. Wolf [ID](#)

#### **Karlsruher Institut fuer Technologie, Karlsruhe, Germany**

S. Brommer [ID](#), M. Burkart, E. Butz [ID](#), T. Chwalek [ID](#), A. Dierlamm [ID](#), A. Droll, N. Faltermann [ID](#), M. Giffels [ID](#), A. Gottmann [ID](#), F. Hartmann<sup>31</sup> [ID](#), R. Hofsaess [ID](#), M. Horzela [ID](#), U. Husemann [ID](#), M. Klute [ID](#), R. Koppenhöfer [ID](#), M. Link, A. Lintuluoto [ID](#), S. Maier [ID](#), S. Mitra [ID](#), M. Mormile [ID](#), Th. Müller [ID](#), M. Neukum, M. Oh [ID](#), G. Quast [ID](#), K. Rabbertz [ID](#), B. Regnery [ID](#), N. Shadskiy [ID](#), I. Shvetsov [ID](#), H.J. Simonis [ID](#), N. Trevisani [ID](#), R. Ulrich [ID](#), J. van der Linden [ID](#), R.F. Von Cube [ID](#), M. Wassmer [ID](#), S. Wieland [ID](#), F. Wittig, R. Wolf [ID](#), S. Wunsch, X. Zuo [ID](#)

**Institute of Nuclear and Particle Physics (INPP), NCSR Demokritos, Aghia Paraskevi,**

**Greece**

G. Anagnostou, P. Assiouras , G. Daskalakis , A. Kyriakis, A. Papadopoulos<sup>31</sup>, A. Stakia 

**National and Kapodistrian University of Athens, Athens, Greece**

P. Kontaxakis , G. Melachroinos, A. Panagiotou, I. Papavergou , I. Paraskevas , N. Saoulidou , K. Theofilatos , E. Tziaferi , K. Vellidis , I. Zisopoulos 

**National Technical University of Athens, Athens, Greece**

G. Bakas , T. Chatzistavrou, G. Karapostoli , K. Kousouris , I. Papakrivopoulos , E. Siamarkou, G. Tsipolitis, A. Zacharopoulou

**University of Ioánnina, Ioánnina, Greece**

K. Adamidis, I. Bestintzanos, I. Evangelou , C. Foudas, P. Gianneios , C. Kamtsikis, P. Katsoulis, P. Kokkas , P.G. Kosmoglou Kioseoglou , N. Manthos , I. Papadopoulos , J. Strologas 

**HUN-REN Wigner Research Centre for Physics, Budapest, Hungary**

M. Bartók<sup>32</sup> , C. Hajdu , D. Horvath<sup>33,34</sup> , F. Sikler , V. Veszpremi 

**MTA-ELTE Lendület CMS Particle and Nuclear Physics Group, Eötvös Loránd University, Budapest, Hungary**

M. Csand , K. Farkas , M.M.A. Gadallah<sup>35</sup> , . Kadlecsik , P. Major , K. Mandal , G. Pasztor , A.J. Radl<sup>36</sup> , G.I. Veres 

**Faculty of Informatics, University of Debrecen, Debrecen, Hungary**

P. Raics, B. Ujvari<sup>37</sup> , G. Zilizi 

**Institute of Nuclear Research ATOMKI, Debrecen, Hungary**

G. Bencze, S. Czellar, J. Karancsi<sup>32</sup> , J. Molnar, Z. Szillasi

**Karoly Robert Campus, MATE Institute of Technology, Gyongyos, Hungary**

T. Csorgo<sup>36</sup> , F. Nemes<sup>36</sup> , T. Novak 

**Panjab University, Chandigarh, India**

J. Babbar , S. Bansal , S.B. Beri, V. Bhatnagar , G. Chaudhary , S. Chauhan , N. Dhingra<sup>38</sup> , R. Gupta, A. Kaur , A. Kaur , H. Kaur , M. Kaur , S. Kumar , M. Meena , K. Sandeep , T. Sheokand, J.B. Singh , A. Singla 

**University of Delhi, Delhi, India**

A. Ahmed , A. Bhardwaj , A. Chhetri , B.C. Choudhary , A. Kumar , M. Naimuddin , K. Ranjan , S. Saumya 

**Saha Institute of Nuclear Physics, HBNI, Kolkata, India**

S. Acharya<sup>39</sup> , S. Baradia , S. Barman<sup>40</sup> , S. Bhattacharya , D. Bhowmik, S. Dutta , S. Dutta, B. Gomber<sup>39</sup> , P. Palit , G. Saha , B. Sahu<sup>39</sup> , S. Sarkar

**Indian Institute of Technology Madras, Madras, India**

M.M. Ameen , P.K. Behera , S.C. Behera , S. Chatterjee , P. Jana , P. Kalbhor , J.R. Komaragiri<sup>41</sup> , D. Kumar<sup>41</sup> , L. Panwar<sup>41</sup> , R. Pradhan , P.R. Pujahari , N.R. Saha , A. Sharma , A.K. Sikdar , S. Verma 

**Tata Institute of Fundamental Research-A, Mumbai, India**

T. Aziz, I. Das , S. Dugad, M. Kumar , G.B. Mohanty , P. Suryadevara

**Tata Institute of Fundamental Research-B, Mumbai, India**

A. Bala , S. Banerjee , R.M. Chatterjee, M. Guchait , Sh. Jain , S. Karmakar 

S. Kumar , G. Majumder , K. Mazumdar , S. Mukherjee , A. Thachayath 

**National Institute of Science Education and Research, An OCC of Homi Bhabha National Institute, Bhubaneswar, Odisha, India**

S. Bahinipati<sup>42</sup> , A.K. Das, C. Kar , D. Maity<sup>43</sup> , P. Mal , T. Mishra , V.K. Muraleedharan Nair Bindhu<sup>43</sup> , K. Naskar<sup>43</sup> , A. Nayak<sup>43</sup> , P. Sadangi, P. Saha , S.K. Swain , S. Varghese<sup>43</sup> , D. Vats<sup>43</sup> 

**Indian Institute of Science Education and Research (IISER), Pune, India**

A. Alpana , S. Dube , B. Kansal , A. Laha , A. Rastogi , S. Sharma 

**Isfahan University of Technology, Isfahan, Iran**

H. Bakhshiansohi<sup>44</sup> , E. Khazaie<sup>44</sup> , M. Zeinali<sup>45</sup> 

**Institute for Research in Fundamental Sciences (IPM), Tehran, Iran**

S. Chenarani<sup>46</sup> , S.M. Etesami , M. Khakzad , M. Mohammadi Najafabadi 

**University College Dublin, Dublin, Ireland**

M. Grunewald 

**INFN Sezione di Bari<sup>a</sup>, Università di Bari<sup>b</sup>, Politecnico di Bari<sup>c</sup>, Bari, Italy**

M. Abbrescia<sup>a,b</sup> , R. Aly<sup>a,c,47</sup> , A. Colaleo<sup>a,b</sup> , D. Creanza<sup>a,c</sup> , B. D'Anzi<sup>a,b</sup> , N. De Filippis<sup>a,c</sup> , M. De Palma<sup>a,b</sup> , A. Di Florio<sup>a,c</sup> , W. Elmetenawee<sup>a,b,47</sup> , L. Fiore<sup>a</sup> , G. Iaselli<sup>a,c</sup> , G. Maggi<sup>a,c</sup> , M. Maggi<sup>a</sup> , I. Margjeka<sup>a,b</sup> , V. Mastrapasqua<sup>a,b</sup> , S. My<sup>a,b</sup> , S. Nuzzo<sup>a,b</sup> , A. Pellecchia<sup>a,b</sup> , A. Pompili<sup>a,b</sup> , G. Pugliese<sup>a,c</sup> , R. Radogna<sup>a</sup> , G. Ramirez-Sanchez<sup>a,c</sup> , D. Ramos<sup>a</sup> , A. Ranieri<sup>a</sup> , L. Silvestris<sup>a</sup> , F.M. Simone<sup>a,b</sup> , Ü. Sözbilir<sup>a</sup> , A. Stamerra<sup>a</sup> , R. Venditti<sup>a</sup> , P. Verwilligen<sup>a</sup> , A. Zaza<sup>a,b</sup> 

**INFN Sezione di Bologna<sup>a</sup>, Università di Bologna<sup>b</sup>, Bologna, Italy**

G. Abbiendi<sup>a</sup> , C. Battilana<sup>a,b</sup> , D. Bonacorsi<sup>a,b</sup> , L. Borgonovi<sup>a</sup> , R. Campanini<sup>a,b</sup> , P. Capiluppi<sup>a,b</sup> , A. Castro<sup>a,b</sup> , F.R. Cavallo<sup>a</sup> , M. Cuffiani<sup>a,b</sup> , G.M. Dallavalle<sup>a</sup> , T. Diotalevi<sup>a,b</sup> , A. Fanfani<sup>a,b</sup> , D. Fasanella<sup>a,b</sup> , P. Giacomelli<sup>a</sup> , L. Giommi<sup>a,b</sup> , C. Grandi<sup>a</sup> , L. Guiducci<sup>a,b</sup> , S. Lo Meo<sup>a,48</sup> , L. Lunerti<sup>a,b</sup> , S. Marcellini<sup>a</sup> , G. Masetti<sup>a</sup> , F.L. Navarria<sup>a,b</sup> , A. Perrotta<sup>a</sup> , F. Primavera<sup>a,b</sup> , A.M. Rossi<sup>a,b</sup> , T. Rovelli<sup>a,b</sup> , G.P. Siroli<sup>a,b</sup> 

**INFN Sezione di Catania<sup>a</sup>, Università di Catania<sup>b</sup>, Catania, Italy**

S. Costa<sup>a,b,49</sup> , A. Di Mattia<sup>a</sup> , R. Potenza<sup>a,b</sup> , A. Tricomi<sup>a,b,49</sup> , C. Tuve<sup>a,b</sup> 

**INFN Sezione di Firenze<sup>a</sup>, Università di Firenze<sup>b</sup>, Firenze, Italy**

G. Barbagli<sup>a</sup> , G. Bardelli<sup>a,b</sup> , B. Camaiani<sup>a,b</sup> , A. Cassese<sup>a</sup> , R. Ceccarelli<sup>a</sup> , V. Ciulli<sup>a,b</sup> , C. Civinini<sup>a</sup> , R. D'Alessandro<sup>a,b</sup> , E. Focardi<sup>a,b</sup> , T. Kello<sup>a</sup> , G. Latino<sup>a,b</sup> , P. Lenzi<sup>a,b</sup> , M. Lizzo<sup>a</sup> , M. Meschini<sup>a</sup> , S. Paoletti<sup>a</sup> , A. Papanastassiou<sup>a,b</sup> , G. Sguazzoni<sup>a</sup> , L. Viliani<sup>a</sup> 

**INFN Laboratori Nazionali di Frascati, Frascati, Italy**

L. Benussi , S. Bianco , S. Meola<sup>50</sup> , D. Piccolo 

**INFN Sezione di Genova<sup>a</sup>, Università di Genova<sup>b</sup>, Genova, Italy**

P. Chatagnon<sup>a</sup> , F. Ferro<sup>a</sup> , E. Robutti<sup>a</sup> , S. Tosi<sup>a,b</sup> 

**INFN Sezione di Milano-Bicocca<sup>a</sup>, Università di Milano-Bicocca<sup>b</sup>, Milano, Italy**

A. Benaglia<sup>a</sup> , G. Boldrini<sup>a</sup> , F. Brivio<sup>a</sup> , F. Cetorelli<sup>a</sup> , F. De Guio<sup>a,b</sup> , M.E. Dinardo<sup>a,b</sup> , P. Dini<sup>a</sup> , S. Gennai<sup>a</sup> , A. Ghezzi<sup>a,b</sup> , P. Govoni<sup>a,b</sup> , L. Guzzi<sup>a</sup> 

M.T. Lucchini<sup>a,b</sup> , M. Malberti<sup>a</sup> , S. Malvezzi<sup>a</sup> , A. Massironi<sup>a</sup> , D. Menasce<sup>a</sup> , L. Moroni<sup>a</sup> , M. Paganoni<sup>a,b</sup> , D. Pedrini<sup>a</sup> , B.S. Pinolini<sup>a</sup>, S. Ragazzi<sup>a,b</sup> , N. Redaelli<sup>a</sup> , T. Tabarelli de Fatis<sup>a,b</sup> , D. Zuolo<sup>a</sup> 

**INFN Sezione di Napoli<sup>a</sup>, Università di Napoli 'Federico II'<sup>b</sup>, Napoli, Italy; Università della Basilicata<sup>c</sup>, Potenza, Italy; Scuola Superiore Meridionale (SSM)<sup>d</sup>, Napoli, Italy**

S. Buontempo<sup>a</sup> , A. Cagnotta<sup>a,b</sup> , F. Carnevali<sup>a,b</sup> , N. Cavallo<sup>a,c</sup> , A. De Iorio<sup>a,b</sup> , F. Fabozzi<sup>a,c</sup> , A.O.M. Iorio<sup>a,b</sup> , L. Lista<sup>a,b,51</sup> , P. Paolucci<sup>a,31</sup> , B. Rossi<sup>a</sup> , C. Sciacca<sup>a,b</sup> 

**INFN Sezione di Padova<sup>a</sup>, Università di Padova<sup>b</sup>, Padova, Italy; Università di Trento<sup>c</sup>, Trento, Italy**

R. Ardino<sup>a</sup> , P. Azzi<sup>a</sup> , N. Bacchetta<sup>a,52</sup> , D. Bisello<sup>a,b</sup> , P. Bortignon<sup>a</sup> , A. Bragagnolo<sup>a,b</sup> , R. Carlin<sup>a,b</sup> , P. Checchia<sup>a</sup> , T. Dorigo<sup>a</sup> , U. Gasparini<sup>a,b</sup> , G. Grossi<sup>a</sup>, L. Layer<sup>a,53</sup> , E. Lusiani<sup>a</sup> , M. Margoni<sup>a,b</sup> , A.T. Meneguzzo<sup>a,b</sup> , M. Michelotto<sup>a</sup> , M. Migliorini<sup>a,b</sup> , F. Montecassiano<sup>a</sup> , J. Pazzini<sup>a,b</sup> , P. Ronchese<sup>a,b</sup> , R. Rossin<sup>a,b</sup> , F. Simonetto<sup>a,b</sup> , G. Strong<sup>a</sup> , M. Tosi<sup>a,b</sup> , A. Triossi<sup>a,b</sup> , S. Ventura<sup>a</sup> , H. Yarai<sup>a,b</sup> , P. Zotto<sup>a,b</sup> , A. Zucchetta<sup>a,b</sup> , G. Zumerle<sup>a,b</sup> 

**INFN Sezione di Pavia<sup>a</sup>, Università di Pavia<sup>b</sup>, Pavia, Italy**

S. Abu Zeid<sup>a,54</sup> , C. Aimè<sup>a,b</sup> , A. Braghieri<sup>a</sup> , S. Calzaferri<sup>a,b</sup> , D. Fiorina<sup>a,b</sup> , P. Montagna<sup>a,b</sup> , V. Re<sup>a</sup> , C. Riccardi<sup>a,b</sup> , P. Salvini<sup>a</sup> , I. Vai<sup>a,b</sup> , P. Vitulo<sup>a,b</sup> 

**INFN Sezione di Perugia<sup>a</sup>, Università di Perugia<sup>b</sup>, Perugia, Italy**

S. Ajmal<sup>a,b</sup> , P. Asenov<sup>a,55</sup> , G.M. Bilei<sup>a</sup> , D. Ciangottini<sup>a,b</sup> , L. Fanò<sup>a,b</sup> , M. Magherini<sup>a,b</sup> , G. Mantovani<sup>a,b</sup> , V. Mariani<sup>a,b</sup> , M. Menichelli<sup>a</sup> , F. Moscatelli<sup>a,55</sup> , A. Piccinelli<sup>a,b</sup> , M. Presilla<sup>a,b</sup> , A. Rossi<sup>a,b</sup> , A. Santocchia<sup>a,b</sup> , D. Spiga<sup>a</sup> , T. Tedeschi<sup>a,b</sup> 

**INFN Sezione di Pisa<sup>a</sup>, Università di Pisa<sup>b</sup>, Scuola Normale Superiore di Pisa<sup>c</sup>, Pisa, Italy; Università di Siena<sup>d</sup>, Siena, Italy**

P. Azzurri<sup>a</sup> , G. Bagliesi<sup>a</sup> , R. Bhattacharya<sup>a</sup> , L. Bianchini<sup>a,b</sup> , T. Boccali<sup>a</sup> , E. Bossini<sup>a</sup> , D. Bruschini<sup>a,c</sup> , R. Castaldi<sup>a</sup> , M.A. Ciocci<sup>a,b</sup> , M. Cipriani<sup>a,b</sup> , V. D'Amante<sup>a,d</sup> , R. Dell'Orso<sup>a</sup> , S. Donato<sup>a</sup> , A. Giassi<sup>a</sup> , F. Ligabue<sup>a,c</sup> , D. Matos Figueiredo<sup>a</sup> , A. Messineo<sup>a,b</sup> , M. Musich<sup>a,b</sup> , F. Palla<sup>a</sup> , S. Parolia<sup>a</sup> , A. Rizzi<sup>a,b</sup> , G. Rolandi<sup>a,c</sup> , S. Roy Chowdhury<sup>a</sup> , T. Sarkar<sup>a</sup> , A. Scribano<sup>a</sup> , P. Spagnolo<sup>a</sup> , R. Tenchini<sup>a</sup> , G. Tonelli<sup>a,b</sup> , N. Turini<sup>a,d</sup> , A. Venturi<sup>a</sup> , P.G. Verdini<sup>a</sup> 

**INFN Sezione di Roma<sup>a</sup>, Sapienza Università di Roma<sup>b</sup>, Roma, Italy**

P. Barria<sup>a</sup> , M. Campana<sup>a,b</sup> , F. Cavallari<sup>a</sup> , L. Cunqueiro Mendez<sup>a,b</sup> , D. Del Re<sup>a,b</sup> , E. Di Marco<sup>a</sup> , M. Diemoz<sup>a</sup> , F. Errico<sup>a,b</sup> , E. Longo<sup>a,b</sup> , P. Meridiani<sup>a</sup> , J. Mijuskovic<sup>a,b</sup> , G. Organtini<sup>a,b</sup> , F. Pandolfi<sup>a</sup> , R. Paramatti<sup>a,b</sup> , C. Quaranta<sup>a,b</sup> , S. Rahatlou<sup>a,b</sup> , C. Rovelli<sup>a</sup> , F. Santanastasio<sup>a,b</sup> , L. Soffi<sup>a</sup> , R. Tramontano<sup>a,b</sup> 

**INFN Sezione di Torino<sup>a</sup>, Università di Torino<sup>b</sup>, Torino, Italy; Università del Piemonte Orientale<sup>c</sup>, Novara, Italy**

N. Amapane<sup>a,b</sup> , R. Arcidiacono<sup>a,c</sup> , S. Argiro<sup>a,b</sup> , M. Arneodo<sup>a,c</sup> , N. Bartosik<sup>a</sup> , R. Bellan<sup>a,b</sup> , A. Bellora<sup>a,b</sup> , C. Biino<sup>a</sup> , N. Cartiglia<sup>a</sup> , M. Costa<sup>a,b</sup> , R. Covarelli<sup>a,b</sup> , N. Demaria<sup>a</sup> , L. Finco<sup>a</sup> , M. Grippo<sup>a,b</sup> , B. Kiani<sup>a,b</sup> , F. Legger<sup>a</sup> , F. Luongo<sup>a,b</sup> , C. Mariotti<sup>a</sup> , S. Maselli<sup>a</sup> , A. Mecca<sup>a,b</sup> , E. Migliore<sup>a,b</sup> , M. Monteno<sup>a</sup> , R. Mulargia<sup>a</sup> , M.M. Obertino<sup>a,b</sup> , G. Ortona<sup>a</sup> , L. Pacher<sup>a,b</sup> , N. Pastrone<sup>a</sup> , M. Pelliccioni<sup>a</sup> , M. Ruspa<sup>a,c</sup> , F. Siviero<sup>a,b</sup> , V. Sola<sup>a,b</sup> , A. Solano<sup>a,b</sup> , D. Soldi<sup>a,b</sup> , A. Staiano<sup>a</sup> , C. Tarricone<sup>a,b</sup> , M. Tornago<sup>a,b</sup> , D. Trocino<sup>a</sup> , G. Umoret<sup>a,b</sup> 

E. Vlasov<sup>a,b</sup> 

**INFN Sezione di Trieste<sup>a</sup>, Università di Trieste<sup>b</sup>, Trieste, Italy**

S. Belforte<sup>a</sup> , V. Candelise<sup>a,b</sup> , M. Casarsa<sup>a</sup> , F. Cossutti<sup>a</sup> , K. De Leo<sup>a,b</sup> , G. Della Ricca<sup>a,b</sup> 

**Kyungpook National University, Daegu, Korea**

S. Dogra , J. Hong , C. Huh , B. Kim , D.H. Kim , J. Kim, H. Lee, S.W. Lee , C.S. Moon , Y.D. Oh , M.S. Ryu , S. Sekmen , Y.C. Yang 

**Chonnam National University, Institute for Universe and Elementary Particles, Kwangju, Korea**

G. Bak , P. Gwak , H. Kim , D.H. Moon 

**Hanyang University, Seoul, Korea**

E. Asilar , D. Kim , T.J. Kim , J.A. Merlin, J. Park 

**Korea University, Seoul, Korea**

S. Choi , S. Han, B. Hong , K. Lee, K.S. Lee , S. Lee , J. Park, S.K. Park, J. Yoo 

**Kyung Hee University, Department of Physics, Seoul, Korea**

J. Goh 

**Sejong University, Seoul, Korea**

H. S. Kim , Y. Kim, S. Lee

**Seoul National University, Seoul, Korea**

J. Almond, J.H. Bhyun, J. Choi , W. Jun , J. Kim , J.S. Kim, S. Ko , H. Kwon , H. Lee , J. Lee , J. Lee , B.H. Oh , S.B. Oh , H. Seo , U.K. Yang, I. Yoon 

**University of Seoul, Seoul, Korea**

W. Jang , D.Y. Kang, Y. Kang , S. Kim , B. Ko, J.S.H. Lee , Y. Lee , I.C. Park , Y. Roh, I.J. Watson , S. Yang 

**Yonsei University, Department of Physics, Seoul, Korea**

S. Ha , H.D. Yoo 

**Sungkyunkwan University, Suwon, Korea**

M. Choi , M.R. Kim , H. Lee, Y. Lee , I. Yu 

**College of Engineering and Technology, American University of the Middle East (AUM), Dasman, Kuwait**

T. Beyrouty, Y. Maghrbi 

**Riga Technical University, Riga, Latvia**

K. Dreimanis , A. Gaile , G. Pikurs, A. Potrebko , M. Seidel , V. Veckalns<sup>56</sup> 

**University of Latvia (LU), Riga, Latvia**

N.R. Strautnieks 

**Vilnius University, Vilnius, Lithuania**

M. Ambrozas , A. Juodagalvis , A. Rinkevicius , G. Tamulaitis 

**National Centre for Particle Physics, Universiti Malaya, Kuala Lumpur, Malaysia**

N. Bin Norjoharuddeen , I. Yusuff<sup>57</sup> , Z. Zolkapli

**Universidad de Sonora (UNISON), Hermosillo, Mexico**

J.F. Benitez , A. Castaneda Hernandez , H.A. Encinas Acosta, L.G. Gallegos Maríñez,

M. León Coello , J.A. Murillo Quijada , A. Sehrawat , L. Valencia Palomo 

**Centro de Investigacion y de Estudios Avanzados del IPN, Mexico City, Mexico**

G. Ayala , H. Castilla-Valdez , E. De La Cruz-Burelo , I. Heredia-De La Cruz<sup>58</sup> , R. Lopez-Fernandez , C.A. Mondragon Herrera, A. Sánchez Hernández 

**Universidad Iberoamericana, Mexico City, Mexico**

C. Oropeza Barrera , M. Ramírez García 

**Benemerita Universidad Autonoma de Puebla, Puebla, Mexico**

I. Bautista , I. Pedraza , H.A. Salazar Ibarguen , C. Uribe Estrada 

**University of Montenegro, Podgorica, Montenegro**

I. Bubanja, N. Raicevic 

**University of Canterbury, Christchurch, New Zealand**

P.H. Butler 

**National Centre for Physics, Quaid-I-Azam University, Islamabad, Pakistan**

A. Ahmad , M.I. Asghar, A. Awais , M.I.M. Awan, H.R. Hoorani , W.A. Khan 

**AGH University of Krakow, Faculty of Computer Science, Electronics and Telecommunications, Krakow, Poland**

V. Avati, L. Grzanka , M. Malawski 

**National Centre for Nuclear Research, Swierk, Poland**

H. Bialkowska , M. Bluj , B. Boimska , M. Górski , M. Kazana , M. Szleper , P. Zalewski 

**Institute of Experimental Physics, Faculty of Physics, University of Warsaw, Warsaw, Poland**

K. Bunkowski , K. Doroba , A. Kalinowski , M. Konecki , J. Krolikowski , A. Muhammad 

**Warsaw University of Technology, Warsaw, Poland**

K. Pozniak , W. Zabolotny 

**Laboratório de Instrumentação e Física Experimental de Partículas, Lisboa, Portugal**

M. Araujo , D. Bastos , C. Beirão Da Cruz E Silva , A. Boletti , M. Bozzo , P. Faccioli , M. Gallinaro , J. Hollar , N. Leonardo , T. Niknejad , A. Petrilli , M. Pisano , J. Seixas , J. Varela , J.W. Wulff

**Faculty of Physics, University of Belgrade, Belgrade, Serbia**

P. Adzic , P. Milenovic 

**VINCA Institute of Nuclear Sciences, University of Belgrade, Belgrade, Serbia**

M. Dordevic , J. Milosevic , V. Rekovic

**Centro de Investigaciones Energéticas Medioambientales y Tecnológicas (CIEMAT), Madrid, Spain**

M. Aguilar-Benitez, J. Alcaraz Maestre , Cristina F. Bedoya , M. Cepeda , M. Cer- rada , N. Colino , B. De La Cruz , A. Delgado Peris , D. Fernández Del Val , J.P. Fernández Ramos , J. Flix , M.C. Fouz , O. Gonzalez Lopez , S. Goy Lopez , J.M. Hernandez , M.I. Josa , J. León Holgado , D. Moran , C. M. Morcillo Perez , Á. Navarro Tobar , C. Perez Dengra , A. Pérez-Calero Yzquierdo , J. Puerta Pelayo , I. Redondo , D.D. Redondo Ferrero , L. Romero, S. Sánchez Navas , L. Urda Gómez , J. Vazquez Escobar , C. Willmott

**Universidad Autónoma de Madrid, Madrid, Spain**J.F. de Trocóniz **Universidad de Oviedo, Instituto Universitario de Ciencias y Tecnologías Espaciales de Asturias (ICTEA), Oviedo, Spain**B. Alvarez Gonzalez , J. Cuevas , J. Fernandez Menendez , S. Folgueras , I. Gonzalez Caballero , J.R. González Fernández , E. Palencia Cortezon , C. Ramón Álvarez , V. Rodríguez Bouza , A. Soto Rodríguez , A. Trapote , C. Vico Villalba , P. Vischia **Instituto de Física de Cantabria (IFCA), CSIC-Universidad de Cantabria, Santander, Spain**S. Bhowmik , S. Blanco Fernández , J.A. Brochero Cifuentes , I.J. Cabrillo , A. Calderon , J. Duarte Campderros , M. Fernandez , C. Fernandez Madrazo , G. Gomez , C. Lasaosa García , C. Martinez Rivero , P. Martinez Ruiz del Arbol , F. Matorras , P. Matorras Cuevas , E. Navarrete Ramos , J. Piedra Gomez , L. Scodellaro , I. Vila , J.M. Vizan Garcia **University of Colombo, Colombo, Sri Lanka**M.K. Jayananda , B. Kailasapathy<sup>59</sup> , D.U.J. Sonnadara , D.D.C. Wickramarathna **University of Ruhuna, Department of Physics, Matara, Sri Lanka**W.G.D. Dharmaratna<sup>60</sup> , K. Liyanage , N. Perera , N. Wickramage **CERN, European Organization for Nuclear Research, Geneva, Switzerland**D. Abbaneo , C. Amendola , E. Auffray , G. Auzinger , J. Baechler, D. Barney , A. Bermúdez Martínez , M. Bianco , B. Bilin , A.A. Bin Anuar , A. Bocci , E. Brondolin , C. Caillol , T. Camporesi , G. Cerminara , N. Chernyavskaya , D. d'Enterria , A. Dabrowski , A. David , A. De Roeck , M.M. Defranchis , M. Deile , M. Dobson , F. Fallavollita<sup>61</sup> , L. Forthomme , G. Franzoni , W. Funk , S. Giani, D. Gigi, K. Gill , F. Glege , L. Gouskos , M. Haranko , J. Hegeman , V. Innocente , T. James , P. Janot , J. Kieseler , S. Laurila , P. Lecoq , E. Leutgeb , C. Lourenço , B. Maier , L. Malgeri , M. Mannelli , A.C. Marini , F. Meijers , S. Mersi , E. Meschi , V. Milosevic , F. Moortgat , M. Mulders , S. Orfanelli, F. Pantaleo , M. Peruzzi , G. Petrucciani , A. Pfeiffer , M. Pierini , D. Piparo , H. Qu , D. Rabady , G. Reales Gutierrez, M. Rovere , H. Sakulin , S. Scarfi , M. Selvaggi , A. Sharma , K. Shchelina , P. Silva , P. Sphicas<sup>62</sup> , A.G. Stahl Leiton , A. Steen , S. Summers , D. Treille , P. Tropea , A. Tsirou, D. Walter , J. Wanczyk<sup>63</sup> , K.A. Wozniak<sup>64</sup> , P. Zehetner , P. Zejdl , W.D. Zeuner**Paul Scherrer Institut, Villigen, Switzerland**T. Bevilacqua<sup>65</sup> , L. Caminada<sup>65</sup> , A. Ebrahimi , W. Erdmann , R. Horisberger , Q. Ingram , H.C. Kaestli , D. Kotlinski , C. Lange , M. Missiroli<sup>65</sup> , L. Noehte<sup>65</sup> , T. Rohe **ETH Zurich - Institute for Particle Physics and Astrophysics (IPA), Zurich, Switzerland**T.K. Arrestad , K. Androsov<sup>63</sup> , M. Backhaus , A. Calandri , C. Cazzaniga , K. Datta , A. De Cosa , G. Dissertori , M. Dittmar, M. Donegà , F. Eble , M. Galli , K. Gedia , F. Glessgen , C. Grab , D. Hits , W. Lustermann , A.-M. Lyon , R.A. Manzoni , M. Marchegiani , L. Marchese , C. Martin Perez , A. Mascellani<sup>63</sup> , F. Nessi-Tedaldi , F. Pauss , V. Perovic , S. Pigazzini , M.G. Ratti , M. Reichmann , C. Reissel , T. Reitenspiess , B. Ristic , F. Riti , D. Ruini, D.A. Sanz Becerra , R. Seidita , J. Steggemann<sup>63</sup> , D. Valsecchi , R. Wallny **Universität Zürich, Zurich, Switzerland**

C. Amsler<sup>66</sup> , P. Bärtschi , C. Botta , D. Brzhechko, M.F. Canelli , K. Cormier , R. Del Burgo, J.K. Heikkilä , M. Huwiler , W. Jin , A. Jofrehei , B. Kilminster , S. Leontsinis , S.P. Liechti , A. Macchiolo , P. Meiring , V.M. Mikuni , U. Molinatti , I. Neutelings , A. Reimers , P. Robmann, S. Sanchez Cruz , K. Schweiger , M. Senger , Y. Takahashi 

#### National Central University, Chung-Li, Taiwan

C. Adloff<sup>67</sup>, C.M. Kuo, W. Lin, P.K. Rout , P.C. Tiwari<sup>41</sup> , S.S. Yu 

#### National Taiwan University (NTU), Taipei, Taiwan

L. Ceard, Y. Chao , K.F. Chen , P.s. Chen, Z.g. Chen, W.-S. Hou , T.h. Hsu, Y.w. Kao, R. Khurana, G. Kole , Y.y. Li , R.-S. Lu , E. Paganis , A. Psallidas, X.f. Su , J. Thomas-Wilsker , H.y. Wu, E. Yazgan 

#### High Energy Physics Research Unit, Department of Physics, Faculty of Science, Chulalongkorn University, Bangkok, Thailand

C. Asawatangtrakuldee , N. Srimanobhas , V. Wachirapusanand 

#### Çukurova University, Physics Department, Science and Art Faculty, Adana, Turkey

D. Agyel , F. Boran , Z.S. Demiroglu , F. Dolek , I. Dumanoglu<sup>68</sup> , E. Eskut , Y. Guler<sup>69</sup> , E. Gurpinar Guler<sup>69</sup> , C. Isik , O. Kara, A. Kayis Topaksu , U. Kiminsu , G. Onengut , K. Ozdemir<sup>70</sup> , A. Polatoz , B. Tali<sup>71</sup> , U.G. Tok , S. Turkcapar , E. Uslan , I.S. Zorbakir 

#### Middle East Technical University, Physics Department, Ankara, Turkey

M. Yalvac<sup>72</sup> 

#### Bogazici University, Istanbul, Turkey

B. Akgun , I.O. Atakisi , E. Gülmez , M. Kaya<sup>73</sup> , O. Kaya<sup>74</sup> , S. Tekten<sup>75</sup> 

#### Istanbul Technical University, Istanbul, Turkey

A. Cakir , K. Cankocak<sup>68</sup> , Y. Komurcu , S. Sen<sup>76</sup> 

#### Istanbul University, Istanbul, Turkey

O. Aydilek , S. Cerci<sup>71</sup> , V. Epshteyn , B. Hacisahinoglu , I. Hos<sup>77</sup> , B. Isildak<sup>78</sup> , B. Kaynak , S. Ozkorucuklu , O. Potok , H. Sert , C. Simsek , D. Sunar Cerci<sup>71</sup> , C. Zorbilmez 

#### Institute for Scintillation Materials of National Academy of Science of Ukraine, Kharkiv, Ukraine

A. Boyaryntsev , B. Grynyov 

#### National Science Centre, Kharkiv Institute of Physics and Technology, Kharkiv, Ukraine

L. Levchuk 

#### University of Bristol, Bristol, United Kingdom

D. Anthony , J.J. Brooke , A. Bundred , F. Bury , E. Clement , D. Cussans , H. Flacher , M. Glowacki, J. Goldstein , H.F. Heath , L. Kreczko , B. Krikler , S. Paramesvaran , S. Seif El Nasr-Storey, V.J. Smith , N. Stylianou<sup>79</sup> , K. Walkingshaw Pass, R. White 

#### Rutherford Appleton Laboratory, Didcot, United Kingdom

A.H. Ball, K.W. Bell , A. Belyaev<sup>80</sup> , C. Brew , R.M. Brown , D.J.A. Cockerill , C. Cooke , K.V. Ellis, K. Harder , S. Harper , M.-L. Holmberg<sup>81</sup> , J. Linacre , K. Manolopoulos, D.M. Newbold , E. Olaiya, D. Petyt , T. Reis , G. Salvi , T. Schuh,

C.H. Shepherd-Themistocleous , I.R. Tomalin , T. Williams 

#### **Imperial College, London, United Kingdom**

R. Bainbridge , P. Bloch , C.E. Brown , O. Buchmuller, V. Cacchio, C.A. Carrillo Montoya , G.S. Chahal<sup>82</sup> , D. Colling , J.S. Dancu, P. Dauncey , G. Davies , J. Davies, M. Della Negra , S. Fayer, G. Fedi , G. Hall , M.H. Hassanshahi , A. Howard, G. Iles , M. Knight , J. Langford , L. Lyons , A.-M. Magnan , S. Malik, A. Martelli , M. Mieskolainen , J. Nash<sup>83</sup> , M. Pesaresi , B.C. Radburn-Smith , A. Richards, A. Rose , C. Seez , R. Shukla , A. Tapper , K. Uchida , G.P. Uttley , L.H. Vage, T. Virdee<sup>31</sup> , M. Vojinovic , N. Wardle , D. Winterbottom 

#### **Brunel University, Uxbridge, United Kingdom**

K. Coldham, J.E. Cole , A. Khan, P. Kyberd , I.D. Reid 

#### **Baylor University, Waco, Texas, USA**

S. Abdullin , A. Brinkerhoff , B. Caraway , J. Dittmann , K. Hatakeyama , J. Hiltbrand , A.R. Kanuganti , B. McMaster , M. Saunders , S. Sawant , C. Sutantawibul , M. Toms<sup>84</sup> , J. Wilson 

#### **Catholic University of America, Washington, DC, USA**

R. Bartek , A. Dominguez , C. Huerta Escamilla, A.E. Simsek , R. Uniyal , A.M. Vargas Hernandez 

#### **The University of Alabama, Tuscaloosa, Alabama, USA**

R. Chudasama , S.I. Cooper , S.V. Gleyzer , C.U. Perez , P. Rumerio<sup>85</sup> , E. Usai , C. West , R. Yi 

#### **Boston University, Boston, Massachusetts, USA**

A. Akpinar , A. Albert , D. Arcaro , C. Cosby , Z. Demiragli , C. Erice , E. Fontanesi , D. Gastler , S. Jeon , J. Rohlf , K. Salyer , D. Sperka , D. Spitzbart , I. Suarez , A. Tsatsos , S. Yuan 

#### **Brown University, Providence, Rhode Island, USA**

G. Benelli , X. Coubez<sup>26</sup> , D. Cutts , M. Hadley , U. Heintz , J.M. Hogan<sup>86</sup> , T. Kwon , G. Landsberg , K.T. Lau , D. Li , J. Luo , S. Mondal , M. Narain<sup>†</sup> , N. Pervan , S. Sagir<sup>87</sup> , F. Simpson , M. Stamenkovic , W.Y. Wong, X. Yan , W. Zhang 

#### **University of California, Davis, Davis, California, USA**

S. Abbott , J. Bonilla , C. Brainerd , R. Breedon , M. Calderon De La Barca Sanchez , M. Chertok , M. Citron , J. Conway , P.T. Cox , R. Erbacher , F. Jensen , O. Kukral , G. Mocellin , M. Mulhearn , D. Pellett , W. Wei , Y. Yao , F. Zhang 

#### **University of California, Los Angeles, California, USA**

M. Bachtis , R. Cousins , A. Datta , J. Hauser , M. Ignatenko , M.A. Iqbal , T. Lam , E. Manca , W.A. Nash , D. Saltzberg , B. Stone , V. Valuev 

#### **University of California, Riverside, Riverside, California, USA**

R. Clare , M. Gordon, G. Hanson , W. Si , S. Wimpenny<sup>†</sup> 

#### **University of California, San Diego, La Jolla, California, USA**

J.G. Branson , S. Cittolin , S. Cooperstein , D. Diaz , J. Duarte , R. Gerosa , L. Giannini , J. Guiang , R. Kansal , V. Krutelyov , R. Lee , J. Letts , M. Masciovecchio , F. Mokhtar , M. Pieri , M. Quinnan , B.V. Sathia Narayanan , V. Sharma , M. Tadel , E. Vourliotis , F. Würthwein , Y. Xiang , A. Yagil 

**University of California, Santa Barbara - Department of Physics, Santa Barbara, California, USA**

A. Barzdukas [ID](#), L. Brennan [ID](#), C. Campagnari [ID](#), G. Collura [ID](#), A. Dorsett [ID](#), J. Incandela [ID](#), M. Kilpatrick [ID](#), J. Kim [ID](#), A.J. Li [ID](#), P. Masterson [ID](#), H. Mei [ID](#), M. Oshiro [ID](#), J. Richman [ID](#), U. Sarica [ID](#), R. Schmitz [ID](#), F. Setti [ID](#), J. Sheplock [ID](#), D. Stuart [ID](#), S. Wang [ID](#)

**California Institute of Technology, Pasadena, California, USA**

A. Bornheim [ID](#), O. Cerri, A. Latorre, J.M. Lawhorn [ID](#), J. Mao [ID](#), H.B. Newman [ID](#), T. Q. Nguyen [ID](#), M. Spiropulu [ID](#), J.R. Vlimant [ID](#), C. Wang [ID](#), S. Xie [ID](#), R.Y. Zhu [ID](#)

**Carnegie Mellon University, Pittsburgh, Pennsylvania, USA**

J. Alison [ID](#), S. An [ID](#), M.B. Andrews [ID](#), P. Bryant [ID](#), V. Dutta [ID](#), T. Ferguson [ID](#), A. Harilal [ID](#), C. Liu [ID](#), T. Mudholkar [ID](#), S. Murthy [ID](#), M. Paulini [ID](#), A. Roberts [ID](#), A. Sanchez [ID](#), W. Terrill [ID](#)

**University of Colorado Boulder, Boulder, Colorado, USA**

J.P. Cumalat [ID](#), W.T. Ford [ID](#), A. Hassani [ID](#), G. Karathanasis [ID](#), E. MacDonald, N. Manganelli [ID](#), F. Marini [ID](#), A. Perloff [ID](#), C. Savard [ID](#), N. Schonbeck [ID](#), K. Stenson [ID](#), K.A. Ulmer [ID](#), S.R. Wagner [ID](#), N. Zipper [ID](#)

**Cornell University, Ithaca, New York, USA**

J. Alexander [ID](#), S. Bright-Thonney [ID](#), X. Chen [ID](#), D.J. Cranshaw [ID](#), J. Fan [ID](#), X. Fan [ID](#), D. Gadkari [ID](#), S. Hogan [ID](#), J. Monroy [ID](#), J.R. Patterson [ID](#), J. Reichert [ID](#), M. Reid [ID](#), A. Ryd [ID](#), J. Thom [ID](#), P. Wittich [ID](#), R. Zou [ID](#)

**Fermi National Accelerator Laboratory, Batavia, Illinois, USA**

M. Albrow [ID](#), M. Alyari [ID](#), O. Amram [ID](#), G. Apollinari [ID](#), A. Apresyan [ID](#), L.A.T. Bauerdick [ID](#), D. Berry [ID](#), J. Berryhill [ID](#), P.C. Bhat [ID](#), K. Burkett [ID](#), J.N. Butler [ID](#), A. Canepa [ID](#), G.B. Cerati [ID](#), H.W.K. Cheung [ID](#), F. Chlebana [ID](#), G. Cummings [ID](#), J. Dickinson [ID](#), I. Dutta [ID](#), V.D. Elvira [ID](#), Y. Feng [ID](#), J. Freeman [ID](#), A. Gandrakota [ID](#), Z. Gecse [ID](#), L. Gray [ID](#), D. Green, A. Grummer [ID](#), S. Grünendahl [ID](#), D. Guerrero [ID](#), O. Gutsche [ID](#), R.M. Harris [ID](#), R. Heller [ID](#), T.C. Herwig [ID](#), J. Hirschauer [ID](#), L. Horyn [ID](#), B. Jayatilaka [ID](#), S. Jindariani [ID](#), M. Johnson [ID](#), U. Joshi [ID](#), T. Klijnsma [ID](#), B. Klime [ID](#), K.H.M. Kwok [ID](#), S. Lammel [ID](#), D. Lincoln [ID](#), R. Lipton [ID](#), T. Liu [ID](#), C. Madrid [ID](#), K. Maeshima [ID](#), C. Mantilla [ID](#), D. Mason [ID](#), P. McBride [ID](#), P. Merkel [ID](#), S. Mrenna [ID](#), S. Nahn [ID](#), J. Ngadiuba [ID](#), D. Noonan [ID](#), V. Papadimitriou [ID](#), N. Pastika [ID](#), K. Pedro [ID](#), C. Pena<sup>88</sup> [ID](#), F. Ravera [ID](#), A. Reinsvold Hall<sup>89</sup> [ID](#), L. Ristori [ID](#), E. Sexton-Kennedy [ID](#), N. Smith [ID](#), A. Soha [ID](#), L. Spiegel [ID](#), S. Stoynev [ID](#), J. Strait [ID](#), L. Taylor [ID](#), S. Tkaczyk [ID](#), N.V. Tran [ID](#), L. Uplegger [ID](#), E.W. Vaandering [ID](#), I. Zoi [ID](#)

**University of Florida, Gainesville, Florida, USA**

C. Aruta [ID](#), P. Avery [ID](#), D. Bourilkov [ID](#), L. Cadamuro [ID](#), P. Chang [ID](#), V. Cherepanov [ID](#), R.D. Field, E. Koenig [ID](#), M. Kolosova [ID](#), J. Konigsberg [ID](#), A. Korytov [ID](#), K.H. Lo, K. Matchev [ID](#), N. Menendez [ID](#), G. Mitselmakher [ID](#), A. Muthirakalayil Madhu [ID](#), N. Rawal [ID](#), D. Rosenzweig [ID](#), S. Rosenzweig [ID](#), K. Shi [ID](#), J. Wang [ID](#)

**Florida State University, Tallahassee, Florida, USA**

T. Adams [ID](#), A. Al Kadhim [ID](#), A. Askew [ID](#), N. Bower [ID](#), R. Habibullah [ID](#), V. Hagopian [ID](#), R. Hashmi [ID](#), R.S. Kim [ID](#), S. Kim [ID](#), T. Kolberg [ID](#), G. Martinez, H. Prosper [ID](#), P.R. Prova, O. Viazlo [ID](#), M. Wulansatiti [ID](#), R. Yohay [ID](#), J. Zhang

**Florida Institute of Technology, Melbourne, Florida, USA**

B. Alsufyani, M.M. Baarmann [ID](#), S. Butalla [ID](#), T. Elkafrawy<sup>54</sup> [ID](#), M. Hohlmann [ID](#), R. Kumar Verma [ID](#), M. Rahmani

**University of Illinois Chicago, Chicago, USA, Chicago, USA**

M.R. Adams [id](#), C. Bennett, R. Cavanaugh [id](#), S. Dittmer [id](#), R. Escobar Franco [id](#), O. Evdokimov [id](#), C.E. Gerber [id](#), D.J. Hofman [id](#), J.h. Lee [id](#), D. S. Lemos [id](#), A.H. Merrit [id](#), C. Mills [id](#), S. Nanda [id](#), G. Oh [id](#), B. Ozek [id](#), D. Pilipovic [id](#), T. Roy [id](#), S. Rudrabhatla [id](#), M.B. Tonjes [id](#), N. Varelas [id](#), X. Wang [id](#), Z. Ye [id](#), J. Yoo [id](#)

#### **The University of Iowa, Iowa City, Iowa, USA**

M. Alhusseini [id](#), D. Blend, K. Dilsiz<sup>90</sup> [id](#), L. Emediato [id](#), G. Karaman [id](#), O.K. Köseyan [id](#), J.-P. Merlo, A. Mestvirishvili<sup>91</sup> [id](#), J. Nachtman [id](#), O. Neogi, H. Ogul<sup>92</sup> [id](#), Y. Onel [id](#), A. Penzo [id](#), C. Snyder, E. Tiras<sup>93</sup> [id](#)

#### **Johns Hopkins University, Baltimore, Maryland, USA**

B. Blumenfeld [id](#), L. Corcodilos [id](#), J. Davis [id](#), A.V. Gritsan [id](#), L. Kang [id](#), S. Kyriacou [id](#), P. Maksimovic [id](#), M. Roguljic [id](#), J. Roskes [id](#), S. Sekhar [id](#), M. Swartz [id](#), T.Á. Vámi [id](#)

#### **The University of Kansas, Lawrence, Kansas, USA**

A. Abreu [id](#), L.F. Alcerro Alcerro [id](#), J. Anguiano [id](#), P. Baringer [id](#), A. Bean [id](#), Z. Flowers [id](#), D. Grove [id](#), J. King [id](#), G. Krintiras [id](#), M. Lazarovits [id](#), C. Le Mahieu [id](#), C. Lindsey, J. Marquez [id](#), N. Minafra [id](#), M. Murray [id](#), M. Nickel [id](#), M. Pitt [id](#), S. Popescu<sup>94</sup> [id](#), C. Rogan [id](#), C. Royon [id](#), R. Salvatico [id](#), S. Sanders [id](#), C. Smith [id](#), Q. Wang [id](#), G. Wilson [id](#)

#### **Kansas State University, Manhattan, Kansas, USA**

B. Allmond [id](#), A. Ivanov [id](#), K. Kaadze [id](#), A. Kalogeropoulos [id](#), D. Kim, Y. Maravin [id](#), K. Nam, J. Natoli [id](#), D. Roy [id](#), G. Sorrentino [id](#)

#### **Lawrence Livermore National Laboratory, Livermore, California, USA**

F. Rebassoo [id](#), D. Wright [id](#)

#### **University of Maryland, College Park, Maryland, USA**

E. Adams [id](#), A. Baden [id](#), O. Baron, A. Belloni [id](#), A. Bethani [id](#), Y.M. Chen [id](#), S.C. Eno [id](#), N.J. Hadley [id](#), S. Jabeen [id](#), R.G. Kellogg [id](#), T. Koeth [id](#), Y. Lai [id](#), S. Lascio [id](#), A.C. Mignerey [id](#), S. Nabili [id](#), C. Palmer [id](#), C. Papageorgakis [id](#), M.M. Paranjpe, L. Wang [id](#), K. Wong [id](#)

#### **Massachusetts Institute of Technology, Cambridge, Massachusetts, USA**

J. Bendavid [id](#), W. Busza [id](#), I.A. Cali [id](#), Y. Chen [id](#), M. D'Alfonso [id](#), J. Eysermans [id](#), C. Freer [id](#), G. Gomez-Ceballos [id](#), M. Goncharov, P. Harris, D. Hoang, D. Kovalevskyi [id](#), J. Krupa [id](#), L. Lavezzi [id](#), Y.-J. Lee [id](#), K. Long [id](#), C. Mironov [id](#), C. Paus [id](#), D. Rankin [id](#), C. Roland [id](#), G. Roland [id](#), S. Rothman [id](#), Z. Shi [id](#), G.S.F. Stephans [id](#), J. Wang, Z. Wang [id](#), B. Wyslouch [id](#), T. J. Yang [id](#)

#### **University of Minnesota, Minneapolis, Minnesota, USA**

B. Crossman [id](#), B.M. Joshi [id](#), C. Kapsiak [id](#), M. Krohn [id](#), D. Mahon [id](#), J. Mans [id](#), B. Marzocchi [id](#), S. Pandey [id](#), M. Revering [id](#), R. Rusack [id](#), R. Saradhy [id](#), N. Schroeder [id](#), N. Strobbe [id](#), M.A. Wadud [id](#)

#### **University of Mississippi, Oxford, Mississippi, USA**

L.M. Cremaldi [id](#)

#### **University of Nebraska-Lincoln, Lincoln, Nebraska, USA**

K. Bloom [id](#), M. Bryson, D.R. Claes [id](#), C. Fangmeier [id](#), F. Golf [id](#), G. Haza [id](#), J. Hossain [id](#), C. Joo [id](#), I. Kravchenko [id](#), I. Reed [id](#), J.E. Siado [id](#), G.R. Snow<sup>†</sup>, W. Tabb [id](#), A. Vagnerini [id](#), A. Wightman [id](#), F. Yan [id](#), D. Yu [id](#), A.G. Zecchinelli [id](#)

#### **State University of New York at Buffalo, Buffalo, New York, USA**

G. Agarwal [id](#), H. Bandyopadhyay [id](#), L. Hay [id](#), I. Iashvili [id](#), A. Kharchilava [id](#), C. McLean [id](#), M. Morris [id](#), D. Nguyen [id](#), J. Pekkanen [id](#), S. Rappoccio [id](#), H. Rejeb Sfar, A. Williams [id](#)

**Northeastern University, Boston, Massachusetts, USA**

G. Alverson [ID](#), E. Barberis [ID](#), Y. Haddad [ID](#), Y. Han [ID](#), A. Krishna [ID](#), J. Li [ID](#), M. Lu [ID](#), G. Madigan [ID](#), D.M. Morse [ID](#), V. Nguyen [ID](#), T. Orimoto [ID](#), A. Parker [ID](#), L. Skinnari [ID](#), A. Tishelman-Charny [ID](#), B. Wang [ID](#), D. Wood [ID](#)

**Northwestern University, Evanston, Illinois, USA**

S. Bhattacharya [ID](#), J. Bueghly, Z. Chen [ID](#), K.A. Hahn [ID](#), Y. Liu [ID](#), Y. Miao [ID](#), D.G. Monk [ID](#), M.H. Schmitt [ID](#), A. Taliercio [ID](#), M. Velasco

**University of Notre Dame, Notre Dame, Indiana, USA**

R. Band [ID](#), R. Bucci, S. Castells [ID](#), M. Cremonesi, A. Das [ID](#), R. Goldouzian [ID](#), M. Hildreth [ID](#), K.W. Ho [ID](#), K. Hurtado Anampa [ID](#), C. Jessop [ID](#), K. Lannon [ID](#), J. Lawrence [ID](#), N. Loukas [ID](#), L. Lutton [ID](#), J. Mariano, N. Marinelli, I. Mcalister, T. McCauley [ID](#), C. McGrady [ID](#), K. Mohrman [ID](#), C. Moore [ID](#), Y. Musienko<sup>16</sup> [ID](#), H. Nelson [ID](#), M. Osherson [ID](#), R. Ruchti [ID](#), A. Townsend [ID](#), M. Wayne [ID](#), H. Yockey, M. Zarucki [ID](#), L. Zygalda [ID](#)

**The Ohio State University, Columbus, Ohio, USA**

A. Basnet [ID](#), B. Bylsma, M. Carrigan [ID](#), L.S. Durkin [ID](#), C. Hill [ID](#), M. Joyce [ID](#), A. Lesauvage [ID](#), M. Nunez Ornelas [ID](#), K. Wei, B.L. Winer [ID](#), B. R. Yates [ID](#)

**Princeton University, Princeton, New Jersey, USA**

F.M. Addesa [ID](#), H. Bouchamaoui [ID](#), P. Das [ID](#), G. Dezoort [ID](#), P. Elmer [ID](#), A. Frankenthal [ID](#), B. Greenberg [ID](#), N. Haubrich [ID](#), S. Higginbotham [ID](#), G. Kopp [ID](#), S. Kwan [ID](#), D. Lange [ID](#), A. Loeliger [ID](#), D. Marlow [ID](#), I. Ojalvo [ID](#), J. Olsen [ID](#), D. Stickland [ID](#), C. Tully [ID](#)

**University of Puerto Rico, Mayaguez, Puerto Rico, USA**

S. Malik [ID](#)

**Purdue University, West Lafayette, Indiana, USA**

A.S. Bakshi [ID](#), V.E. Barnes [ID](#), S. Chandra [ID](#), R. Chawla [ID](#), S. Das [ID](#), A. Gu [ID](#), L. Gutay, M. Jones [ID](#), A.W. Jung [ID](#), D. Kondratyev [ID](#), A.M. Koshy, M. Liu [ID](#), G. Negro [ID](#), N. Neumeister [ID](#), G. Paspalaki [ID](#), S. Piperov [ID](#), A. Purohit [ID](#), V. Scheurer, J.F. Schulte [ID](#), M. Stojanovic [ID](#), J. Thieman [ID](#), A. K. Virdi [ID](#), F. Wang [ID](#), W. Xie [ID](#)

**Purdue University Northwest, Hammond, Indiana, USA**

J. Dolen [ID](#), N. Parashar [ID](#), A. Pathak [ID](#)

**Rice University, Houston, Texas, USA**

D. Acosta [ID](#), A. Baty [ID](#), T. Carnahan [ID](#), S. Dildick [ID](#), K.M. Ecklund [ID](#), P.J. Fernández Manteca [ID](#), S. Freed, P. Gardner, F.J.M. Geurts [ID](#), A. Kumar [ID](#), W. Li [ID](#), O. Miguel Colin [ID](#), B.P. Padley [ID](#), R. Redjimi, J. Rotter [ID](#), E. Yigitbasi [ID](#), Y. Zhang [ID](#)

**University of Rochester, Rochester, New York, USA**

A. Bodek [ID](#), P. de Barbaro [ID](#), R. Demina [ID](#), J.L. Dulemba [ID](#), C. Fallon, A. Garcia-Bellido [ID](#), O. Hindrichs [ID](#), A. Khukhunaishvili [ID](#), P. Parygin<sup>84</sup> [ID](#), E. Popova<sup>84</sup> [ID](#), R. Taus [ID](#), G.P. Van Onsem [ID](#)

**The Rockefeller University, New York, New York, USA**

K. Goulianatos [ID](#)

**Rutgers, The State University of New Jersey, Piscataway, New Jersey, USA**

B. Chiarito, J.P. Chou [ID](#), Y. Gershtein [ID](#), E. Halkiadakis [ID](#), A. Hart [ID](#), M. Heindl [ID](#), D. Jaroslawski [ID](#), O. Karacheban<sup>29</sup> [ID](#), I. Laflotte [ID](#), A. Lath [ID](#), R. Montalvo, K. Nash, H. Routray [ID](#), S. Salur [ID](#), S. Schnetzer, S. Somalwar [ID](#), R. Stone [ID](#), S.A. Thayil [ID](#), S. Thomas, J. Vora [ID](#), H. Wang [ID](#)

**University of Tennessee, Knoxville, Tennessee, USA**

H. Acharya, D. Ally , A.G. Delannoy , S. Fiorendi , T. Holmes , N. Karunarathna , L. Lee , E. Nibigira , S. Spanier 

**Texas A&M University, College Station, Texas, USA**

D. Aebi , M. Ahmad , O. Bouhali<sup>95</sup> , M. Dalchenko , R. Eusebi , J. Gilmore , T. Huang , T. Kamon<sup>96</sup> , H. Kim , S. Luo , S. Malhotra, R. Mueller , D. Overton , D. Rathjens , A. Safonov 

**Texas Tech University, Lubbock, Texas, USA**

N. Akchurin , J. Damgov , V. Hegde , A. Hussain , Y. Kazhykarim, K. Lamichhane , S.W. Lee , A. Mankel , T. Mengke, S. Muthumuni , T. Peltola , I. Volobouev , A. Whitbeck 

**Vanderbilt University, Nashville, Tennessee, USA**

E. Appelt , S. Greene, A. Gurrola , W. Johns , R. Kunawalkam Elayavalli , A. Melo , F. Romeo , P. Sheldon , S. Tuo , J. Velkovska , J. Viinikainen 

**University of Virginia, Charlottesville, Virginia, USA**

B. Cardwell , B. Cox , J. Hakala , R. Hirosky , A. Ledovskoy , A. Li , C. Neu , C.E. Perez Lara 

**Wayne State University, Detroit, Michigan, USA**

P.E. Karchin 

**University of Wisconsin - Madison, Madison, Wisconsin, USA**

A. Aravind, S. Banerjee , K. Black , T. Bose , S. Dasu , I. De Bruyn , P. Everaerts , C. Galloni, H. He , M. Herndon , A. Herve , C.K. Koraka , A. Lanaro, R. Loveless , J. Madhusudanan Sreekala , A. Mallampalli , A. Mohammadi , S. Mondal, G. Parida , D. Pinna, A. Savin, V. Shang , V. Sharma , W.H. Smith , D. Teague, H.F. Tsoi , W. Vetens , A. Warden 

**Authors affiliated with an institute or an international laboratory covered by a cooperation agreement with CERN**

S. Afanasiev , V. Andreev , Yu. Andreev , T. Aushev , M. Azarkin , A. Babaev , A. Belyaev , V. Blinov<sup>97</sup> , E. Boos , V. Borshch , D. Budkouski , V. Bunichev , M. Chadeeva<sup>97</sup> , V. Chekhovsky, R. Chistov<sup>97</sup> , A. Dermenev , T. Dimova<sup>97</sup> , D. Druzhkin<sup>98</sup> , M. Dubinin<sup>88</sup> , L. Dudko , A. Ershov , G. Gavrilov , V. Gavrilov , S. Gninenko , V. Golovtcov , N. Golubev , I. Golutvin , I. Gorbunov , A. Gribushin , Y. Ivanov , V. Kachanov , L. Kardapoltsev<sup>97</sup> , V. Karjavine , A. Karneyeu , V. Kim<sup>97</sup> , M. Kirakosyan, D. Kirpichnikov , M. Kirsanov , V. Klyukhin , O. Kodolova<sup>99</sup> , D. Konstantinov , V. Korenkov , A. Kozyrev<sup>97</sup> , N. Krasnikov , A. Lanev , P. Levchenko<sup>100</sup> , N. Lychkovskaya , V. Makarenko , A. Malakhov , V. Matveev<sup>97</sup> , V. Murzin , A. Nikitenko<sup>101,99</sup> , S. Obraztsov , V. Oreshkin , V. Palichik , V. Perelygin , M. Perfilov, S. Petrushanko , S. Polikarpov<sup>97</sup> , V. Popov , O. Radchenko<sup>97</sup> , M. Savina , V. Savrin , V. Shalaev , S. Shmatov , S. Shulha , Y. Skovpen<sup>97</sup> , S. Slabospitskii , V. Smirnov , D. Sosnov , V. Sulimov , E. Tcherniaev , A. Terkulov , O. Teryaev , I. Tlisova , A. Toropin , L. Uvarov , A. Uzunian , A. Vorobyev<sup>†</sup>, N. Voytishin , B.S. Yuldashev<sup>102</sup>, A. Zarubin , I. Zhizhin , A. Zhokin 

<sup>†</sup>: Deceased

<sup>1</sup>Also at Yerevan State University, Yerevan, Armenia

<sup>2</sup>Also at TU Wien, Vienna, Austria

- <sup>3</sup>Also at Institute of Basic and Applied Sciences, Faculty of Engineering, Arab Academy for Science, Technology and Maritime Transport, Alexandria, Egypt
- <sup>4</sup>Also at Ghent University, Ghent, Belgium
- <sup>5</sup>Also at Universidade Estadual de Campinas, Campinas, Brazil
- <sup>6</sup>Also at Federal University of Rio Grande do Sul, Porto Alegre, Brazil
- <sup>7</sup>Also at UFMS, Nova Andradina, Brazil
- <sup>8</sup>Also at Nanjing Normal University, Nanjing, China
- <sup>9</sup>Now at Henan Normal University, Xinxiang, China
- <sup>10</sup>Now at The University of Iowa, Iowa City, Iowa, USA
- <sup>11</sup>Also at University of Chinese Academy of Sciences, Beijing, China
- <sup>12</sup>Also at China Center of Advanced Science and Technology, Beijing, China
- <sup>13</sup>Also at University of Chinese Academy of Sciences, Beijing, China
- <sup>14</sup>Also at China Spallation Neutron Source, Guangdong, China
- <sup>15</sup>Also at Université Libre de Bruxelles, Bruxelles, Belgium
- <sup>16</sup>Also at an institute or an international laboratory covered by a cooperation agreement with CERN
- <sup>17</sup>Now at British University in Egypt, Cairo, Egypt
- <sup>18</sup>Now at Cairo University, Cairo, Egypt
- <sup>19</sup>Also at Birla Institute of Technology, Mesra, Mesra, India
- <sup>20</sup>Also at Purdue University, West Lafayette, Indiana, USA
- <sup>21</sup>Also at Université de Haute Alsace, Mulhouse, France
- <sup>22</sup>Also at Department of Physics, Tsinghua University, Beijing, China
- <sup>23</sup>Also at The University of the State of Amazonas, Manaus, Brazil
- <sup>24</sup>Also at Erzincan Binali Yıldırım University, Erzincan, Turkey
- <sup>25</sup>Also at University of Hamburg, Hamburg, Germany
- <sup>26</sup>Also at RWTH Aachen University, III. Physikalisches Institut A, Aachen, Germany
- <sup>27</sup>Also at Isfahan University of Technology, Isfahan, Iran
- <sup>28</sup>Also at Bergische University Wuppertal (B UW), Wuppertal, Germany
- <sup>29</sup>Also at Brandenburg University of Technology, Cottbus, Germany
- <sup>30</sup>Also at Forschungszentrum Jülich, Juelich, Germany
- <sup>31</sup>Also at CERN, European Organization for Nuclear Research, Geneva, Switzerland
- <sup>32</sup>Also at Institute of Physics, University of Debrecen, Debrecen, Hungary
- <sup>33</sup>Also at Institute of Nuclear Research ATOMKI, Debrecen, Hungary
- <sup>34</sup>Now at Universitatea Babes-Bolyai - Facultatea de Fizica, Cluj-Napoca, Romania
- <sup>35</sup>Also at Physics Department, Faculty of Science, Assiut University, Assiut, Egypt
- <sup>36</sup>Also at HUN-REN Wigner Research Centre for Physics, Budapest, Hungary
- <sup>37</sup>Also at Faculty of Informatics, University of Debrecen, Debrecen, Hungary
- <sup>38</sup>Also at Punjab Agricultural University, Ludhiana, India
- <sup>39</sup>Also at University of Hyderabad, Hyderabad, India
- <sup>40</sup>Also at University of Visva-Bharati, Santiniketan, India
- <sup>41</sup>Also at Indian Institute of Science (IISc), Bangalore, India
- <sup>42</sup>Also at IIT Bhubaneswar, Bhubaneswar, India
- <sup>43</sup>Also at Institute of Physics, Bhubaneswar, India
- <sup>44</sup>Also at Department of Physics, Isfahan University of Technology, Isfahan, Iran
- <sup>45</sup>Also at Sharif University of Technology, Tehran, Iran
- <sup>46</sup>Also at Department of Physics, University of Science and Technology of Mazandaran, Behshahr, Iran
- <sup>47</sup>Also at Helwan University, Cairo, Egypt
- <sup>48</sup>Also at Italian National Agency for New Technologies, Energy and Sustainable Economic

Development, Bologna, Italy

<sup>49</sup>Also at Centro Siciliano di Fisica Nucleare e di Struttura Della Materia, Catania, Italy

<sup>50</sup>Also at Università degli Studi Guglielmo Marconi, Roma, Italy

<sup>51</sup>Also at Scuola Superiore Meridionale, Università di Napoli 'Federico II', Napoli, Italy

<sup>52</sup>Also at Fermi National Accelerator Laboratory, Batavia, Illinois, USA

<sup>53</sup>Also at Università di Napoli 'Federico II', Napoli, Italy

<sup>54</sup>Also at Ain Shams University, Cairo, Egypt

<sup>55</sup>Also at Consiglio Nazionale delle Ricerche - Istituto Officina dei Materiali, Perugia, Italy

<sup>56</sup>Also at Riga Technical University, Riga, Latvia

<sup>57</sup>Also at Department of Applied Physics, Faculty of Science and Technology, Universiti Kebangsaan Malaysia, Bangi, Malaysia

<sup>58</sup>Also at Consejo Nacional de Ciencia y Tecnología, Mexico City, Mexico

<sup>59</sup>Also at Trincomalee Campus, Eastern University, Sri Lanka, Nilaveli, Sri Lanka

<sup>60</sup>Also at Saegis Campus, Nugegoda, Sri Lanka

<sup>61</sup>Also at INFN Sezione di Pavia, Università di Pavia, Pavia, Italy

<sup>62</sup>Also at National and Kapodistrian University of Athens, Athens, Greece

<sup>63</sup>Also at Ecole Polytechnique Fédérale Lausanne, Lausanne, Switzerland

<sup>64</sup>Also at University of Vienna Faculty of Computer Science, Vienna, Austria

<sup>65</sup>Also at Universität Zürich, Zurich, Switzerland

<sup>66</sup>Also at Stefan Meyer Institute for Subatomic Physics, Vienna, Austria

<sup>67</sup>Also at Laboratoire d'Annecy-le-Vieux de Physique des Particules, IN2P3-CNRS, Annecy-le-Vieux, France

<sup>68</sup>Also at Near East University, Research Center of Experimental Health Science, Mersin, Turkey

<sup>69</sup>Also at Konya Technical University, Konya, Turkey

<sup>70</sup>Also at Izmir Bakircay University, Izmir, Turkey

<sup>71</sup>Also at Adiyaman University, Adiyaman, Turkey

<sup>72</sup>Also at Bozok Universitetesi Rektörlüğü, Yozgat, Turkey

<sup>73</sup>Also at Marmara University, Istanbul, Turkey

<sup>74</sup>Also at Milli Savunma University, Istanbul, Turkey

<sup>75</sup>Also at Kafkas University, Kars, Turkey

<sup>76</sup>Also at Hacettepe University, Ankara, Turkey

<sup>77</sup>Also at Istanbul University - Cerrahpasa, Faculty of Engineering, Istanbul, Turkey

<sup>78</sup>Also at Yildiz Technical University, Istanbul, Turkey

<sup>79</sup>Also at Vrije Universiteit Brussel, Brussel, Belgium

<sup>80</sup>Also at School of Physics and Astronomy, University of Southampton, Southampton, United Kingdom

<sup>81</sup>Also at University of Bristol, Bristol, United Kingdom

<sup>82</sup>Also at IPPP Durham University, Durham, United Kingdom

<sup>83</sup>Also at Monash University, Faculty of Science, Clayton, Australia

<sup>84</sup>Now at an institute or an international laboratory covered by a cooperation agreement with CERN

<sup>85</sup>Also at Università di Torino, Torino, Italy

<sup>86</sup>Also at Bethel University, St. Paul, Minnesota, USA

<sup>87</sup>Also at Karamanoğlu Mehmetbey University, Karaman, Turkey

<sup>88</sup>Also at California Institute of Technology, Pasadena, California, USA

<sup>89</sup>Also at United States Naval Academy, Annapolis, Maryland, USA

<sup>90</sup>Also at Bingol University, Bingol, Turkey

<sup>91</sup>Also at Georgian Technical University, Tbilisi, Georgia

<sup>92</sup>Also at Sinop University, Sinop, Turkey

<sup>93</sup>Also at Erciyes University, Kayseri, Turkey

<sup>94</sup>Also at Horia Hulubei National Institute of Physics and Nuclear Engineering (IFIN-HH), Bucharest, Romania

<sup>95</sup>Also at Texas A&M University at Qatar, Doha, Qatar

<sup>96</sup>Also at Kyungpook National University, Daegu, Korea

<sup>97</sup>Also at another institute or international laboratory covered by a cooperation agreement with CERN

<sup>98</sup>Also at Universiteit Antwerpen, Antwerpen, Belgium

<sup>99</sup>Also at Yerevan Physics Institute, Yerevan, Armenia

<sup>100</sup>Also at Northeastern University, Boston, Massachusetts, USA

<sup>101</sup>Also at Imperial College, London, United Kingdom

<sup>102</sup>Also at Institute of Nuclear Physics of the Uzbekistan Academy of Sciences, Tashkent, Uzbekistan